F 1503/2

BULETINUL INSTITUTULUI POLITEHNIC DIN IAŞI

Tomul XXXIX (XLIII)
Fasc. 1–4

Secţia II

CHIMIE ŞI INGINERIE CHIMICĂ

1993

BULETINUL INSTITUTULUI POLITEHNIC DIN IAŞI

ORSZÁGOS MŰSZAKI INFORMÁCIÓS KÖZPONT ÉS KÖNYVTÁR
1883

Tomul XXXIX (XLIII)
Fasc. 1–4

Secţia II

CHIMIE şi INGINERIE CHIMICĂ

1993

EDITORIAL STAFF

Prof. dr. eng. **VITALIE BELOUSOV** (President)
Prof. dr. eng. **PAULICĂ RĂILEANU** (Secretary)
Prof. dr. eng. **EFTIMIE NIŢESCU**
Prof. dr. doc. **ALFRED BRAIER** (Editor)
Prof. dr. eng. **HUGO ROSMAN** (Editor)
Prof. dr. eng. **MIHAIL VOICU** (Head of the Exchange Service)
Prof. dr. **AUREL BEJANCU**
Prof. dr. eng. **VICTOR BULACOVSCHI**
Prof. dr. eng. **DIMITRIE ALEXA**
Prof. dr. eng. **SPIRIDON CREŢU**
Prof. dr. eng. **ADRIAN RADU**
Prof. dr. eng. **ION GIURMĂ**
Prof. dr. eng. **MIRCEA MATEESCU**

TEXredaction:
Computing Centre of the Technical University of Iaşi

BULETINUL INSTITUTULUI POLITEHNIC DIN IAŞI
BULLETIN OF THE POLYTECHNIC INSTITUTE OF JASSY
Tomul XXXIX (XLIII), Fasc. 1–4 1993

Secţia II

CHIMIE ŞI INGINERIE CHIMICĂ

SUMAR

Pag.

DOINA BEJAN, AL. DUCA, MARIA GABURICI şi MIOARA SURPĂŢEANU, Caracterizarea fenilen-diaminelor prin voltametrie ciclică (engl., rez. rom.) 7

I. ROŞCA, DANIEL SUTIMAN, N. FOCA, ELENA ŞTEFANCU, DOINA SIBIESCU şi AL. CONSTANTINESCU, Recuperarea vanadiului din catalizator uzat prin extracţie în mediu bazic (germ., rez. rom.) 17

DOINA BEJAN şi AL. DUCA, Voltametria ciclică a anilinei şi a unor derivaţi *para*-substituiţi: *para*-aminofenol şi *para*-toluidină (engl., rez. rom.) 23

AL. NACU, LAVINIA TOFAN şi DOINA BÎLBĂ, Determinarea extractiv-spectrofotometrică a Mo(VI) din fonte şi oţeluri aliate cu *o*-xilidida acidului 1-mercaptopropionic (engl., rez. rom.) 33

I. ROŞCA, N. FOCA, DANIEL SUTIMAN şi D. CONDURACHE, Studiul spectrofotometric al echilibrelor chimice din sistemul $K_2[PdCl_4]$–arsenazo (III) (engl., rez. rom.) 39

GH. IONESCU, DOINA HRIŢCU şi D. ROŞCA, Studiul proprietăţilor intrinseci ale curgerii vâscoase în sistemul 1,3-butandiol–metanol (engl., rez. rom.) 49

LUCIA ODOCHIAN, CORNELIA VASILE, INGEBORG TENCHEA şi M. GRĂMĂTICU, Studiul modificărilor fizico-chimice şi structurale ale uleiurilor minerale în condiţii de utilizare (engl., rez. rom.) 57

MARIA APOSTOLESCU, FLORIN BANDRABUR, ŞT. IVĂŞCAN şi VALERIU JUMANCA, Comportarea la coroziune a aluminiului în soluţii de carbonat de etilenă (engl., rez. rom.) 65

CAROLINA HAGIU şi RODICA DIACONESCU, Analiza instalaţiei Norsk-Hydro de obţinere a nitrofosfaţilor. II. Utilizarea calculatorului pentru analiza procesului tehnologic „dezagregare nitrică“ (franc., rez. rom.) 71

AL. SZÉP şi GH. MIHĂILĂ, Studiul comparativ al procesului de descompunere termică a unor carbonaţi naturali (engl., rez. rom.) 79

MARCEL-IONEL POPA, Cromatografia în fază lichidă de înaltă performanţă a clorului din polimeri (engl., rez. rom.) 89

I. SĂNDULESCU, P. ONU, V. POPA şi D. GÂNJU, Aciditatea şi activitatea catalitică a mordeniţilor (engl., rez. rom.) 95

NATALIA HURDUC, LUCIA ODOCHIAN, C. LUCA, ELENA MIHAI şi ELENA IONESCU, Cercetări privind obţinerea monometiladipatului de înaltă puritate (engl., rez. rom.) 101

Pag.

I. MAZILU şi LUCIA TĂTARU, Polimeri ferocenici catalizatori în reacţia de deshidratare a ciclohexanolului (engl., rez. rom.) 107

CORNELIU ONISCU, EUGEN HOROBA, DAN CAŞCAVAL şi ADINA DUMITRAŞCU, Studiul cinetic al reacţiei de saponificare a 2-clor-4-dimetilamidosulfonil fenoxiacetatului de metil (engl., rez. rom.) 115

SAVEL IFRIM, O nouă categorie de coloranţi azoici (franc., rez. rom.) 121

EMIL DUMITRIU, V. HULEA şi MIRCEA PALAMARU, Câteva observaţii asupra mecanismului alchilării toluenului cu metanol catalizată de zeoliţi (engl., rez. rom.) 127

GH. SURPĂŢEANU, N. HURDUC şi VICTOR BULACOVSCHI, Cataliza cu transfer interfazic în procesele de policondensare. X. Energiile de rotaţie internă la polieterii pe bază de 3,3-bis(clorometil)oxetan şi 4,4′-dihidroxiazobenzen (engl., rez. rom.) .. 133

TATIANA LIXANDRU 139

BULETINUL INSTITUTULUI POLITEHNIC DIN IAŞI
BULLETIN OF THE POLYTECHNIC INSTITUTE OF JASSY
Tome XXXIX (XLIII), Fasc. 1–4 1993

Section II

CHEMISTRY and CHEMICAL ENGINEERING

CONTENTS

Pp.

DOINA BEJAN, AL. DUCA, MARIA GABURICI and MIOARA SURPĂŢEANU, Characterization of Phenylen-Diamines by Cyclic Voltammetry (English, Romanian summary) 7

I. ROŞCA, DANIEL SUTIMAN, N. FOCA, ELENA ŞTEFANCU, DOINA SIBIESCU und AL. CONSTANTINESCU, Rückgewinnung von Vanadium aus einem verbrauchten Katalysator durch Extraktion in einem basischen Medium (German, Romanian summary) 17

DOINA BEJAN and AL. DUCA, Cyclic Voltammetry of Aniline and Some of Its *Para*-Substituted Derivatives: *Para*-Aminophenol and *Para*-Toluidine (English, Romanian summary) 23

AL. NACU, LAVINIA TOFAN and DOINA BÎLBĂ, Extraction-Spectrophotometric Determination of Molybdenum (VI) in Cast Iron and Alloy Steels with *o*-Xylidide of 1-Mercaptopropionic Acid (English, Romanian summary) 33

I. ROŞCA, N. FOCA, DANIEL SUTIMAN and D. CONDURACHE, Spectrophotometric Study on Chemical Equilibria in $K_2[PdCl_4]$ – Arsenazo (III) System (English, Romanian summary) 39

GH. IONESCU, DOINA HRIŢCU and D. ROŞCA, Study of the Intrinsic Properties of Viscous Flow in the 1,3-Butandiol–Methanol System (English, Romanian summary) 49

LUCIA ODOCHIAN, CORNELIA VASILE, INGEBORG TENCHEA and M. GRĂMĂTICU, Study of the Physico-Chemical and Structural Modifications of Mineral Oils During Their Utilization (English, Romanian summary) 57

MARIA APOSTOLESCU, FLORIN BANDRABUR, ŞT. IVĂŞCAN and VALERIU JUMANCA, Corrosion Behaviour of Aluminium in Ethylene Carbonate Solutions (English, Romanian summary) 65

CAROLINA HAGIU et RODICA DIACONESCU, Analyse de l'installation Norsk-Hydro d'obtention des nitrophosphates. II. Utilisation de l'ordinateur dans l'analyse du processus technologique de „désagrégation nitrique" (French, Romanian summary) 71

AL. SZÉP and GH. MIHĂILĂ, A Comparative Study on the Thermal Decomposition of Some Natural Carbonates (English, Romanian summary) 79

MARCEL-IONEL POPA, High Performance Liquid Chromatography of Chloride in Polymers (English, Romanian summary) 89

Pp.

I. SĂNDULESCU, P. ONU, V. POPA and D. GÂNJU, Acidity and Catalytic Activity of Dealuminated Mordenites (English, Romanian summary) 95

NATALIA HURDUC, LUCIA ODOCHIAN, C. LUCA, ELENA MIHAI and ELENA IONESCU, Investigations Concerning the Obtainment of High Purity Monomethyladipate (English, Romanian summary) 101

I. MAZILU and LUCIA TĂTARU, Ferrocene Polymers as Catalysts in the Dehydration Reaction of Cyclohexanol (English, Romanian summary) 107

CORNELIU ONISCU, EUGEN HOROBA, DAN CAŞCAVAL and ADINA DUMITRAŞCU, Kinetic Study on Saponification of Methyl 2-Chloro-Dimethylamidosulphonyl-Phenoxyacetate (English, Romanian summary) 115

SAVEL IFRIM, Une nouvelle catégorie de colorants azoïques (French, Romanian summary) 121

EMIL DUMITRIU, V. HULEA and MIRCEA PALAMARU, Some Remarks on Mechanism of Zeolite Catalyzed Alkylation of Toluene with Methanol (English, Romanian summary) 127

GH. SURPĂŢEANU, N. HURDUC and VICTOR BULACOVSCHI, Phase Transfer Catalysis in Polycondensation Processes. X. Internal Rotation Energies in Polyethers Based on 3,3-Bis(Chloromethyl)Oxetane and 4,4′-Dihydroxyazobenzene (English, Romanian summary) 133

TATIANA LIXANDRU 139

BULETINUL INSTITUTULUI POLITEHNIC DIN IAŞI
Tomul XXXIX (XLIII), Fasc. 1–4, 1993
Secţia II
CHIMIE ŞI INGINERIE CHIMICĂ

D.C. 547.553.1; 537.741.3

CHARACTERIZATION OF PHENYLEN-DIAMINES BY CYCLIC VOLTAMMETRY

BY

DOINA BEJAN, AL. DUCA, MARIA GABURICI
and MIOARA SURPĂŢEANU

1. Introduction

The cyclic voltammetry on carbon electrodes is largely applied for electrochemical characterization and determination of organic compounds of different classes [1],...,[10].

Information concerning the anodic oxidation of *p*-disubstituted benzene [11] and other aromatic compounds [12], indicate the oxidation of aromatic substrat to proceed firstly, followed by the reaction with nucleophils, such as CN^-, HO^-, $-NH_2$, $-OCH_3$ and –OAc.

References on the electrochemical behaviour of phenylene-diamines are rather few in literature. A study on *p*FDA is given in [1]. For this reason, in present paper *ortho*- and *para*-phenylene-diamines are studied comparatively.

The runs were made with paste carbon electrode (P.C.E.) and spectral carbon electrode (Sp.C.E.), 10^{-1}M Na_2SO_4 solution as a support electrolyte and the cyclic voltammograms were recorded within the $-\,0.3\ \text{V} \rightleftharpoons +\,1.4\ \text{V}$ potential domain with respect to the saturated calomel electrode (S.C.E.) at a potential scanning rate of 50 mV/s.

The shape and the caracteristics of the voltammograms of *o*FDA and of the *o*FDA – *p*FDA mixture, have been followed as well as the possibilities of characterization and analysis of the real samples.

2. Experimental

Standard solutions of *p*FDA and *o*FDA (STOC) of 5×10^{-3} mol.L^{-1} concentration prepared with analytical grade reagents and twice-distilled water.

a) *p*FDA solutions (synthetical samples) of 10^{-2} mol.L^{-1} and 2×10^{-3} mol.L^{-1} concentrations, prepared with twice-distilled water.

b) 10^{-1} M Na_2SO_4 solution prepared with analytical grade reagent and twice-distilled water.

c) The paste carbon electrode (P.C.E.) was prepared as described in [1], [13],

[14].

d) The spectral carbon electrode was prepared as described in [1], [13].

The determined quantities of working solution and support-electrolyte were introduced into the polarographic cell, till a total volume of 10 mL, pure nitrogen bubbled 10 min. and the cyclic voltammogram recorded at a rate of 50 mV/s on a OH-102 Radelkis Polarograph.

3. Results and Discussion

The phenylene-diamines can be obtained by the reduction of *m*-dinitrobenzene or corresponding nitroanilines. They are crystalline compounds more sensitive to oxidation than the monoamines [15].

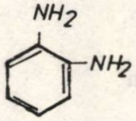

ortho-phenylene-diamine

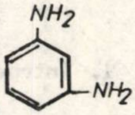

meta-phenylene-diamine

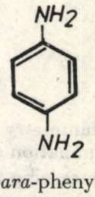

para-phenylene-diamine

Their aqueous solutions show slightly basic character (Ex: for *p*FDA, $Kb_1 = 1.1 \times 10^{-8}$ and $Kb_2 = 3.5 \times 10^{-12}$) and are unstable in air becoming quikly brown-coloured.

In the present paper the results obtained on the electrochemical behaviour of *o*FDA and *p*FDA are reported. The influence of $-NH_2$ group position in benzene ring on the voltammogram shape and voltammetric characteristics were followed on both P.C.E. (Figs. 1 *a* and 2 *a*) and Sp.C.E. (Figs. 1 *b* and 2 *b*).

The influence of depolarizer concentration on the intensity of voltammetric currents is depicted for *p*FDA in [1] and for *o*FDA in Fig. 3.

The $ip - C$ dependence is linear for both *p*FDA and *o*FDA which is indicative of the predominant diffusional character of the voltammetric currents. However, a rather great residual current is noticed on Sp.C.E., probably due to same possible side reactions on its surface.

By taking into account the obtained values for the potential difference, $\Delta E\,(V)$, and for the ip_a/ip_c ratio of the corresponding anodic and cathodic peaks, it may be noticed that *p*FDA suffers a quasireversible redox process on both Sp.C.E. and P.C.E. while *o*FDA is oxidized practically irreversible on the two electrodes, this irreversibility being more pronounced on P.C.E.

The *o*FDA voltammograms obtained on both Sp.C.E. and P.C.E. are wide, the peaks slightly defined and superimposed, so that the $b_{1/2}(V)$ (the peak half-width) cannot be well appreciated. The enlarging of the voltammograms makes evident the repulsion of the electroactive centers in the molecule during the oxydation process.

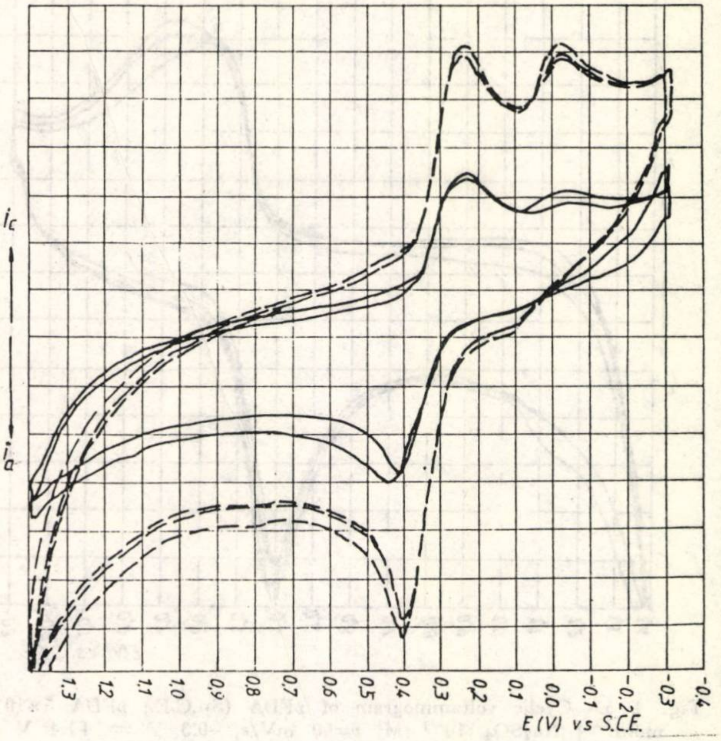

Fig. 1 *a*.– Cyclic voltammogram of *p*FDA (P.C.E.; *p*FDA 5×10^{-4} mol.L^{-1}; Na_2SO_4 10^{-1} M; v=50 mV/s; –0.3 V $\rightleftharpoons$ +1.4 V with respect to S.C.E.); —— $S=4\times10^{-7}$ A/div.; - - - $S=2\times10^{-7}$ A/div.

The stabilization of the electrod process is satisfactory on the both electrodes for *p*FDA, fairly good for *o*FDA on Sp.C.E. and rather low on P.C.E. (lower for high concentrations). In the last case the intensity of the anodic peaks within the +0.440 V → +1.40 V potential range decreases continuously with increasing scanning cycles.

The determination sensivity is higher on Sp.C.E. for *p*FDA, while for *o*FDA the sensivity is about the same for the both electrodes.

Since the real samples often contain the two isomers in different proportions, they may be estimated qualitatively or semiquantitatively from the cyclic voltammogram.

In this connection a study in model system was performed, by drawing the cyclic voltammograms on Sp.C.E. and P.C.E. (Na_2SO_4 10^{-1} M; $S = 4 \times 10^{-7}$ A/div. and $S = 2 \times 10^{-7}$ A/div. respectively; v=50 mV/s; potential domain –0.3 $\rightleftharpoons$ +1.4 V with respect to S.C.E.) for a series of standard solutions with different proportions of the two isomers (100% *p*FDA; 50% *p*FDA + 50% *o*FDA; 10% *p*FDA + 90% *o*FDA; 100% *o*FDA).

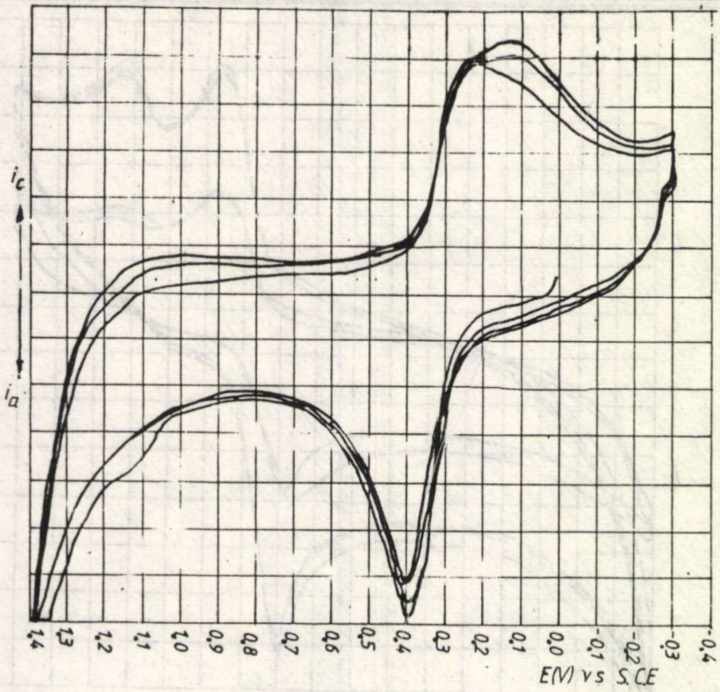

Fig. 1 *b*.– Cyclic voltammogram of *p*FDA (Sp.C.E.; *p*FDA 5×10^{-4} mol.L^{-1}; Na$_2$SO$_4$ 10^{-1} M; v=50 mV/s; –0.3 V ⇄ +1.4 V with respect to S.C.E.; $S=4\times10^{-7}$ A/div.).

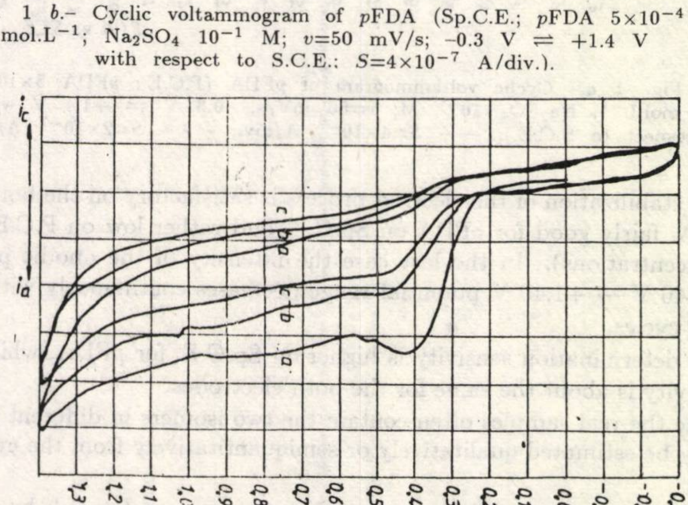

Fig. 2 *a*.– Cyclic voltammogram of *o*FDA (P.C.E.; Na$_2$SO$_4$ 10^{-1} M; *o*FDA 5×10^{-4} mol.L^{-1}; v=50 mV/s; –0.3 V ⇄ +1.4 V with respect to S.C.E.; $S=4\times10^{-7}$ A/div.).

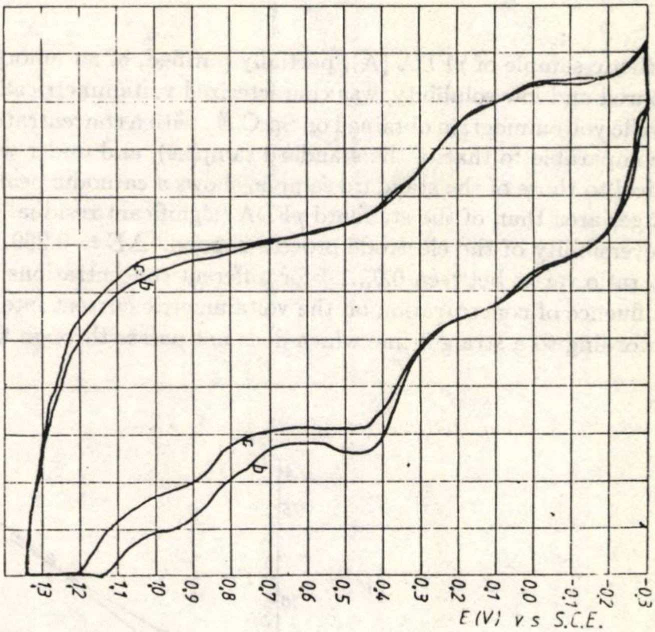

Fig. 2 *b*.– Cyclic voltammogram of *o*FDA (Sp.C.E.; Na_2SO_4 10^{-1} M; *o*FDA 5×10^{-4} mol.L^{-1}; v=50 mV/s; –0.3 V ⇄ +1.4 V with respect to S.C.E.; $S=4\times10^{-7}$ A/div.).

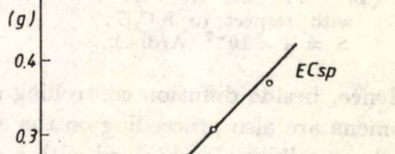

Fig. 3.– Influence of *o*FDA concentration on the area (grams) of cyclic voltammogram (Na_2SO_4 10^{-1} M; v=50 mV/s; $S=4\times10^{-7}$ A/div.; –0.3 ⇄ +1.4 V with respect to S.C.E.); —— Sp.C.E.; - - - P.C.E.

The fact was noticed that a content of 10% of an isomer modifies only slightly the voltammogram of the other while a content of 50% induces significant modifications in its shape being a hybrid of the cyclic voltammograms of the pure isomers.

A synthetic sample of *p*FDA (A), partially purified, of an amorphous aspect, brown-coloured and low solubility, was characterized voltammetrically.

The cyclic voltammogram obtained on Sp.C.E., with a concentration of 6×10^{-4} mol.L^{-1} (comparable to that of the standard samples), and under working conditions identical to those of the standard sample, shows a cathodic peak sharper and of much larger area than of the standard *p*FDA (significant residual current).

The reversibility of the electrode process is good: $\Delta E = 0.260...0.280$ V and the ip_a/ip_c ratio varies between 0.9...1.1 for different concentrations.

The influence of concentration on the voltammetric current intensity is linear (Fig. 4) according to a straight line which does not passes through the origin.

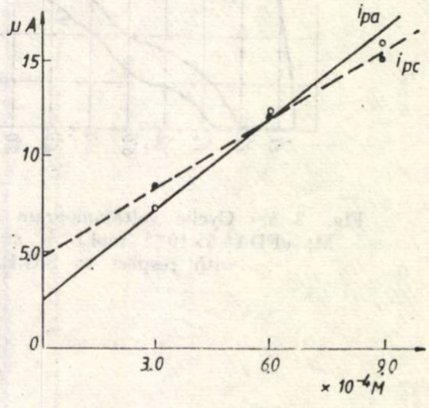

Fig. 4.– Influence of concentration on voltammetric currents (*p*FDA synthetical sample (A); Sp.C.E.; Na_2SO_4 10^{-1} M; $-0.3 \rightleftharpoons +1.4$ V with respect to S.C.E.; $S = 4\times10^{-7}$ A/div.).

Hence, beside diffusion controlling in a great extent the anodic peak, other phenomena are also proceeding on the electrode surface (adsorption and others). A good reversibility is obtained with a concentrations of about 5×10^{-4} mol.L^{-1} when $ip_a = ip_c$ (s. Fig. 4).

Another two synthetical *p*FDA samples (*I*, *II*) have been studied on P.C.E. (Na_2SO_4 10^{-1} M; v=50 mV/s; $S = 8\times10^{-8}$ A/div.) by cyclic voltammetry, within the $-0.3 \rightleftharpoons +1.4$ V domain with respect to S.C.E.

The shape of their voltammograms would indicate the sample under study to be impurified by the *ortho* isomer. The characteristics of the voltammograms of the samples *I*, *II* are presented in Table 1 in comparison with the *p*FDA and *o*FDA standard samples.

The presence of a cathodic peak at $Ep_a = +0.400$ V (approaching to *o*FDA), the general shape of the anodic branch, the rather weak stabilization of the oxidative process, similar to *o*FDA, support the above mentioned hypothesis.

The cathodic branch of the voltammogram show elements characteristics of both *p*FDA and *o*FDA, the potentials being slightly modified. Besides, the ip_a/ip_c

Table 1

Characteristics of Voltammograms of the Samples I and II in Comparison with pFDA and oFDA Standard Samples

Ep_a, [V]				Ep_c, [V]			
*p*FDA	*o*FDA	Sample *I*	Sample *II*	*p*FDA	*o*FDA	Sample *I*	Sample *II*
+0.100	+0.100	+0.100	+0.200	–	+0.580	+0.400	+0.400
–	–	+0.180	+0.325	+0.230	+0.300	+0.200	+0.160
+0.440	+0.440	+0.440	+0.480	–0.030	0.000	–0.160	–
	+0.700						
	+0.900						
	+1.050						

ratio for the correspondent peaks is much different from the standard *p*FDA tending to values characteristics of the *p*FDA +*o*FDA mixture (Table 2).

Table 2

Influence of Sample Composition on the ip_a/ip_c *Ratio*

Sample	*p*FDA standard	Sample *II*	Sample *I*	50% *p*FDA 50% *o*FDA
ip_a/ip_c	1.33	1.72	2.92	5.14

It can be seen that the presence of *o*FDA along with *p*FDA results in the increase of ip_a/ip_c ratio. One can estimate by a rough calculation that sample *I* has a higher content of *o*FDA than the sample *II* (the rough calculation takes into account the increase in the ip_a/ip_c ratio value in function of the percentage participation of *o*FDA: for 50% *o*FDA the increase in the ip_a/ip_c ratio is of $5.14...1.33 \cong 3.81$; for the samples *I* and *II* the increase in this ratio is of 1.59 and 0.39 respectively. Consequently, the composition of the sample *I* would be 79% *p*FDA and 21% *o*FDA and that of the sample *II*, 94.75% *p*FDA and 5.25% *o*FDA).

The synthetical sample *II*, showing the voltammetric characteristics closer to those of the standard *p*FDA, has been used for settling the *ip* vs. *C* dependence, in order to appreciate the character of the electrode process.

The dependence *ip* [μA] vs. *C* [mol.L^{-1}], (Fig.5), is linear for the anodic peaks, the straight lines passing either through the origin or very close to it, which confirms the diffusion to control predominantly the oxidative electrode process.

For the cathodic peaks, the ip_c vs. *C* linear dependence is valid till the concentration of 3×10^{-4} mol.L^{-1} only. Above this value, the curve is flat due to a saturation effect exerced by the accumulation of reduction products on the electrode surface.

The dependence of the overall electrode process suported by *p*FDA (*II*) on the concentration may be expressed by the function *A* [g] vs. *C* [mol.L^{-1}], where *A* [g] is the area of the cyclic voltammogram in grams. This dependence is linear, which supports the conclusions drawn from the interpretation of the functions *ip* vs. *C*.

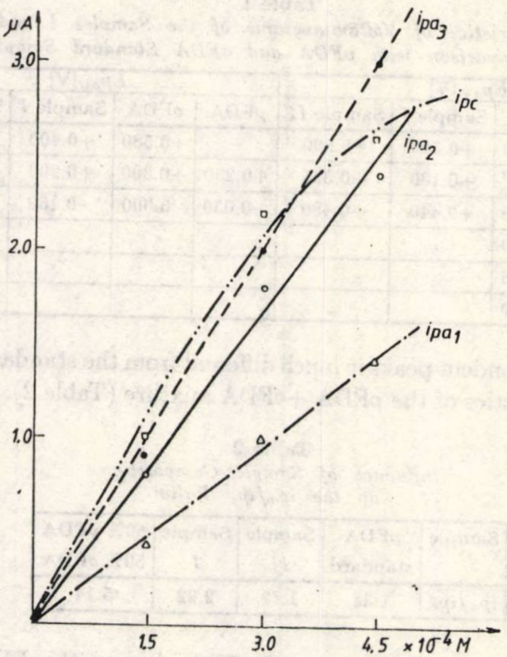

Fig. 5.- Influence of concentration of *p*FDA synthetical sample (*II*) on the intensity of anodic and cathodic currents obtained by cyclic voltammetry (P.C.E.; Na_2SO_4 10^{-1} M; $v = 50$ mV/s; -0.3 V $\rightleftharpoons$ $+1.4$ V with respect to S.C.E.; $S = 4\times10^{-7}$ A/div.).

4. Conclusions

The phenylene-diamines can be characterized electrochemically by cyclic voltammetry in neutral salt solution (Na_2SO_4, 10^{-1} M), by using carbon electrodes (Sp.C.E. and P.C.E.), within the $-0.3 \rightleftharpoons +1.4$ V potential domain with respect to S.C.E.

The relative position of the two $-NH_2$ groups in benzene ring causes the different behaviour of the *o*- and *p*FDA on both Sp.C.E. and P.C.E. The mechanism and kinetics of oxidation and reduction are therefore different.

The voltammetric currents are controlled exclusively or predominantly by diffusion, some side electrode processes resulting in the increase in the residual current being also possible.

The cyclic voltammogram of one isomer is modified by the presence of the other in a content of 10...90%. The study in a model system of some mixed solutions of *o*FDA and *p*FDA (standard samples), made possible the qualitative and semiquantitative interpretation of some samples, obtained by synthesis and partially purified.

In all synthetic samples, the isomer *o*FDA was found to exist in different contents along with *p*FDA.

The amount of *o*FDA from *p*FDA, synthetical samples, can be estimated by the difference in the voltammogram, widths (anodic branch) and taking the ip_a/ip_c ratio into account. The possibility of controlling and optimizing the synthesis process by electrochemical way by cyclic voltammetry on carbon electrodes is suggested.

Received, January 18, 1991

Polytechnic Institute, Jassy,
Department of
Analytical Chemistry

REFERENCES

1. Duca Al., Bejan D., Rev. roum. de chimie, **36**, *4-7*, 439 (1991).

2. Adam R.N., *Electrochemistry at Solid Electrodes.* Marcel Dekker, New York, 1969, 327 (*cf.* Bull. Soc. Chim. Fr., **5**, 794 (1987)).

3. Al-Arab M.M., Barquawi K.R., Tabba H.D., Bull. Soc. chim. Fr., **5**, 787 (1987).

4. Malik W.U., Goyal R.N., Rajeshwari W.A., Bull. Soc. Chim. Fr., **5**, 791 (1987).

5. Chibani A., Hazard A., Jubault M., Tallec A., Bull. Soc. chim. Fr., **5**, 795 (1987).

6. Chen H., Chen J., Environ. chem., **8**, *2*, 76 (1989) (*cf.* Refer. Zhur., **19**, *3* (1990)).

7. Rodriquez J.R.B., Barcia A.C., Blanco P.T., Analyst, **114**, *8*, 939 (1989) (*cf.* Refer. Zhur., **19**, *3*, 3G382 (1990)).

8. Maslowska J., Malicka M., Chem. anal., **33**, *6*, 903 (1988) (*cf.* Refer. Zhur., **19**, *4* (1990)).

9. Lyne P.D., O'Neill R.D., Anal. chem., **61**, 20, 2323 (1989).

10. Anderson J.E., Tallman E.D., Chesney D.J., Anderson J.L., Anal. chem., **50**, *8*, 1051 (1978).

11. Rozhkov I.N., Alyev I.Y., Tetrahedron, **31**, 977 (1975) (*cf.* Bull. Soc. Chim. Fr., **5**, 790 (1987)).

12. Eberson L., *Organic Electrochemistry.* Ed. M. Baizer, Marcel Dekker, New York, 1973, 447-468 and 781-804 (*cf.* Bull. Soc. Chim. Fr., **5**, 790 (1987)).

13. Kekedy L., *Senzori electrochimici metalici şi ion-selectivi.* Ed. Acad., Buc., 1987, 33.

14. Guadalupe A.R., Jhaweri S.S., Lin K.E., Abruña H.D., Anal. chem., **59**, *19*, 2436 (1987).

15. Neniţescu C.D., *Chimie organică.* Vol. **I**, Ed. Tehnică, Bucureşti, 1960, 521.

16. Beral E., Zapan M., *Chimie organică.* Ed. Tehnică, Bucureşti, 1973, 104; 457.

CARACTERIZAREA FENILEN-DIAMINELOR PRIN VOLTAMETRIE CICLICĂ

(Rezumat)

Izomerii *orto-* şi *para-* ai diaminobenzenului (*orto*-fenilendiamina şi *para*-fenilendiamina) au fost caracterizaţi electrochimic folosind doi electrozi pe bază de cărbune: un electrod pastă de cărbune (E.P.C) şi un electrod din cărbune spectral (E.C.Sp).

Studiul s-a efectuat prin voltametrie ciclică, utilizând ca electrolit suport soluţia de Na_2SO_4 10^{-1} M, în domeniul de potenţial $-0{,}3 \rightleftharpoons +1{,}4$ V faţă de E.S.C.

Rezultatele au fost extinse la câteva sisteme reale (probe de *p*FDA obţinute în laborator), după analiza în sistem model a unor amestecuri de *p*FDA şi *o*FDA în proporţii variabile.

Se poate trage concluzia că puritatea unor probe reale de *p*FDA sau *o*FDA se poate aprecia prin voltametrie ciclică.

De asemenea, este posibilă optimizarea procesului de sinteză a compuşilor studiaţi şi se pot obţine informaţii despre ei.

BULETINUL INSTITUTULUI POLITEHNIC DIN IAŞI
Tomul XXXIX (XLIII), Fasc. 1–4, 1993
Secţia II
CHIMIE ŞI INGINERIE CHIMICĂ

D.K. 669.922; 542.973.8

RÜCKGEWINNUNG VON VANADIUM AUS EINEM VERBRAUCHTEN KATALYSATOR DURCH EXTRAKTION IN EINEM BASISCHEN MEDIUM

VON

**I. ROŞCA, DANIEL SUTIMAN, N. FOCA, ELENA ŞTEFANCU,
DOINA SIBIESCU und AL. CONSTANTINESCU**

1. Vorwort

Einer der in der chemisch-anorganischen Industrie am meisten verwendeten Katalysatoren ist der auf der Grundlage von Vanadiumpentaoxyd mit Siliziumdioxyd als Katalysatorträger, der bei der Oxydierung der Schwefelgase in der Schwefelsäureherstellung Anwendung findet.

Je nach dem Hersteller enthält dieser Katalysator zwischen 4% und 7% Vanadiumpentaoxyd [1]. Infolge der großen Katalysatormengen und der Tatsache, daß es sich um keinen einheimischen Rohstoff handelt, ist die Verwertung des in diesem Katalysator enthaltenen Vanadiumpentaoxyds von besonderem Interesse.

In der Fachliteratur findet man eine relativ große Anzahl von Arbeiten auf diesem Fachgebiet [1],...,[8], aber die vorgeschlagenen Verfahren sind industriemäßig schwer anwendbar, entweder wegen des hohen Arbeitsdruckes [1], [2], der Komplexität des technologischen Prozesses [3],...,[5], der Verwendung von wenig wirksamen Reduktionsmitteln [6] bzw. der Korrosion [3] oder wegen der Extraktion von mehreren Verbindungen, deren nachfolgende Trennung schwierig ist.

In Rumänien gibt es noch kein industriemäßiges Verfahren für eine Verwertung des Vanadiums aus dem verbrauchten Katalysator der Schwefelsäureindustrie.

In dieser Arbeit werden unsere Bemühungen um die Herstellung von Ammoniummetavanadat aus dem verbrauchtem Katalysator von Vanadiumpentaoxyd vorgestellt.

2. Experimenteller Teil

Der zur Wiedergewinnung verwendete Katalysator hat folgende Zusammensetzung: V_2O_4= 3,24%; V_2O_5= 2,01%; Fe_2O_3= 2,5%; Al_2O_3=3,33%; K_2O=6,02%; SiO_2=76,55%.

Er wurde bis zu einer Teilchengröße unter 0,1 mm gemahlen. Unter Berücksichtigung der Eigenschaften der Vanadium(IV)- und Vanadium(V)-Salze [7], [11], [12] wird die Extraktion unter der Form von Kalium- oder Natriummetavanadat, also eines Vanadium(V)-Salzes bei einem aus den experimentellen Daten optimal bestimmten pH-Wert verfolgt. Infolge des großen Anteils von Vanadium(IV) im verbrauchten Katalysator wurden in der ersten Phase die Vanadium(IV)-Salze zu Vanadium(V)-Verbindungen oxydiert. In einem Sulfonierkolben, vorgesehen mit Rührer, Thermometer und Rückflußkühler, wurde zur Extraktion der Katalysator (400 g) und destilliertes Wasser (2 l) eingeführt. Auf der Grundlage von experimentellen Bestimmungen wurde geschlußfolgert, daß das optimale Extraktionsverhältnis zwischen Feststoff und Flüssigkeit 1:5 beträgt. Die Suspension hat einen stark sauren pH-Wert. Zur Oxydation von Vanadium(IV) zu Vanadium(V) wurden mehrere Oxydationsmittel getestet und zwar: Kaliumpermanganat, Kaliumbichromat, Wasserstoffperoxyd und Natriumhypochlorit. In Abb. 1 ist die Veränderung der Vanadiumpentaoxydkonzentration in Abhängigkeit von der Zeit für verschiedenen Oxydationsmittel dargestellt.

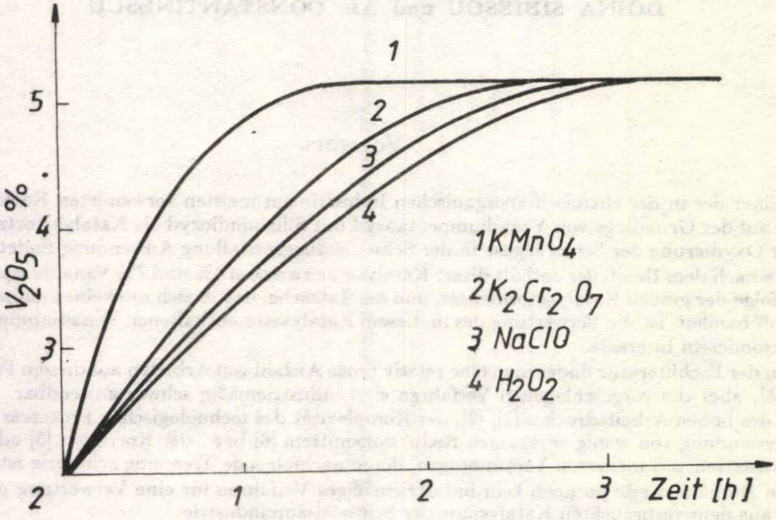

Abb. 1.– Zeitabhängige Veränderung der V_2O_5-Konzentration in der Suspension für verschiedene Oxydationsmittel.

Aus ökonomischen Gründen und der fast gleichen Oxydationskraft der getesteten Oxydationsmittel wurde zur Oxydation von Vanadium(IV) zu Vanadium(V) das Natriumhypochlorit ausgewählt. Dieses ist zur industriellen Nutzung sehr gut geeignet. Dann wurde der optimale Extraktions-pH-Wert bestimmt. In die vorher beschriebene Anlage wurden 400 g verbrauchter Katalysator, destilliertes Wasser im Feststoff – Flüssigkeitsverhältnis von 1:5 und das Oxydationsmittel Natriumhypochlorit eingefüllt. Die Oxydation im kalten Zustand dauerte 2,5 Stunden, danach wurde eine 10%-ige Natriumhydroxydlösung hinzugefügt, um den gewünschten pH-Wert zu erhalten. In Abb. 2 wird die zeitabhängige Veränderung der Konzentration von Vanadiumpentaoxyd in der flüssigen Phase bei verschiedenen pH-Werten dargestellt.

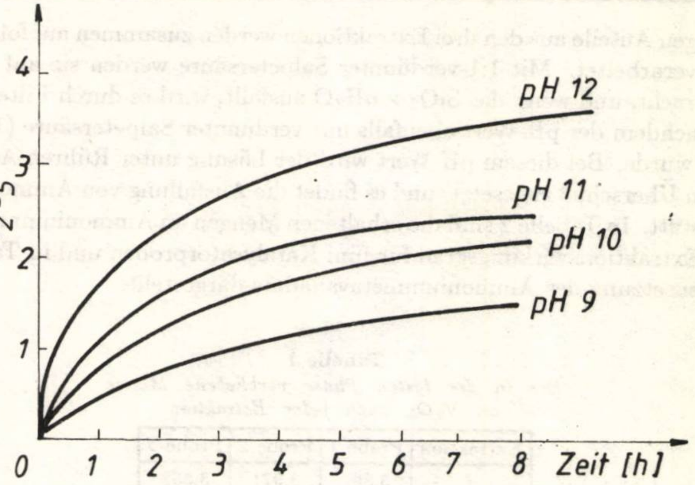

Abb. 2.– Zeitabhängige Veränderung der V_2O_5-Konzentration in der flüssigen Phase bei verschiedenen pH-Werten (Oxydationsmittel NaClO).

Nach der Bestimmung des optimalen pH-Wertes für die Extraktion wurde die Vanadiummenge bestimmt, die in Form von Ammoniummetavanadat zurückgewonnen werden kann.

In die Anlage wurden 400 g verbrauchter Katalysator, 2 l destilliertes Wasser eingefüllt, die Suspension wurde gerührt, kalt 50...70 ml Natriumhypochlorit zugefügt und danach, zur Anregung des Oxydationsprozesses, einige ml 10%-ige Natriumhydroxydlösung. Man nimmt an, erwähnt auch von einigen Autoren in der Fachliteratur [13], daß die Oxydation mit Hypochlorit durch den aus dem Hypochlorit erhaltenen Singlet-Sauerstoff begünstigt wird. Nach 2,5-stündigem Rühren beginnt das Gemisch sich zu erwärmen, wobei 10%-iges Natriumhydroxyd bis zum pH=12 Wert hinzugefügt wird. Dieser Wert darf nicht überschritten werden, weil durch Versuche festgestellt wurde, daß größere pH-Werte zur Extraktion großer Siliziummengen führen, die in ihrem Niederschlag große Mengen von Vanadiumverbindungen einschließen, wodurch der Extraktionsgrad stark abfällt. Die Suspension wird auf eine Temperatur von 90°C gebracht, die 5 Stunden beibehalten wird. Dann filtriert man die Suspension in einem Büchner-Trichter mit Filterpapier Blau, und der flüssige Teil wird weiterverarbeitet, um Ammoniummetavanadat zu erhalten. Infolge der großen Absorptionskraft des katalytischen Trägers wird dieser zur kompletten Wiedergewinnung der Vanadiumverbindungen noch zweimal mit destilliertem Wasser im Feststoff – Flüssigkeits-Verhältnis von 1:3 mit Korrigierung des pH-Wertes der Suspension auf 12 mit Hilfe von 10%-iger Natriumhydroxydlösung zwei Stunden bei 90°C versetzt. Die feste Phase wird von der flüssigen Phase durch Filterung getrennt.

In Tabelle 1 ist der Vanadiumgehalt, ausgedrückt in Prozenten an Vanadiumpentaoxyd, verblieben in der festen Phase nach jeder Extraktion, wiedergegeben.

Die flüssigen Anteile aus den drei Extraktionen werden zusammen auf folgende Weise weiterverarbeitet. Mit 1:1-verdünnter Salpetersäure werden sie auf den pH=8 Wert gebracht, und wenn das $SiO_2 \times nH_2O$ ausfällt, wird es durch Filterung abgetrennt, nachdem der pH-Wert ebenfalls mit verdünnter Salpetersäure (1:1) auf 6,5 gebracht wurde. Bei diesem pH-Wert wird der Lösung unter Rühren Ammoniumchlorid im Überschuß zugesetzt, und es findet die Ausfällung von Ammoniummetavanadat statt. In Tabelle 2 sind die erhaltenen Mengen an Ammoniummetavanadat und der Extraktionswirkungsgrad für fünf Katalysatorproben und in Tabelle 3 die Zusammensetzung des Ammoniummetavanadats dargestellt.

Tabelle 1

Die in der festen Phase verbliebene Menge an V_2O_5 nach jeder Extraktion

Extraktion	Probe *1*	Probe *2*	Probe *3*
I	3,897	3,971	3,852
II	2,602	2,581	2,671
III	0,982	1,010	0,953
IV	0,945	0,933	0,937
V	0,901	0,911	0,887

Tabelle 2

Erhaltene Menge an Ammoniummetavanadat und Ausnutzungsgrad

Probe	*I*	*II*	*III*	*IV*	*V*
Menge	0,401	5,150	4,617	4,758	5,217
Ausnutzungsgrad, [%]	65,2	76,3	68,4	70,5	77,3

Tabelle 3

Zusammensetzung des Ammoniummetavanadats

Komponente	NH_4VO_3	Cl^-	SO_4^{2-}	Fe^{3+}	Na^+	K^+
%	99,2	0,19	0,45	0,012	0,12	0,15

3. Interpretation der Ergebnisse und Schlußfolgerungen

1. Aus Abb. 1 folgt, daß, unabhängig vom verwendeten Oxydationsmittel, der Prozeß nach drei Stunden beendet ist, wobei die Reaktionsgeschwindigkeit vom Oxydationsmittel abhängt; bei $KMnO_4$ ist diese größer als bei H_2O_2.

2. Aus den experimentell erhaltenen Daten folgt, daß die maximale Menge an Vanadium sich praktisch in den ersten drei Extraktionen abscheidet (Tab. 1).

3. Der Ausnutzungsgrad variiert zwischen 65% und 75%.

4. Die Reinheit des Ammoniummetavanadats erlaubt seine Verwendung als Katalysator in der organisch-chemischen Industrie, bei der Oxydation der Adipinsäure.

5. Das Verfahren ist einfach und leicht industriemäßig und mit geringem Energieverbrauch anzuwenden.

Eingegangen am 25. Oktober 1991

Technische Hochschule, Jassy,
Lehrstühl für
Anorganische Chemie

LITERATURVERZEICHNIS

1. Calistru C., Leonte C., *Tehnologia substanţelor anorganice.* EDP, Bucureşti, 1972.

2. * * * Patent R.S.R., Nr. *88425* (1982).

3. * * * Patent R.S.R., Nr. *88435* (1982).

4. * * * Patent R.S.R., Nr. *88436* (1982).

5. * * * Patent R.S.R., Nr. *77275* (1978).

6. * * * Patent R.S.R., Nr. *78284* (1978).

7. * * * Patent R.S.R., Nr. *59754* (1974).

8. Pascal P., *Nouveau Traité de Chimie Minérale.* Vol. **XII**, Masson et Cie, Paris, 1958.

9. Minova A., Ivashantev V., Zh. Prikl.'Khim., **52**, *1*, 26 (1979).

10. Vleva A.N., Khim. Ind., **35**, *2*, 50 (1963).

11. Golovka N.A., Brodanich K.J., Zarogolova N.D., Khim. Prom. Ukr., **5**, 49-51 (1966).

12. Rîpan R., Ceteanu I., *Chimia metalelor.* Vol. **II**, EDP, Bucureşti, 1969.

13. Constantinescu G.C., *Chimie anorganică.* Vol. **II**, Ed. Tehn., Bucureşti, 1986.

14. Roşca I., Palamaru M., *Reactivitatea oxigenului singlet*, im Bd. *Ştiinţa, tehnica şi civilizaţia umană în perspectiva viitorului.* Zilele Academice Ieşene, Iaşi, 1987, 7.

RECUPERAREA VANADIULUI DIN CATALIZATOR UZAT PRIN EXTRACŢIE ÎN MEDIU BAZIC

(Rezumat)

Este prezentat un mod de valorificare a catalizatorului uzat pe bază de pentaoxid de vanadiu folosit în cataliza de oxidare a dioxidului de sulf la trioxid de sulf.

În prima fază este urmărită oxidarea compuşilor vanadiului (IV) la vanadiu (V) cu diverşi oxidanţi, apoi este determinată valoarea optimă a pH-ului de extracţie şi, în final, se prezintă metoda experimentală de recuperare a vanadiului sub formă de metavanadat de amoniu, prin precipitare cu clorură de amoniu dintr-o soluţie de metavanadat.

Prin această metodă se obţine un produs a cărui puritate permite utilizarea lui drept catalizator la oxidarea acidului adipic.

BULETINUL INSTITUTULUI POLITEHNIC DIN IAŞI
Tomul XXXIX (XLIII), Fasc. 1–4, 1993
Secţia II
CHIMIE ŞI INGINERIE CHIMICĂ

D.C. 547.564.4; 547.565.2; 537.741.3

CYCLIC VOLTAMMETRY OF ANILINE AND SOME OF ITS *PARA*-SUBSTITUTED DERIVATIVES: *PARA*-AMINOPHENOL AND *PARA*-TOLUIDINE

BY

DOINA BEJAN and AL. DUCA

1. Introduction

References on the electrochemical behaviour of the primary aromatic amines [1], [2] and electrochemical oxidation of the *p*-disubstituted benzene [3], [4] are to be found in literature.

In some papers [5] the mechanism of electrooxidation of these compounds into several stages is presented: the first is the irreversible oxidation by losing an electron and a proton and conversion into a free, unstable radical, which leads to a hydrazo-compound by dimerization; the second stage is a reversible redox process leading to an azo-compound by the participation of two electrons and two protons.

The general mechanism may be represented as follows:

$$\text{R-NH} \xrightarrow{-e^- \, -H^+} \text{R-}\dot{\text{N}}\text{H} \longrightarrow \text{R-NH-NH-R} \overset{-2e^- \, -2H^+}{\rightleftharpoons} \text{R-N=N-R}$$

In the above mentioned reference this mechanism is applied to 2-amino-4-phenylthiazol.

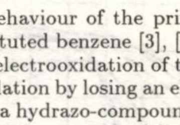

The aim of the present paper is the characterization of the three compounds by cyclic voltammetry on carbon electrodes (Spectral Carbon Electrode – Sp.C.E. and Paste Carbon Electrode – P.C.E.) and revealing of the principal behaviour similarities and differences in connection with the structure and substituent nature.

The three compounds show a slight basic character: pK_b (aniline) = 9.42; pK_b (*p*-toluidine) = 9.0; pK_b (*p*-aminophenol) = 8.50. Their aqueous solutions are unstable, sensitive to the air oxidation.

2. Experimental

a) Standard solutions of aniline (5×10^{-3} M), *p*-aminophenol (10^{-2} M), *p*-toluidine (5×10^{-3} M), prepared with analytical grade reagents and twice-distilled watter.

b) 10^{-1} M Na_2SO_4 solution prepared with analytical grade substance and twice-distilled watter.

c) Paste carbon electrode (P.C.E.) prepared as described in [7],...,[9].

d) Spectral carbon electrode (Sp.C.E.) prepared and used according to [7], [8].

The corresponding volumes of solutions were introduced into the cell for the voltammetric analysis, then support – electrolyte added till a volume of 10 mL, pure nitrogen bubbled for 10 min. and recordings made on an Polarograph OH-102 Radelkis.

3. Results and Discussion

3.1. Voltammetric Characterization of Aniline

The cyclic voltammograms of aniline ($C = 5.10^{-4}$ mol.l^{-1}) recorded on P.C.E. are given in Fig. 1, for $S = 4.10^{-7}$ A/div. and potential scanning rate of 50 mV/s and 100 mV/s.

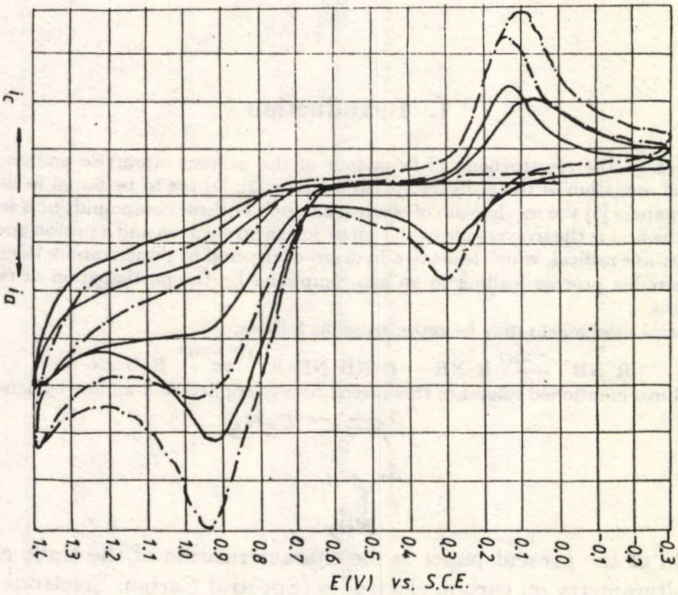

Fig. 1.– Cyclic voltammograms of aniline (P.C.E.; Na_2SO_4 10^{-1} M; $C = 5.10^{-4}$ mol.l^{-1}; $S = 4.10^{-7}$ A/div.; -0.3 V ⇌ +1.4 V potential domain with respect to S.C.E.); —— 50 mV/s, -.-.-.- 100 mV/s.

Within the 0.0 V→ +1.4 V domain a particularly high anodic peak can be noticed at Ep_a=+0.93 V, which corresponds to an intense oxidative process.

The intensity of this peak decreases with increasing number of the recording cycles, the anodic curve shape being significantly modified.

Based on its cyclic voltammogram obtained with P.C.E., the aniline can be appreciated to suffer an initial irreversible oxidation ($Ep_a = +0.93$ V) followed by a quasireversible redox process: $Ep_c = +0.080$ V and $Ep_a = +0.30$ V ($v = 50$ mV/s).

As results from the lg i_p vs. lg v diagrams, the voltammetric current is diffusional in case of the anodic peak with $Ep_a = +0.930$ V for which the slope of the function is $\mathrm{tg}\alpha = 0.444$, hence very close to 0.50 (cycle a) as well as for the anodic peak with $Ep_a = +0.300$ V ($\mathrm{tg}\alpha = 0.53$) noticed in the scanning cycle b.

The voltammetric current of the peak $Ep_a = +0.93$ V, cycle b, is controlled by both diffusion and adsorption ($\mathrm{tg}\alpha = 0.65$, theat means $0.50 < \mathrm{tg}\alpha < 1.0$ [7]). Due to the possible adsorption of the oxidation products on the electrode surface, the voltammetric current of the cathodic peak is exclusively controlled by adsorption ($\mathrm{tg}\alpha = 1.0$).

Based on the above considerations, the aniline may be assumed to oxidize in at least two main stages, namely: an irreversible oxidation strictly controlled by diffusion and a practically reversible (at least during the second scanning cycle within the $+1.4$ V $\rightleftharpoons$ -0.3 V domain) redox process where the oxidation is controlled by diffusion only and the reduction by adsorption.

The values $\Delta E \neq 0$, which are not very high, are indicative of a rather slow electron transfer (slow electrode kinetics). The calculation of charging on the electrode surface ($\Gamma = Q/nFA$) reveals the fact that a molecular monolayer of the electroactive species was fixed on P.C.E. during the electrochemical process pro- ceeding within the potential domain of $+1.4$ V $\rightleftharpoons$ -0.3 V ($\Gamma p_a = 0.97 \times 10^{-10}$ mol/cm^2, $\Gamma p_c = 1.41 \times 10^{-10}$ mol/cm^2), while the $0.0 \rightarrow +1.4$ V potential domain promotes the fixation of multimolecular layers ($\Gamma p_a = 1.166 \times 10^{-9}$ mol/cm^2) [10].

The voltammogram recorded with Sp.C.E. has a shape similar to that obtained with P.C.E. (Fig. 2).

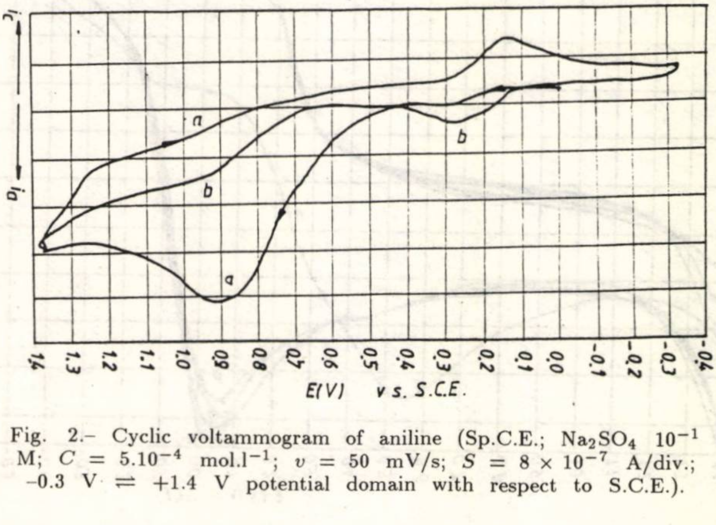

Fig. 2.– Cyclic voltammogram of aniline (Sp.C.E.; Na_2SO_4 10^{-1} M; $C = 5.10^{-4}$ mol.l^{-1}; $v = 50$ mV/s; $S = 8 \times 10^{-7}$ A/div.; -0.3 V $\rightleftharpoons$ $+1.4$ V potential domain with respect to S.C.E.).

The electrod process proceeding on Sp.C.E. at $v = 50$ mV/s is closed to that on P.C.E. at 100 mV/s, hence the Sp.C.E. promotes a more rapid electronic transfer.

Based on the above remarks, the electrode nature may be said to influence significantly the intensity of the anodic process at $Ep_a = +0.930$ V, considered by us as the main electrochemical process.

3.2. Voltammetric Characterization of p-Aminophenol (p-AF)

The aqueous solutions of p-AF suffer more rapide transformations, a behaviour similar to the polyhydroxylic phenols and aromatic diamines [11].

The cyclic voltammogram obtained on P.C.E. was very clear and complex (Fig. 3), showing several possible electrochemical processes.

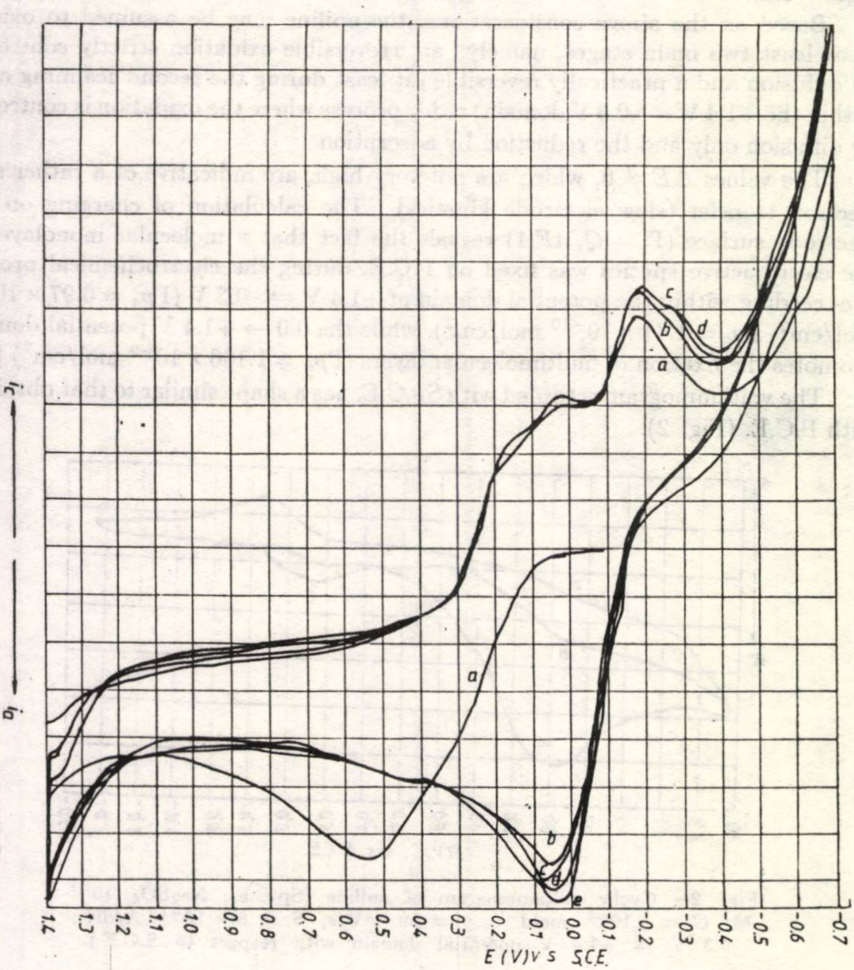

Fig. 3.– Cyclic voltammogram of p-AF (P.C.E.; Na_2SO_4 10^{-1} M; $C = 10^{-3}$ mol.l^{-1}; $v = 50$ mV/s; $S = 2 \times 10^{-7}$ A/div.; −0.7 V ⇌ +1.4 V potential domain with respect to S.C.E.).

The processes on P.C.E. are partially reversible ($\Delta E \neq 0, ip_a/ip_c \neq 1$), with middle-slow kinetics. The initial, quite intense oxidation proceeding, at $Ep_a = = +0.550$ V, is considered irreversible ($\Delta E = 0.350$ V; $ip_a/ip_c = 1.85$).

After the irreversible oxidation within the 0.00 → +1.4 V domain the quasireversible redox process, situated at lower potential values, will prevail, a behaviour also confirmed in [12].

The kinetics of the electron exchange is middle – slow ($\Delta E = 0.210...0.350$ V).

The dependence *ip* vs. *C* was found to be linear for all the mentioned potential values, which indicates the diffusional character of the electrode process.

Since the cyclic voltammogram has a rather complicated shape, the influence of the concentration on the overall electrod process may be also expresed by the function *A*, [g], vs. *C*, [mol.l^{-1}], where *A*, [g], denotes the area of the voltammogram expressed in grammes. In this case the dependence was also linear which confirms the diffusion to be the prevailing transport phenomenon of the electroactive species to the electrode surface. This fact is also supported by the slope values of the function $\lg ip$ vs. $\lg v$, for both anodic and cathodic currents ($\text{tg}\alpha \simeq 0.50$, a proper value of the diffusion current).

The plotting of the *ip* vs. $\sqrt{v}$ function was linear for both reduction and oxidation. In this case, the semi-infinite diffusion of the electrochemical charge is the prevailing phenomenon which was also confirmed by our results.

3.3. Voltammetric Characterization of *p*-Toluidine

The electrochemical behaviour of *p*-toluidine (*p*-Tol) on P.C.E. was particularly interesting, namely the cyclic voltammogramm obtained at a common sensitivity ($S = 2 \times 10^{-7}$ A/div.) was of an asymmetrical shape.

By increasing significantly the sensitivity ($S = 4 \times 10^{-8}$ A/div.) within the critical interval, two cathodic and one anodic peaks were clearly noticed, hence oxidation and reduction processes proceed, although of a low intensity (Fig. 4).

The influence of concentration on the intensity of the voltammetric currents was studied, referring to the anodic peaks clearly evidenced, and a linear *ip* vs. *C* dependence, with straight lines passing near the origin is obtained in every case. We can appreciate that the process of electrochemical oxidation on P.C.E. is irreversible and controlled by diffusion.

The same conclusion can be drawn by means of the *A*, [g], vs. *C*, [mol.l^{-1}], function (Fig. 5).

With Sp.C.E. and the same support – electrolyte and scanning rate, the anodic and cathodic peaks are characterized about by the same potentials.

The influence of concentration on the intensity of anodic and cathodic voltammetric currents is depicted in Figs. 6 *a* and *b*.

The cathodic current is controlled by diffusion at concentrations lower than 3×10^{-4} mol.l^{-1}, while the anodic current obeys the linear dependence of the *ip* vs. *C* function also at higher values (5×10^{-4} mol.l^{-1}).

By taking into account the anodic process on P.C.E. proceeding during the

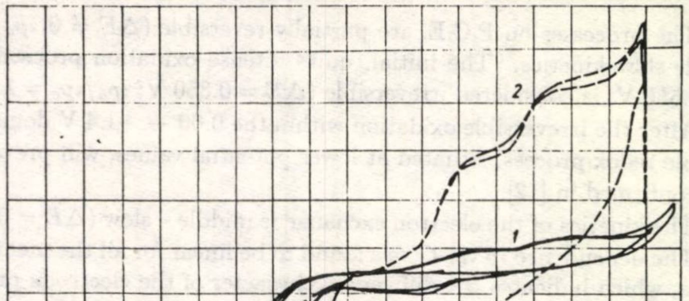

Fig. 4.– Cyclic voltammogram of *p*-toluidine ($C = 5 \times 10^{-4}$ mol.l^{-1}; P.C.E.; Na_2SO_4 10^{-1} M; $v = 50$ mV/s), —— $S = 2 \times 10^{-7}$ A/div., - - - $S = 4 \times 10^{-8}$ A/div.

first scanning cycle (0.00 V → +1.4 V), appreciated by us as representative for the compounds under study, and comparing the potential values of the principal anodic peaks, the conclusion can be drawn that the presence of the $-CH_3$ group does not affect the potential corresponding to the oxidation $-NH_2$ group, since the alkyl groups do not influence significantly the $p-\pi$ conjugation involving the unshared electrons on the nitrogen atom and the π electrons in benzene ring. This fact is due to the rather slight inductive effect of the substituent [6].

Instead, the HO^- group shifts this potential to lower positive values, hence the *p*AF will be oxidized easier. The substituents with unshared electrons (e.g., HO^-) influence the behaviour of the amino compound by means of electronic effects of the type:

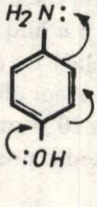

The *p*AF oxydation might proceed according to the following mechanism [13]:

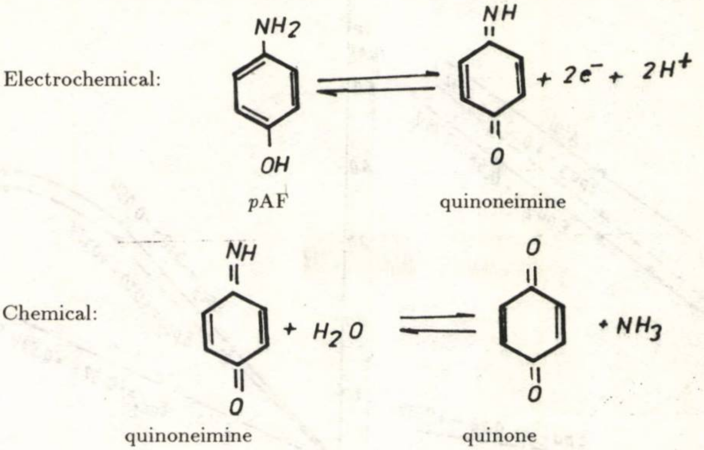
Electrochemical:
NH2
OH
pAF
NH
O
+ 2e⁻ + 2H⁺
quinoneimine
Chemical:
NH
O
quinoneimine
+ H2O
O
O
quinone
+ NH3

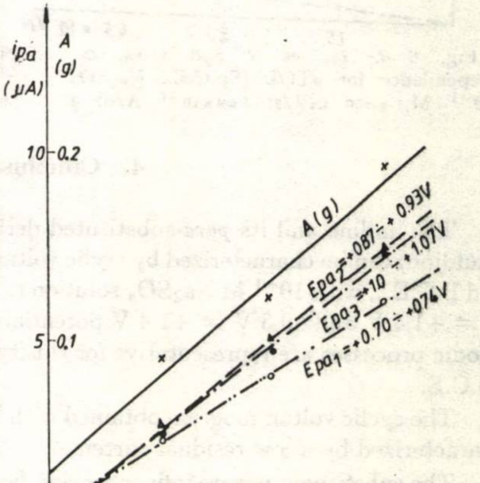

Fig. 5.– Influence of the *p*-Tol concentration on the anodic currents intensity (P.C.E.; Na_2SO_4 10^{-1} M; $v = 50$ mV/s; $S = 2 \times 10^{-7}$ A/div.)

As regards the oxidation, the following order might be considered by taking the potential values of the principal anodic into account:

$$pAF < A \leq pTOL.$$

From the selectivity point of view, the possibility of identifying precisely one of these substances in the presence of the others is quite reduced. Moreover, some peaks representing succesive stages of the oxidation or reduction processes overlap, covering a large voltammogram area.

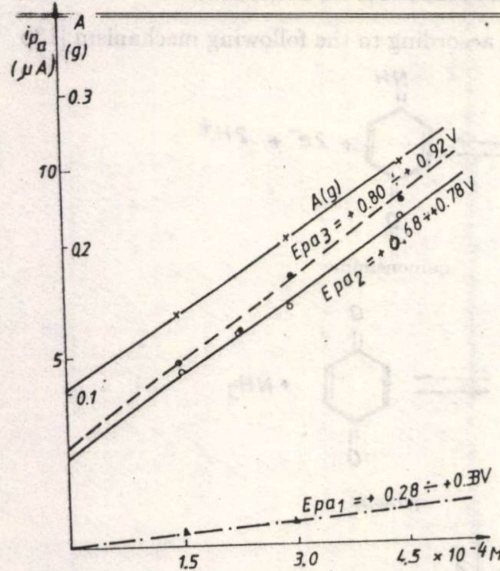

Fig. 6 a.– i_{p_a} vs. C and A vs. C dependence for pTOL (Sp.C.E.; Na_2SO_4 10^{-1} M; $v=50$ mV/s; $S=4\times10^{-7}$ A/div.).

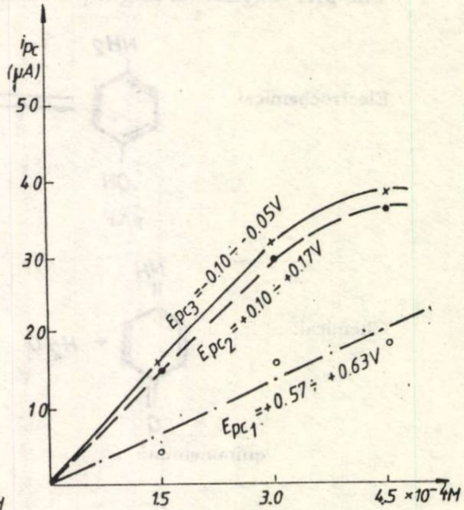

Fig. 6 b.– ip_c vs. C dependence for pTOL (Sp.C.E.; Na_2SO_4 10^{-1} M; $v = 50$ mV/s; $S = 4 \times 10^{-7}$ A/div.).

4. Conclusions

The aniline and its *para*-substituted derivatives (*para*-aminophenol and *para*-toluidine) can be characterized by cyclic voltammetry on carbon electrodes(Sp.C.E. and P.C.E.), with 10^{-1} M Na_2SO_4 solution as a support electrolyte, within the –0.7 V $\rightleftharpoons$ +1.4 V and –0.3 V $\rightleftharpoons$ +1.4 V potential domains, with respect to S.C.E. The anodic processes are representative for this type of substances on both P.C.E. and Sp.C.E.

The cyclic voltammogram obtained with P.C.E. are particularly expressive and characterized by a low residual current.

The substituent nature influences significantly the voltammographic behaviour of the compounds (due to the inductive effects exerted on the benzene ring), as well as the process reversibility of the electrod processes.

The nature of anodic voltammetric currents is prevalently diffusional, while the cathodic currents are controlled either by adsorption (aniline), or by adsorption and diffusion (pTol), or by diffusion only (pAF) within the concentration domain used.

Received, December 16, 1991

Polytechnic Institute, Jassy,
Department of
Analytical Chemistry

REFERENCES

1. Adams R.N., *Electrochemistry at Solid Electrodes.* Marcel Dekker, New York, 1969, 327 (*cf.* Bull. Soc. Chim. Fr., **5**, 791 (1987)).

2. Bacon J., Adams R.N., J. Amer. Chem. Soc., **90**, 6597 (1968).

3. Rozhkov I.N., Alyev I.Y., Tetrahedron, **31**, 977 (1975).

4. Eberson L., in *Organic Electrochemistry*. Ed. M. Baizer, Marcel Dekker, New York, 1973, 447-468 and 781-804.

5. Malik W.U. Goyal R.N., Rajeshwari W.A., Bull. Soc. Chim. Fr., **5**, 793 (1987).

6. Beral E., Zapan M., *Chimie organică*. Ed. Tehnică, Bucureşti, 1973, 117-118.

7. Duca Al., Bejan D., Revue roumaine de chimie, **36**, *4-7*, 439 (1991).

8. Kekedy L., *Senzori electrochimici metalici şi ion-selectivi*. Ed. Acad., Buc., 1987, 33.

9. Guadalupe A.R. Jhaweri S.S., Lin K.E., Abruña H.D., Anal. chem., **59**, *19*, 2436 (1987).

10. Muray R.G., *Electroanalytical Chemistry*. Vol. **13**, Marcel Dekker, Inc., New York and Basel, 1984, 192.

11. Neniţescu C.D., *Chimie organică*. Vol. **II**, Ed.Tehnică, Bucureşti, 1958, 356.

12. Blutis K.J., Wightman R.N., Anal. chem., **55**, *9*, 1576 (1983).

13. Testa A.C., Reinmuth W.H., Anal. chem., **32**, 1512 (1960).

VOLTAMETRIA CICLICĂ A ANILINEI ŞI A UNOR DERIVAŢI *para*-SUBSTITUIŢI: *para*-AMINOFENOL ŞI *para*-TOLUIDINĂ

(Rezumat)

Se prezintă comparativ comportarea electrichimică a anilinei, *para*-toluidinei şi *para*-aminofenolului, punând în evidenţă modificările caracteristicilor voltametrice determinate de substituenţii $-CH_3$ şi HO^-, prezenţi în molecula anilinei.

Studiul a fost efectuat prin voltametrie ciclică, utilizând electrodul pastă de cărbune (E.P.C.) şi electrodul cărbune spectral (E.C.Sp.) în soluţie Na_2SO_4 10^{-1} M, ca electrolit suport, în intervalul +1,4 V $\rightleftharpoons$ -0,3 V faţă de electrodul saturat de calomel (E.S.C.) (anilina şi *p*-toluidina) şi în intervalul +1,4 V $\rightleftharpoons$ -1,0 V (*p*-aminofenol).

Datele experimentale obţinute au permis aprecieri asupra naturii curenţilor voltametrici şi a proceselor de electrod.

Voltamogramele ciclice evidenţiază unele asemănări şi deosebiri în comportarea electrochimică a celor trei compuşi.

BULETINUL INSTITUTULUI POLITEHNIC DIN IAŞI
Tomul XXXIX (XLIII), Fasc. 1–4, 1993
Secţia II
CHIMIE ŞI INGINERIE CHIMICĂ

D.C. 669.825; 535.243

EXTRACTION-SPECTROPHOTOMETRIC DETERMINATION OF MOLYBDENUM (VI) IN CAST IRON AND ALLOY STEELS WITH *O*-XYLIDIDE OF 1-MERCAPTOPROPIONIC ACID

BY

AL. NACU, LAVINIA TOFAN and DOINA BÎLBĂ

1. Introduction

The spectrophotometric methods for molybdenum determination is subdued to many practical difficulties such as the interference of some cations, color intensity variation of the complex with respect to amount of reagent and standing time and the metal extraction dependence on rigid control of some analytical variables. The choice of the proper analysis method is depending on the interfered elements from the sample, the molybdenum content of these as the required precision in analysis.

Among the most used reagents for the spectrophotometric determination of molybdenum are to be mentioned: potasium thiocyanate [1], dithiol [2], [3], dialkyldithiocarbamates [4], mercaptoacids [5].

The anilides of thioglycolic acid, 1- and 2-mercaptoacids were synthetized by Nacu and coworkers [6] and they have been proved to be sensitive and selective reagents in analysis of molybdenum and of other elements such as: cobalt, palladium and rhodium [7],...,[9].

In the present paper, a simple and selective extractive spectrophotometric method is described, for the determination of micro amounts of molybdenum in cast iron and alloy steels with *o*-xylidide of 1-mercaptopropionic acid.

The reagent forms with Mo(VI) in acidic media an yellow complex which is extracted into varied organic solvents.

2. Experimental

To establish the proper conditions for the formation and extraction of the Mo(VI) complex with *o*-xylidide of 1-mercaptopropionic acid, the determination of the initial molar ratio molybdenum : reagent and of the ratio of phases water : organic solvent, the effect of medium acidity, character organic solvent extraction time, possible interferences have been studied.

A high excess of reagent is necessary for the full color of complex development. Thus, for samples of 48 μg Mo(VI) and 5 cm^3 0.25%, 0.5%, 0.75% and 1% (W/V), respectively, solutions of reagent, the best results were obtained with 1%

solution. This complexation reaction is made according to an initial molar ratio molybdenum: reagent of 1:480, in reaction medium.

Concerning the ratio between the volume of aqueous phase and the volume of organic phase, the optimum range for determination is 1:1...2:1.

The acidity effect on the extraction of molybdenum (VI) with *o*-xylidide of 1-mercaptopropionic acid has been studied, with various acids like HCl, H_2SO_4 and $HClO_4$, the proper concentration ranges being: 0.05...4.8 M HCl / 0.025...1.25 M H_2SO_4 / 0.025...2.5 M $HClO_4$. Of these, $HClO_4$ was found to be the most adequate for the extraction purpose, the values of complex absorbance increasing with the increase of acidity from 0.05 M to 2.5 M $HClO_4$.

The Mo(VI) complex can be extracted into various organic solvents such as benzene, ethyl ether, the mixture of isoamyl alcohol and benzene. The 1:1 mixture of isoamyl alcohol and benzene has been selected as solvent because of a higher extractibility as well as a higher stability of the complex.

A period of 10 min. of vigorously shake of phases was sufficient for the complete extraction of the complex. The yellow color of the metal complex was stable for 48 h, at room temperature.

The absorption spectra of *o*-xylidide of 1-mercaptopropionic acid and its Mo (VI) complex are shown in Fig. 1.

The absorption maxima of the reagent and its Mo(VI)-complex were found in different fields of wavelenghts (around 282 nm for reagent and around 305 nm for complex). The molar absorptivity of the complex is around 10^4 $\text{mol}^{-1}\text{cm}^{-1}$ ($c = 10^{-4}$ M, $l = 1$ cm, $\lambda = 305$ nm). Concerning the effect of foreign ions, was found that the following metal ions do not interfere: V(V), Ti(IV), Fe(II), Fe(III), Cr(III), Al(III), Co(II), Ni(II), Zn(II), Mn(II).

3. Method Application

3.1. Calibration Curve Construction

a) *Reagents.* A stock solution of Mo(VI) was prepared from $Na_2MoO_4.2H_2O$ and standardized gravimetrically (8-hydroxiquinoline method).

o-xylidide of 1-mercaptopropionic acid was prepared by the condensation of equimolar amounts of 1-mercaptopropionic acid and *o*-xylidine at 110°...120°C [7]. The product was recrystallized from diluted solution of ethanol and characterized in terms of melting point and absorption spectra. The reagent was used as 1% solution into 1:1 mixture of isoamyl alcohol and benzene.

b) *Procedure.* A portion of solution containing molybdenum was placed in a separatory funnel, the pH of the solution was adjusted and then the solution of reagent was added. After the solution have been vigorously shaken a determined time, the aqueous phase was separated from the organic one. After the separation, the absorbance of the organic phase was measured at 380 nm against a reagent blanck obtained in the same way.

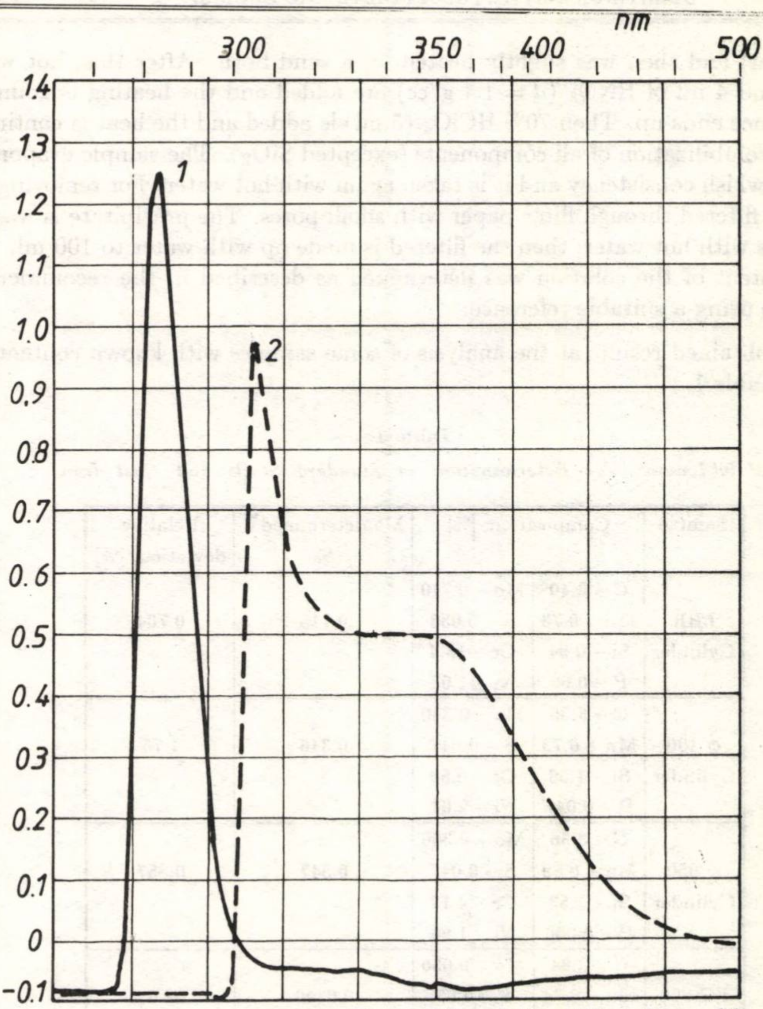

Fig. 1.– Absorption spectra (UV-VIS): *1* – *o*-xylidide of 1-mercaptopropionic acid; *2* – the complex of reagent with Mo(VI).

The Beer's law is kept concerning the concentration range 1...25 μg Mo/ml.

3.2. Mo(VI) Determination in Steels

The proposed method was satisfactorily verified to the determination of molybdenum in standard samples of steels and cast iron.

A sample of 0.5...1.0 g steel or cast iron was decomposed first with 1:9 H_2SO_4

(20...30 ml) and then was slightly heated on a sand both. After this, hot water (20 ml) and 4 ml of HNO_3 ($d = 1.4$ g/cc) are added and the heating is going on effervescence ends up. Then 70% $HClO_4$ (5 ml) is added and the heat is continued until the solubilization of all components (excepted SiO_2). The sample evaporates to the mawkish consistency and it is taken again with hot water. For removing the silice it is filtered through filter paper with small pores. The precipitate is washed 3...4 times with hot water; then the filtered is made up with water to 100 ml. The metal content of the solution was determined as described in the recommended procedure using a suitable reference.

The obtained results at the analysis of some samples with known content are given in Table 1.

Table 1

Molybdenum (VI) Determination in Standard Steels and Cast Iron

Sample	Composition, [%]		Mo determined*) %	Relative deviation, [%]
LBR Cylinder	C – 3.40	Mo – 0.710	0.715	0.704
	Mn – 0.73	S – 0.036		
	Si – 0.94	Cr – 16.4		
	P – 0.06	Ni – 1.07		
ϕ 100 Cylinder	C – 3.36	Mo – 0.340	0.346	1.76
	Mn – 0.73	S – 0.047		
	Si – 1.50	Cr – 0.50		
	P – 0.047	Ni – 2.01		
ϕ 950 Cylinder	C – 3.36	Mo – 0.350	0.347	0.857
	Mn – 0.59	S – 0.047		
	Si – 1.53	Cr – 4.77		
	P – 0.066	Ni – 1.96		
FC-200	C – 3.84	Mo – 0.030	0.0306	2.0
	Mn – 0.74	S – 0.05		
	Si – 1.96	Cr – 0.090		
	P – 0.068	Ni – 2.12		

*) Average of three determinations.

As finds, the proposed method is characterized by satisfactory selectivity and precision, is simple and accessible.

Among the organic reagents with polarized sulphur, the *o*-xylidide of 1-mercaptopropionic acid emphasizes as an important reagent which can be used for Mo(VI) determination in cast iron and alloy steels.

Received, June 17, 1991

Polytechnic Institute, Jassy,
Department of
Inorganic Chemistry

REFERENCES

1. Marčenko Z., *Fotometričeskoe opredelenye elementov.* Izd. Mir, Moskva, 1971.
2. Alimarin I.P., Savvin S.B., Dedkov Y.M., Zh. Anal. Khim., **19**, 328 (1964).
3. Clark L.J., Axiev J.H., Anal. Chem., **27**, 2000 (1955).
4. Haas W., Schwartz T., Microchim. Acta, *253* (1963).
5. Ill F.W., Joe J.H., Anal. Chem., **25**, 1363 (1953).
6. Nacu Al., Nacu D., Alexa M., An. şt. Univ. „Al.I.Cuza", Iaşi, **XVI**, 129 (1970).
7. Nacu Al., Nacu D., An. şt. Univ. „Al.I.Cuza", Iaşi, **XIII**, 29 (1967).
8. Nacu Al., Nacu D., Bîlbă D., An. şt. Univ. „Al.I.Cuza", Iaşi, **XVI**, 129-132 (1970).
9. Nacu Al., Bîlbă D., Revista de chimie, **40**, *4*, 350 (1989).

DETERMINAREA EXTRACTIV-SPECTROFOTOMETRICĂ A Mo(VI) DIN FONTE ŞI OŢELURI ALIATE CU *O*-XILIDIDA ACIDULUI 1-MERCAPTOPROPIONIC

(Rezumat)

Se prezintă o metodă extractiv-spectrofotometrică simplă şi selectivă pentru determinarea unor microcantităţi de molibden (VI) din fonte şi oţeluri aliate, cu ajutorul *o*-xilididei acidului 1-mercaptopropanic.

S-au stabilit condiţiile optime de formare şi extracţie a complexului Mo(VI) cu *o*-xilidida acidului 1-mercaptopropionic (raportul molar iniţial molibden : reactiv, raportul fazelor apă : solvent organic, aciditatea mediului, natura solventului organic, timpul de extracţie, interferenţe posibile).

Metoda propusă a fost verificată cu bune rezultate pentru determinarea molibdenului din probe etalon de fonte şi oţeluri aliate.

BULETINUL INSTITUTULUI POLITEHNIC DIN IAŞI
Tomul XXXIX (XLIII), Fasc. 1–4, 1993
Secţia II
CHIMIE ŞI INGINERIE CHIMICĂ

D.C. 661.718.1; 661.898

SPECTROPHOTOMETRIC STUDY ON CHEMICAL EQUILIBRIA IN $K_2[PdCl_4]$ – ARSENAZO (III) SYSTEM

BY

I. ROŞCA, N. FOCA, DANIEL SUTIMAN and D. CONDURACHE

1. Introduction

The disazo derivatives of the cromotropic acid, especially the arsenazo (III) namely the 2,7 (arsenazophenyl-azo)-1,8-dihidroxinaphtalene 3,6-disulfonic acid, are able to complex with a great number of metallic cations in acid, basic or neutral medium [1], [2].

In the present study the used reagent was a sodium salt wich is water soluble:

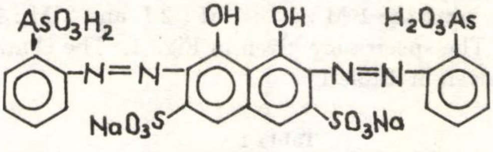

In contrast with the monoazoderivates, the bisazo derivates can coordinate the metallic ions by means of the both azo groups since they contain two –OH groups in the *ortho* position with respect to them.

Consequently, the molecule of the bisazo dye can adopt a plane structure which results in an intensification of the violet or blue colour. The punk colour of the dye acid solution is due to the deviation from the plane structure which is also caused by the presence of a bulky substituents, such as $-NO_2$, $-SO_3H$, also determine a colour intensification [3]. By the reaction between the arsenazo (III) and cations of the metals in the secondary groups complexes with characteristic absorbtion spectra are formed by means of which the metal–ligand (M – L) equilibria can be studied [4].

As shown in literature the M – L combination ratio can be only 1 M : 1 L for the bivalent metals and 1 M : 2 L for the trivalent ones [5],...,[7]. Other combination ratios are not possible. Under unfavourable conditions, at law pH values, the both complex are formed simultaneously.

The study of the $K_2[PdCl_4]$ – arsenazo (III) system by using the tetrachloropalladite in a D.M.F. 85% $-H_2O$ 15% solution and the ligand in aqueous solution reveals the complexity of the interaction between the Pd (II) ion and the arsenazo (III).

The obtained results by studying this system are presented in what follows.

2. Experimental

The arsenazo (III) ligand (L) – the disodic salt – is water soluble and was used as aqueous solutions of concentrations between $1 \times 10^{-3} ... 1 \times 10^{-5}$ mol.l^{-1}.

The Ka tetrachloropalladite was used as a solution in solvent mixture DMF 85% $-H_2O$ 15%, at pH=7.

The absorbtion spectra of the ligand and of the complexes in this system were recorded on a UV-Vis Specord apparatus and the quantitative determination mass by means of a Spekol 20 (Carl Zeiss, Jena) apparatus.

3. Results and Discussion

The Pd (II) ion in the $K_2[PdCl_4]$ complex quickly reacts with the arsenazo (III) (L) giving complexes with characteristic UV and visible absorption spectra.

For qualitative and quantitative study concerning the $K_2[PdCl_4]$ – arsenazo system the absorption spectra of the dye in aqueous solution as well as of the aqueous solution containing the 1 M : 1 L; 1 M : 2 L and 2 M : 1 L combination ratios were recorded. The spectra are given in Fig. 1. The characteristics of the spectra in Fig. 1 are given in Table 1.

Table 1

Nr.	Compound	λ nm	Solvent	ε_{max} l.mol^{-1}cm^{-1}
1	Arsenazo (III); L	400 540	H_2O	11 000 26 000
2	$K_2[PdCl_4]$ (M)	400	DMF	4 000
3	$K_2[PdCl_4]$+ L (1:1)	580 610	H_2O	17 000 16 000
4	$K_2[PdCl_4]$+ L (1:2)	560	H_2O	40 000
5	$K_2[PdCl_4]$+ L (2:1)	628	H_2O	22 500

The analysis of the absorption spectra, their maximum positions and the values of the molar absorption coefficient lead to the following conclusions: a) the ligand shows two absorption maximum in the visible domain; b) $K_2[PdCl_4]$ shows a sharp absorption maximum in the visible domain; c) the interaction between $K_2[PdCl_4]$ and ligand results in the modification of the absorbtion spectra for the 1 M: 1 L; 1 M : 2 L and 2 M : 1 L systems; d) the absorbtion spectrum of the 2 L : 1 M

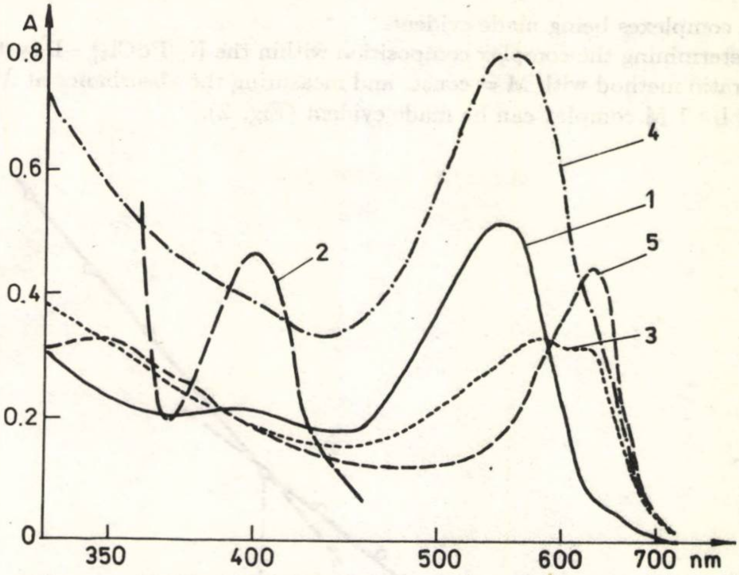

Fig. 1.– Visible absorbtion Spectra of the solution containing: the dye in aqueous solution; $K_2[PdCl_4]$ in DMF solution and the solutions containing the 1 M : 1 L; 1 M : 2 L; 2 M : 1 L combination ratios; layer thickness = 0.2 cm; standard sample – distilled watter.

system covers the absorbtion bands of the free ligand as well as those of the 1 M : 1 L one (Fig. 1, curve *3*).

The absorbtion spectrum of the 2 M : 1 L system is different from those of the free ligand and of the 1 M : 1 L and 2 M : 1 L systems (Fig. 1, curve *4*).

The absorption band characteristic of the 2 M : 1 L system is not to be found from the beginning of the process, but it appears in time, which indicates a certain system evolution [8].

4. Composition of Complexes in the $K_2[PdCl_4]$ – Arsenazo (III) System

The $K_2[PdCl_4]$ – arsenazo (III) system was studied by several methods: the mole ratio method (the Job method); the straight line method (the slope method) [9], [10]. Aqueous solutions have been used and the absorption bands with maxima at 580, 610, 628 nm take into account.

The complex composition in the $K_2[PdCl_4]$ – arsenazo (III) system was determined by the mole ratio method in two variants, namely with M = const. and L – variable and with L = const. and M – variable.

The obtained data demonstrate the complexity of the interactions within the Pd(II)–L system. This fact is revealed by the formation of all possible complexes for a bivalent cation, such as Pd(II), with this ligand, the 1 M : 1 L, 1 M : 2 L and

2 M : 1 L complexes being made evident.

By determining the complex composition within the $K_2[PdCl_4]$ – L system by the mole ratio method with M = const. and measuring the absorbance at $\lambda = 580$ nm, the 2 L : 1 M complex can be made evident (Fig. 2).

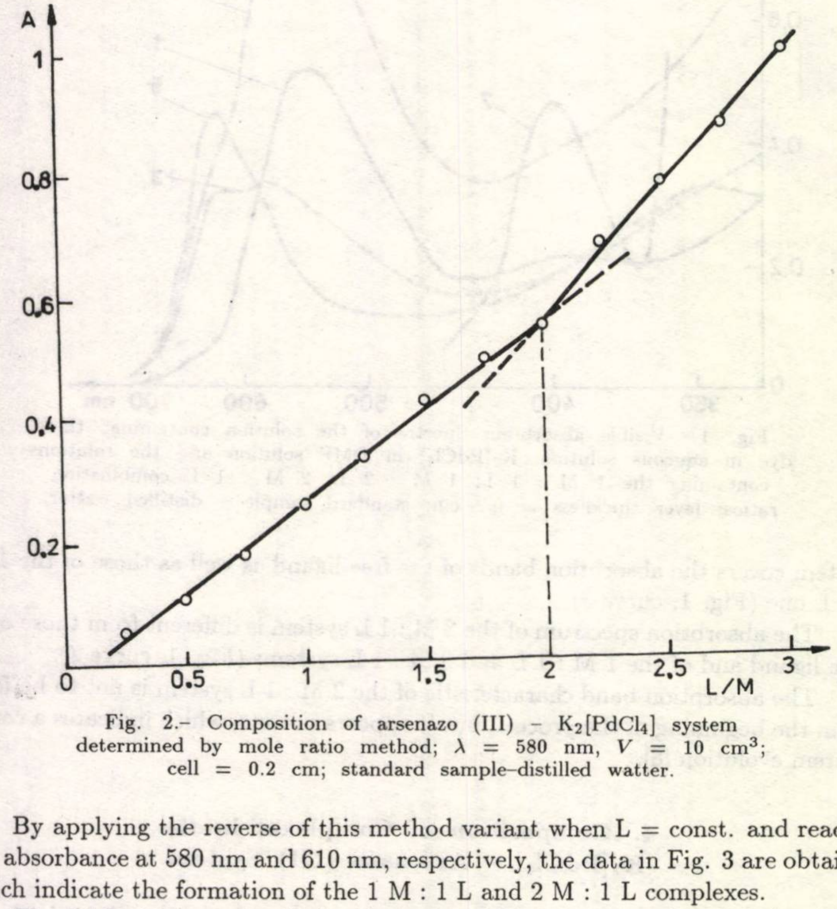

Fig. 2.– Composition of arsenazo (III) – $K_2[PdCl_4]$ system determined by mole ratio method; λ = 580 nm, V = 10 cm^3; cell = 0.2 cm; standard sample–distilled watter.

By applying the reverse of this method variant when L = const. and reading the absorbance at 580 nm and 610 nm, respectively, the data in Fig. 3 are obtained which indicate the formation of the 1 M : 1 L and 2 M : 1 L complexes.

The 2 M : 1 L complex is clearly made evident by measuring the absorbance at solutions with the wavelength of 628 nm where only the complex species absorbs (Fig.4).

By studying the composition of this system with the method of continuous variations at 610 and 628 nm, the formation of two complexes is noticed, namely 1 M : 1 L and 2 M : 1 L, as shown in Fig. 5 *a* and 5 *b* [11].

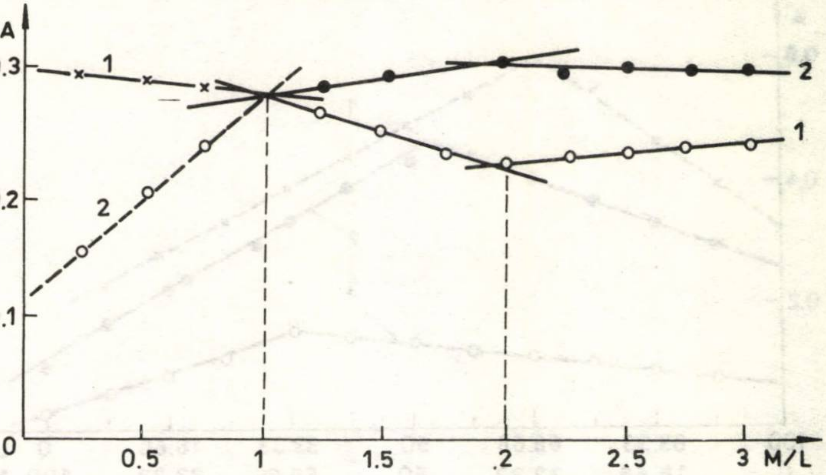

Fig. 3.- Obtained diagrams by studying the arsenazo (III) - $K_2[PdCl_4]$ by the titration of a ligand amount with a variable one of metal: $V_{final}=10$ cm^3, cell = 0.2 cm; *1* - the absorbance at λ = 580 nm; *2* - the absorbance at λ = 610 nm; standard sample-distilled watter.

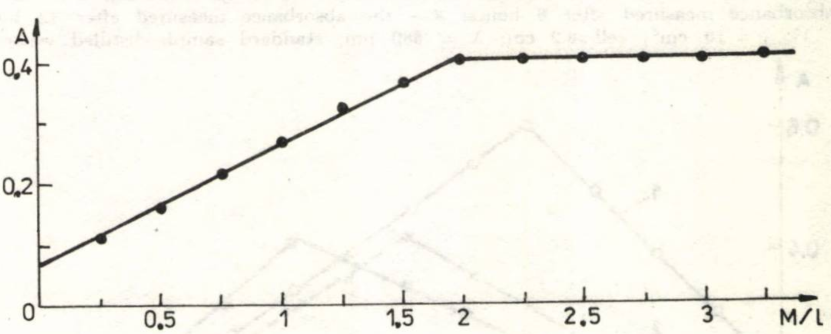

Fig. 4.- Composition of the $K_2[PdCl_4]$ - arsenazo (III) system determined by the mole ratio method: the absorbance of solutions was measured after 12 h at 628 nm; V = 10 cm^3; cell = 0.2 cm; standard sample-distilled watter.

5. Conductometric and pH-metric Study of the $K_2[PdCl_4]$ – Arsenazo (III) Systems

By analysing the spectrophotometric data concerning the metal–ligand combination ratio three complex combinations were found, namely: 1 M : 1 L; 2 L : 1 M and 2 M : 1 L.

As already shown, by the interaction between the Pd(II) ion and arsenazo (III) in strongly acid medium only two complexes are formed: 1 M : 1 L and 2 L : 1 M. This fact is significant for the important role played by the pH of the medium in the complexing process. Consequently, the final pH of the complexed samples was measured after 24 hours. This was necessary because the study was performed

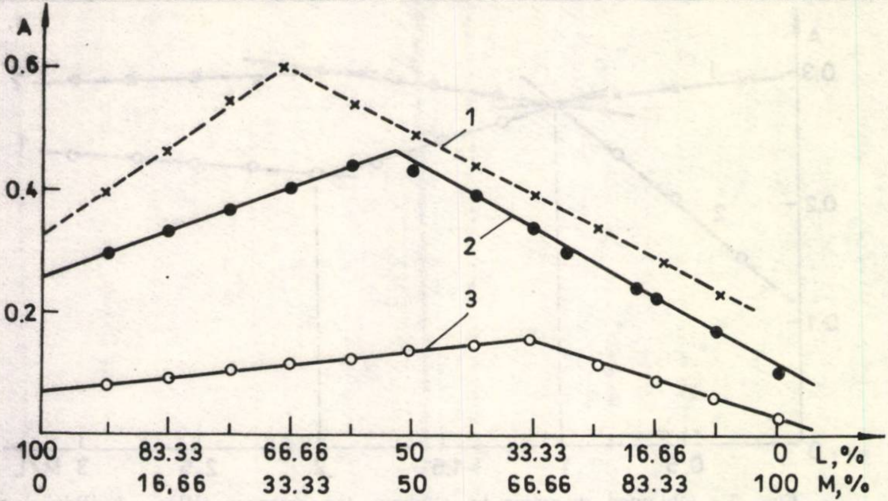

Fig. 5 *a*.– Data obtained by spectrophotometric study concerning the complex composition of the $K_2[PdCl_4]$ – arsenazo (III) system by the Job method: *1* – the absorbance measured in the moment of reagent mixing; *2* – the absorbance measured after 6 hours; *3* – the absorbance measured after 12 hours; $V_{\text{final}} = 10$ cm^3; cell=0.2 cm; λ = 580 nm; standard sample–distilled watter.

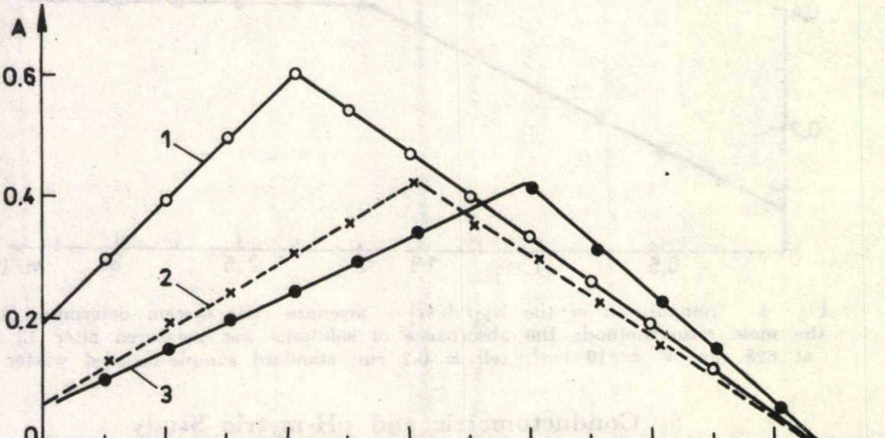

Fig. 5 *b*.– Data obtained by spectrophotometric study concerning the complex composition of the $K_2[PdCl_4]$ – arsenazo (III) system by the Job method: *1* – the absorbance measured in the moment of reagent mixing; *2* – the absorbance measured after 6 hours; *3* – the absorbance measured after 24 hours; $V_{\text{final}} = 15$ cm^3; cell=0.2 cm; λ = 628 nm; standard sample-distilled watter.

by using tetrachloropalladite in DMF–H_2O instead of $PdCl_2$ in a strongly acid medium $H_2[PdCl_4]$.

The following pH values were found: ligand $C = 1 \times 10^{-4}$ mole.l^{-1}, pH = 7.15, complexes: a) 1 M : 1 L, $C_L = C_M = 1 \times 10^{-4}$ moles.l^{-1}, pH = 7.15; b) 2 L : 1 M, $C_L = 2 \times 10^{-4}$ moles.l^{-1}, $C_M = 1 \times 10^{-4}$ moles.l^{-1}, pH = 7.60; c) 2 M : 1 L, $C_M = 2 \times 10^{-4}$ moles.l^{-1}, $C_L = 1 \times 10^{-4}$ moles.l^{-1}, pH = 8.00.

As can be seen the free ligand and the complex of the 1:1 ratio have the same pH as in the 2 L : 1 M and 2 M : 1 L systems; the pH slightly increases, the highest value being noticed in the last case.

It follows the conclusion that the pH is an important factor for the development of the reaction between the Pd(II) ion and the arsenazo (III), the alkali medium promoting the formation of the possible complexes.

The metal–ligand systems: 1 M : 1 L; 2 L : 1 M and 2 M : 1 L have also been studied by the conductometric method. The measurements were made from the solution mixing till the conductibility values remained constant as well as after 24 hours. The obtained data are depicted in Fig. 6.

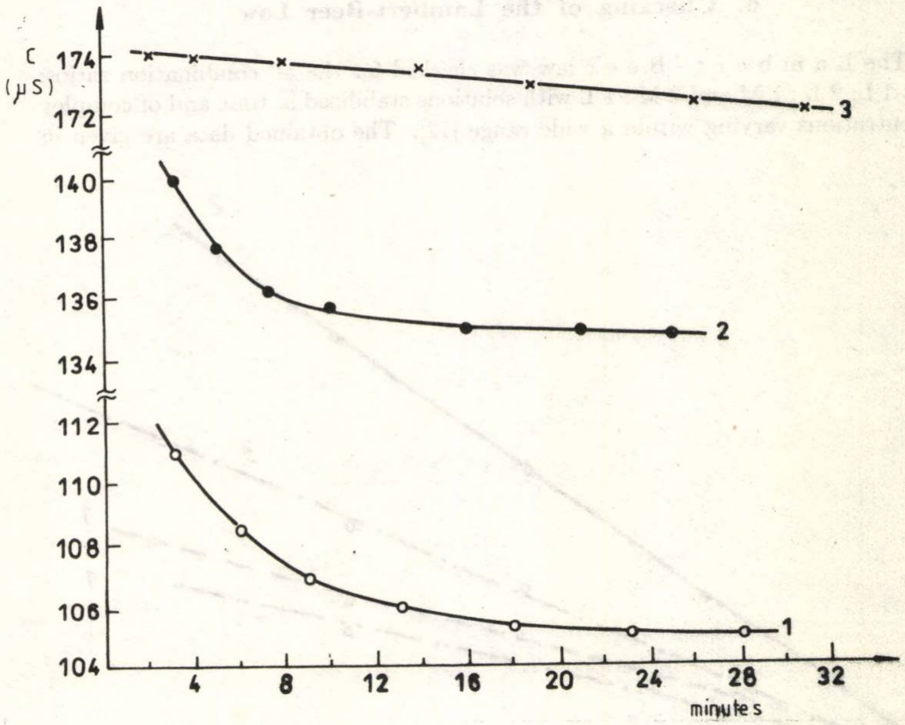

Fig. 6.– Data concerning the variation of the electrical conductibility of the metal–ligand in time: *1* – 1 M : 1 L; *2* – 2 L : 1 M; *3* – 2 M : 1 L; V_{final} = 10 cm^3.

A rapid decrease in the electrical conductibility till a certain value can be noticed. The stabilization time of the electrical conductibility is the longest for the 1 M : 1 L system and the shortest for the 2 M : 1 L.

At the same time the values of the electrical conductivities are noticed to increase in the metal–ligand systems in the following order: 1 M : 1 L; 2 L : 1 M; 2 M : 1 L.

After 24 hours the following values of the electrical conductivity were found for the systems under study:

1 M : 1 L – 106 μS; 2 L : 1 M – 141 μS; 2 M : 1 L – 190 μS.

Hence, the conductibilities increase only in the last two cases, the most important increasing being noticed with the 2 M : 1 L system.

The conductometric analysis of the above mentioned metal–ligand systems indicates a high reaction rate in all cases, but the chemical proceses for the 2 M : : 1 L ratio is evident to be different from the other two cases. This is also supported by the fact that the absorption band characteristic of the 2 M : 1 L system appears in time.

6. Checking of the Lambert-Beer Law

The Lambert-Beer law was checked for the all combination ratios: 1 M : 1 L; 2 L : 1 M and 2 M : 1 L with solutions stabilized in time and of complex concentrations varying within a wide range [12]. The obtained data are given in Fig. 7.

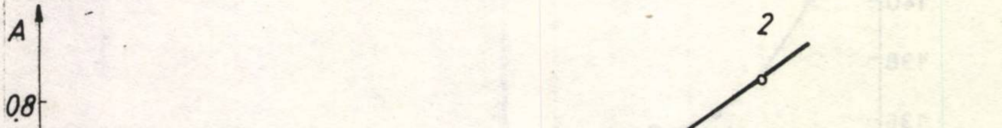

Fig. 7.– Checking of Lambert-Beer law concerning the $K_2[PdCl_4]$ – arsenazo (III) systems: *1* – the system 1 M : 1 L, λ = 610 nm; *2* – the system 2 L : 1 M, λ = 560 nm; *3* – the system 2 M : 1 L, λ = 628 nm; cell = 0.2 cm; standard sample–distilled watter.

The Lambert-Beer law is noticed to hold in all cases and the straight line of the 2 M : 1 L system is situated between those corresponding to the other two cases namely, 1 M : 1 L and 2 L : 1 M.

7. Conclusions

The study of the $K_2[PdCl_4]$ – arsenazo (III) system demonstrates that the metal–ligand interaction in this case have a complex character. By this reaction three combinations are formed with a variable M:L ratio which is determined by several factors such as: reaction medium, pH, etc.

The conclusion can be drawn that the spectrophotometric determination of the Pd(II) concentration by using arsenazo (III) depends on several factors and is not accurate enough.

Received, October 11, 1991

Polytechnic Institute, Jassy,
Department of
Inorganic Chemistry

REFERENCES

1. Popa G., Moldoveanu S., *Reactivi organici în chimia analitică*. Ed. Academiei, Bucureşti, 1976.
2. Bustamente P., Buriel M., Anal. Chem. Acta, **36**, 62 (1962).
3. Zolinger H., *Diazo and Azo Chemistry*. J. Willey, Interscience, NY, 1961.
4. Cornea F., Fulea C., Moldoveanu S., Rev. Roumaine Chim., **15**, 1415 (1970).
5. Luca C., Enea O., *Determinarea constantelor analitice*. EDP, Bucureşti, 1971.
6. Savin B.S., Kuzin L.E., Zh. Analyt. Khim., **26**, 423 (1971).
7. Popa G., Moldoveanu S., Rev. Roumaine Chim., **18**, 1883 (1973).
8. Răileanu M., *Influenţa mediului asupra reactivităţii chimice*. Ed. Scrisul Românesc, Craiova, 1981.
9. Yoe J., Jones A., Ind. Chem. Anal. Ed., **16**, 111 (1944).
10. Job P., Ann., **9**, 118 (1928).
11. Calu N., Duca Al., Nacu Al., *Chimie analitică şi analiză instrumentală*. Vol. **II**, Inst. polit., Iaşi, 1980.
12. Oniciu L., Constantinescu E., *Electrochimie şi Coroziune*. EDP, Bucureşti, 1982.

STUDIUL SPECTROFOTOMETRIC AL ECHILIBRELOR CHIMICE DIN SISTEMUL $K_2[PdCl_4]$-ARSENAZO (III)

(Rezumat)

Se studiază interacţiunea dintre tetracloropaladitul de potasiu şi colorantul 2,7-(arsenazofenilazo)-1,8-dihidroxinaftalin 3,6, utilizat ca sare de sodiu – (arsenazo(III)).

Studiul spectrofotometric al sistemului $K_2[PdCl_4]$ – arsenazo(III) demonstrează complexitatea reacţiei dintre ionul Pd(II) şi ligandul menţionat.

S-au determinat rapoartele de combinare M:L găsindu-se că în urma reacţiei se formează următoarele specii complexe: 1L:1M; 2L:2M; 2M:2L.

Sistemele metal–ligand au fost investigate şi prin alte metode, respectiv, conductometrică şi pH-metrică.

BULETINUL INSTITUTULUI POLITEHNIC DIN IAŞI
Tomul XXXIX (XLIII), Fasc. 1–4, 1993
Secţia II
CHIMIE ŞI INGINERIE CHIMICĂ

D.C. 532; 547.412.1; 547.214

STUDY OF THE INTRINSIC PROPERTIES OF VISCOUS FLOW IN THE 1,3-BUTANDIOL–METHANOL SYSTEM

BY

GH. IONESCU, DOINA HRIŢCU and D. ROŞCA

1. Introduction

1,3-Butandiol (BD)–methanol (MeOH) solutions belong to the diols–methanol systems, known as important agents in the synthesis of polyesteric fibers. The parameters of viscous flow represent essential characteristics involved in the establishment of flow regimes, stirring, distillation, etc.

The present paper is devoted to the determination of certain solutions, concentrated in 1,3-butandiol (the molar fraction ranging between 0.6...0.9), within a 20°...50°C temperature domain.

Processing of the experimental data involved checking of the Guzmán–Andrade and Walther–Ubbelohde equations applicability, referring to the dependence of viscosity on temperature. Also, the applicability of the Eyring equation was tested, as to satisfying the "theory of absolute reaction rates", during viscous flow. Further on, the physical values caracteristic for the process, that is, E_{vis}, $\Delta H^{\neq}_{m}$, $\Delta S^{\neq}_{m}$ and $\Delta G^{\neq}_{m}$, have been calculated.

2. Reactives and Equipments

1,3-Butandiol of p.a. purity is produced by the Swiss "FLUKA AG" company. Methanol has been purified in laboratory conditions, through rectification and dehydration; at 20°C, its characteristic parameters are: density – 0.79136 g/mL, refractive index – 1.32669 and refraction interval – 0.04 degrees, as corrected at 760 Torr. According to literature data [1], the density value is of 0.7914 g/mL and the refractive index – 1.32667.

Viscosity has been determined with a suspended-level Ubbelohde apparatus, assuring flow times of minimum 200 sec. The applied method for measurement being relative, 1,3-butandiol was used as reference liquid.

Density was measured with pycnometer equipped with an internal thermometer.

Temperature variation, both for the determination of viscosity and density, was lower than 0.01 degrees.

Solutions have prepared by weighing. All weighing operations, involved by experiments, had a precision of 0.0001 g.

3. Experimental Data

Utilization of 1,3-butandiol as reference liquid required the establishment of both density and viscosity dependence on temperature, as no complete literature data do exist. According to our determinations, the $\rho = \rho(T)$ and $\eta = \eta(T)$ functions are described by the following equations [2]:

$$\rho_{BD} = 1.0190 - 5.8461 \times 10^{-4} t, [\mathrm{g/mL}], \ (t, \ [^{\circ}\mathrm{C}]), \tag{1}$$

$$\ln \eta_{BD} = -14.936 + \frac{5.878 \times 10^{3}}{T}, \ (\eta, \ [\mathrm{cP}]). \tag{2}$$

Experimental data regarding solutions viscosity, at various temperatures and concentrations, are presented in Table 1.

Table 1

Viscosity of BD–MeOH Solutions

x_{BD}	t, [°C]				
	20	25	30	37	45
(*a*) 1	162.509	115.472	83.734	54.096	33.545
(*b*) 0.8943	100.727	74.330	55.372	36.772	23.599
(*c*) 0.7514	52.449	39.935	30.361	21.436	11.414
(*d*) 0.6354	29.036	22.569	17.925	12.981	9.1665

Densities of the solutions listed in the table, employed in the calculation of viscosity, with the equation:

$$\eta = \frac{\eta_{BD} \tau \rho}{\tau_{BD} \rho_{BD}}, \tag{3}$$

are expressed as functions of temperature, i.e.:

$$\begin{aligned} \rho_b &= 1.0130 - 7.1231 \times 10^{-4} t, \ [\mathrm{g/mL}], \ (t, \ [^{\circ}\mathrm{C}]), \\ \rho_c &= 0.9981 - 7.1990 \times 10^{-4} t, \ [\mathrm{g/mL}], \ (t, \ [^{\circ}\mathrm{C}]), \\ \rho_d &= 0.9757 - 6.5970 \times 10^{-4} t, \ [\mathrm{g/mL}], \ (t, \ [^{\circ}\mathrm{C}]), \end{aligned} \tag{4}$$

(η, τ, ρ values refer to solutions, the same values for 1,3-butandiol being noted with the BD index).

4. Results Interpretation

For correlating the solutions' viscosity with temperature, two equations (of high applicability for compounds that do not dissociate electrolitically) were employed, namely [3], [4]:

$$\ln\eta = \ln B + E_{\text{vis}}/RT, \quad \text{(Guzmán – Andrade)} \tag{5}$$

$$\lg\lg(\nu + 0.6) = m\ln T + n, \quad \text{(Walther – Ubbelohde)}, \tag{6}$$

where: B – viscosity for $T \to 0$; E_{vis} – activation energy of viscous flow for 1 Mole; ν – kinematic viscosity; m and n – experimental constants.

Applicability of Eqs. (5) and (6) to the BD–MeOH solutions involve certain checking operations, starting from experimental data. Consequently, the data listed in Table 1 have been processed as $\ln\eta$ vs. $10^3/T$ and respectively, $\lg\lg(\eta + 0.6)$ vs. $\ln T$ dependences which have a linear character. The processed data are listed in Table 2.

Table 2

Values of $\ln\eta vs.10^3/T$ *and* $\lg\lg(\nu + 0.6) vs. \lg T$

T, [K]		293	298	303	310	318
$10^3/T$, [K^{-1}]		3.4112	3.3540	3.2987	3.2242	3.14320
$\ln\eta$	(a)	5.0910	4.7490	4.4280	3.9910	3.51300
	(b)	4.6100	4.3090	4.0140	3.6050	3.16100
	(c)	3.9600	3.6870	3.4130	3.0650	2.66800
	(d)	3.3690	3.1170	2.8500	2.5630	2.21600
$\lg T$		2.4671	2.4744	2.4817	2.4916	2.50260
$\lg\lg(\nu + 0.6)$	(a)	0.3478	0.3152	0.2832	0.2392	0.19010
	(b)	0.3028	0.2733	0.2427	0.1981	0.14410
	(c)	0.2387	0.2085	0.1773	0.1316	0.07640
	(d)	0.1724	0.1413	0.1091	0.0621	0.00535

Figs. 1 and 2 support, with considerable precision, the linear character of the experimental obtained Eqs. (5) and (6), for all the three solutions studied, at least within the temperature range 20°...45°C.

The coefficients of the straight lines, established by the method of the smallest squares, are given in Table 3.

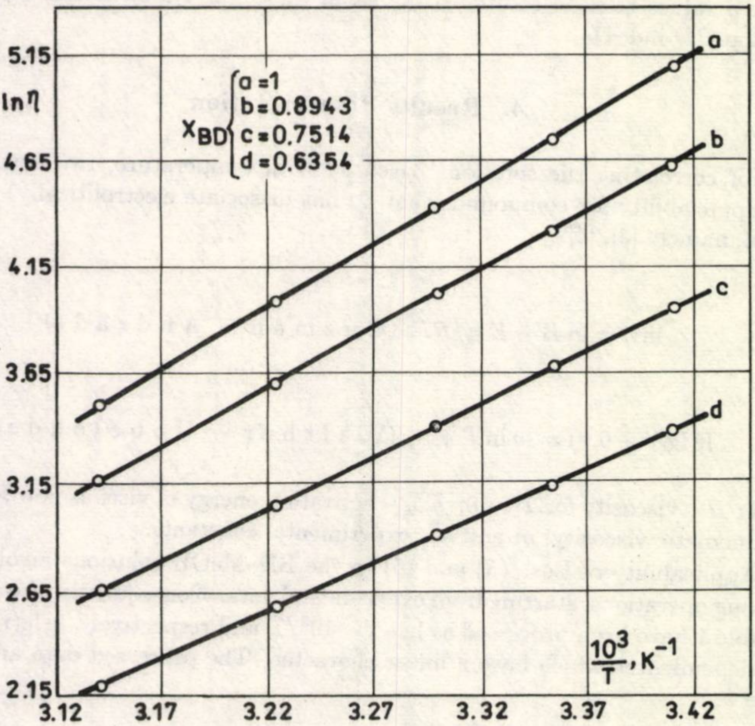

Fig. 1.– The Guzmán – Andrade function.

5. Calculation of Viscous Flow Parameters According to Eyring

The process of viscous flow is interpreted as the molecules' moving from an equilibrium position to another, over a barrier of potential energy separating successive equilibrium states. To such a phenomenon, Eyring has applied the "theory of absolute reaction rates" and established, for further practical application, the following theoretical equation [5], [6]:

$$\eta = \frac{hN}{V_m} \exp \frac{\Delta G^{\neq}_m}{RT}; \; V_m = \frac{M}{\rho}, \tag{7}$$

where: $\Delta G^{\neq}_M$ – Gibbs' free activation energy of flow, for 1 Mole; N – Avogadro's number; V_m – molar volume; h – Planck's constant; M – molar mass; ρ – density.

The generally known thermodynamic equation:

$$\Delta G^{\neq}_m = \Delta H^{\neq}_m - T\Delta S^{\neq}_m, \tag{8}$$

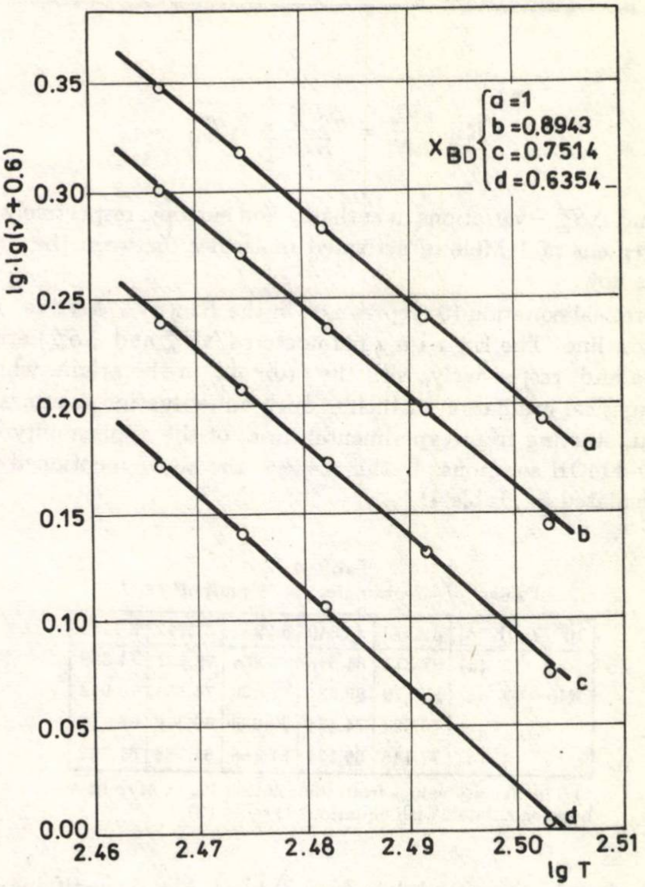

Fig. 2.- The Walther – Ubbelohde function.

Table 3

Numerical Values of the Coefficients of Equations (5) and (6)

Solution	Coefficients			
	$10^6.B$, [cP]	E_{vis}, [KJ/Mole]	m	n
(*a*)	0.3174	48.87	–4.4332	11.2839
(*b*)	0.9456	45.06	–4.4679	11.3282
(*c*)	3.8525	40.04	–4.5686	11.5126
(*d*)	12.5620	35.71	–4.7019	11.7751

associated with equation (7) and with its logarithm, as well, leads to a new equation, namely,

$$R \ln \frac{\eta V_m}{hN} = \frac{\Delta H_m^{\neq}}{RT} - \Delta S_m^{\neq}, \tag{9}$$

with: $\Delta H_m^{\neq}$ and $\Delta S_m^{\neq}$ – variations in enthalpy and entropy, respectively, associated with the movement of 1 Mole of activated molecules, between the liquid layers, during viscous flow.

The theoretical equation (9) represents, in the $R\ln(\eta V_m/hN)$ vs. $1/T$ coordinates, a straight line. The Eyring parameters ($\Delta H_m^{\neq}$ and $\Delta S_m^{\neq}$) are correlated with the slope and, respectively, with the ordinate, in the origin, which leads to a possible numerical evaluation of theirs. Such an evaluation assumes a previous demonstration, starting from experimental data, of the applicability of equation (9) to the BD–MeOH solutions. In this respect, the above mentioned coordinates have been calculated (s. Table 4).

Table 4

*Values of Coordinates in Equation (9)**)

$10^3/T$, [K^{-1}]		3.4112	3.3540	3.2987	3.2242	3.1432
$R\ln\frac{\eta V_m}{hN}$	(*a*)	87.314	84.543	81.864	78.527	74.338
	(*b*)	82.879	80.331	77.870	74.554	70.953
	(*c*)	76.694	74.434	72.250	69.310	66.116
	(*d*)	71.148	69.134	67.188	64.568	61.722

*) The density values from the relation $V_m = M/\rho$ have been calculated with equations (1) and (2).

On employing the numerical data from Table 4, Fig. 3, justifying the applicability of equation (9) to BD-MeOH solutions, has been drawn.

The Eyring parameters, calculated by the method of minimum squares, are listed in Table 5.

Table 5

Variation of $\Delta H_m^{\neq}$ and $\Delta S_m^{\neq}$ Parameters with Concentration

x_{BD}	$\Delta H_m^{\neq}$, [KJ/Mole]	$\Delta S_m^{\neq}$, [KJ/Mole]
1	48.418	77.851
0.8943	44.500	68.923
0.7514	39.469	57.944
0.6354	35.173	48.836

With equation (8), $\Delta G_m^{\neq}$ has been calculated, as a function of temperature and solution concentration (s. Table 6).

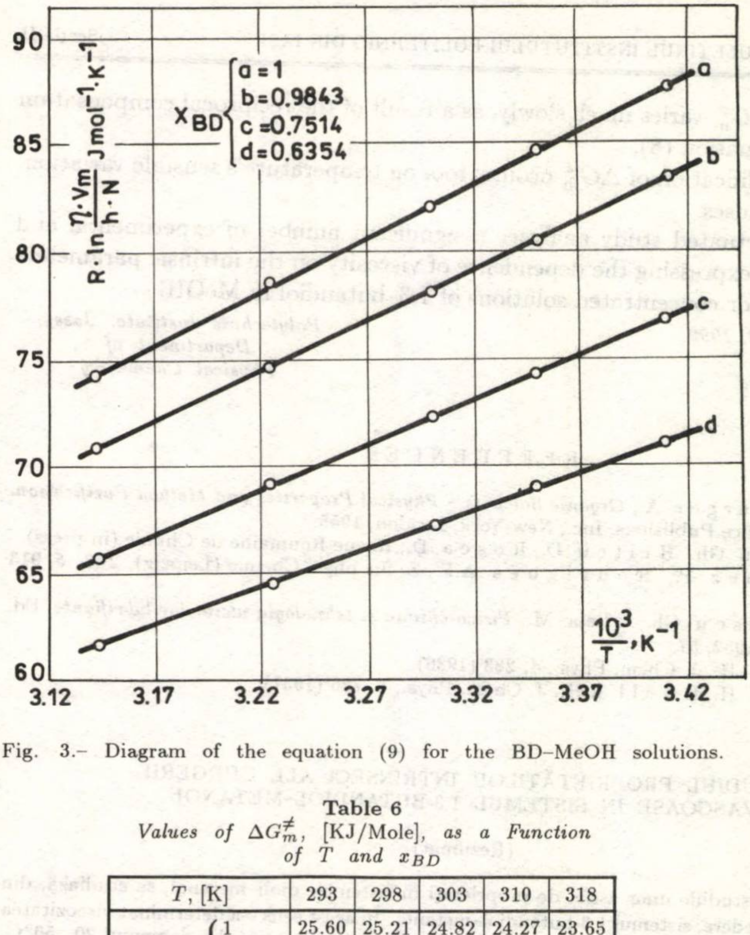

Fig. 3.– Diagram of the equation (9) for the BD–MeOH solutions.

Table 6

Values of $\Delta G_m^{\neq}$, [KJ/Mole], *as a Function of* T *and* x_{BD}

T, [K]	293	298	303	310	318
$x_{BD} =$ 1	25.60	25.21	24.82	24.27	23.65
0.8943	24.30	23.95	23.61	23.12	22.57
0.7514	22.48	22.19	21.90	21.50	21.03
0.6354	20.86	20.61	20.37	20.03	19.64

6. Conclusions

1. As a result of hydrogen bond formation, the solutions' viscosity increases with increasing the concentration of 1,3-butandiol (i.e., with increasing the concentration of the OH-groups).

2. Within the temperature domain selected, viscosity of the pure diol, as well as that of the BD–MeOH solutions, satisfies the Guzmán–Andrade and Walther–Ubbelohde equations.

3. Although $\Delta H_m^{\neq}$ and $\Delta S_m^{\neq}$ are sensibly modified with variation of diol's

concentration, $\Delta G^{\neq}_{m}$ varies much slowly, as a result of the reciprocal compensation of terms from equation (8).

4. Slow modification of $\Delta G^{\neq}_{m}$ ocours, too, on temperature's sensible variation, due to similar causes.

5. The effectuated study analyzes a significant number of experimental and calculated data, expressing the dependence of viscosity on the intrinsic parameters of viscous flow, for concentrated solutions of 1,3–butandiol in MeOH.

Received, March 20, 1992

Polytechnic Institute, Jassy,
Department of
Physical Chemestry

REFERENCES

1. Weissberger A., *Organic Solvents – Physical Properties and Method Purification.* Vol. **VII**, Interscience Publishers, Inc., New-York, London, 1955.

2. Ionescu Gh. Hriţcu D., Roşca D., Revue Roumaine de Chimie (in press).

3. Martineż P., Rodrigues A.F., Z. für phys. Chemie (Leipzig), **268**, *5*, 913 (1987).

4. Rădulescu Gh., Ilea M., *Fizico-chimia şi tehnologia uleiurilor lubrifiante.* Ed. Tehn., Bucureşti, 1982, 57.

5. Eyring H., J. Chem. Phys., **4**, 283 (1936).

6. Eyring H., Ewell R.H., J. Chem. Phys., **5**, 726 (1937).

STUDIUL PROPRIETĂŢILOR INTRINSECI ALE CURGERII VÂSCOASE ÎN SISTEMUL 1,3-BUTANDIOL–METANOL

(Rezumat)

Continuând studiile unor astfel de proprietăţi în sistemele dioli–metanol, se studiază, din acelaşi punct de vedere, sistemul 1,3-butandiol–metanol. În acest sens s-a determinat viscozitatea pentru mai multe concentraţii ale diolului şi pentru câteva temperaturi din domeniul 20...50°C. S-a verificat aplicabilitatea a două ecuaţii, Guzmán – Andrade şi Walther – Ubbelohde, privind variaţia viscozităţii cu temperatura, pentru lichide care nu disociază electrolitic. Utilizând ecuaţia Eyring, care asimilează teoria curgerii vâscoase cu teoria vitezelor absolute de reacţie, s-au determinat parametrii caracteristici ai curgerii vâscoase, E_{vis}, $\Delta H^{\neq}_{m}$, $\Delta S^{\neq}_{m}$ şi $\Delta G^{\neq}_{m}$.

BULETINUL INSTITUTULUI POLITEHNIC DIN IAŞI
Tomul XXXIX (XLIII), Fasc. 1–4, 1993
Secţia II
CHIMIE ŞI INGINERIE CHIMICĂ

D.C. 665.521.5

STUDY OF THE PHYSICO-CHEMICAL AND STRUCTURAL MODIFICATIONS OF MINERAL OILS DURING THEIR UTILIZATION

BY

LUCIA ODOCHIAN, CORNELIA VASILE,
INGEBORG TENCHEA and M. GRĂMĂTICU

1. Introduction

Mineral oils employed in the thermal treatment of alloy steels are paraffinic ones, refined and compounded with various stabilizers, antioxidants, cooling accelerators, etc. [1],...,[3].

During their utilization in various metallurgic processes (thermal treatments of hardening, rolling mills, pipes) mineral oils are subjected both to the action of high temperatures (about 800°C) and to atmospheric oxygen, these agents inducing their physico-chemical and structural deterioration and at the same time, consumption of the stabilizing agents. Also they may result as oils impregnated in various metallic oxides, their recovery, as well as oil cinder's recovery to good account representing a difficult problem.

For the controlled hardening of various metallic pieces, the establishment of the worn out degree of oils, at various durations of utilization, is essential, as the work efficiency of a used oil is lower, while regeneration is only possible for a certain degree of deterioration.

The aim of the present work is, on one hand, to evidence the physico-chemical and structural modifications of mineral oils involved in various metallurgic processes and, on the other hand, to establish some rapid methods for the estimation of their lifetime.

2. Experimental

Two types of hardening oils, TT 11 B and TT 100 A, supplied from Automobils Enterprise of Piteşti, have been employed in different thermal treatments varying between 50 and 200 hours, and also six oils recovered for the oily cinder resulted from the lamination of pipes through a process of destructive distillation at various temperatures.

The studies have been performed comparatively with used oils that, at an industrial level, are sent towards regeneration installations.

For the characterization of oils the following methods have been employed:

thermogravimetry (TG), differential thermal analysis (DTA), IR and H^1-RMN spectroscopy, their results having been correlated with viscosity determinations inflammability points (STAS 5989-66), Conradson coke (STAS 28-69), elemental analysis and fractional distillation.

Derivatogrammes (simultaneous recording of DTA, DTG, TG and T curves) have been recorded by means of a MOM-Budapest Paulik-Paulik-Erdey type derivatograph, under the following conditions: heating rate - 12°C/min., weight of the sample - 20 mg; reference material - Al_2O_3 freshly calcined at 1200°C, the sample having to be energically stirred prior to sample prelevation for subsequent analysis.

IR spectra have been recorded on a Perkin-Elmer 577 spectrometer by spreading a thin oil film on a KBr tablet.

H^1-RMN spectra have been recorded with a JEOL spectrometer at a frequency of 60 MHz on CCl_4 solutions.

3. Results and Discussion

In recent years, the thermal methods of analysis have been intensely employed for the characterization of various types of oils [4],...,[7] as: temperatures characteristic for processes of volatilization–decomposition, the weight loss at various temperatures, the temperatures involved in the process, a.s.o.

The employment of these methods for the cases under study in the present paper are clearly evidenced from the derivatogrammes presented in Figs. 1 and 2 for hardening oils and respectively for the oils obtained from destructive distillation at various temperatures.

In the case of hardening oils, mention must be made of the fact that the aspect of TG, DTG and DTA curves is modified after utilization, volatilization occurring at higher temperatures, on increasing, at the same time, the weight losses corresponding to the second peak of the DTG curve due to the decreasing of the weight losses corresponding of the first peak and also to the surfaces of the exothermal peaks of the DTA curves. These modifications are proportional to the duration of utilization, becoming sensible after 50 hours and increasing further on.

This situation made possible drawing of some calibration curves in coordinates: weight losses corresponding to the first (*I*) and second (*II*) process (Fig. 3) or the ratio of the DTA peaks'surfaces (Fig. 4) as a function of the duration of utilization. These curves may be employed both for the determination of the used degree of oils and for the estimation of their service time considering that, when they have to be regenerated, they should reach the values indicated in Fig. 1, refering to the weight losses and also the values from Fig. 4, i.e. the surfaces'ratio.

The slopes of the straight lines drawn in the two figures lead to the conclusion that the TT 11 B oil is degrading much more rapidly than the TT 100 A one.

In the case of oils resulted from the destructive distillation of the oily cinder resulted from tubes lamination (Fig. 2), one may observe that the oil obtained at increased temperatures is characterized by a high deterioration degree; it volatilizes

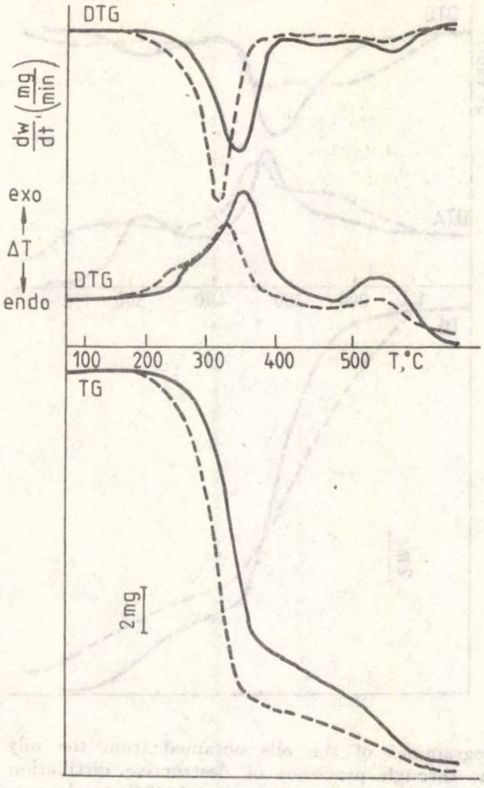

Fig. 1.– Derivatogrammes of hardening oils TT 100 A before utilization (- - -) and of the used oil (——), as well.

at low temperatures, within a large temperature range, resulting consequently an oil having a temperature similar to that of the used one and thus having characteristics that may recommend it for regeneration installations.

Modification of the thermal characteristics of oils results directly in the reduction of their efficiency as cooling agents and also in the possibility of their recovery, for subsequent re-introduction in the process; that is why, the mentioned thermal analyses represent significant and rapid indices for the characterization of such processes.

Changing of the thermal behaviour is explained, of course, through the deterioration of the oils'structure, evidenced in spectral studies. IR spectra show predominantly bands characteristic to paraffins, having long chains, according to their composition [1],...,[3].

The differences appearing between samples with various durations of utilization are recorded in the 1 500 ... 1 800 cm^{-1} region, more exactly as follows: the band from 1 600 cm^{-1}, attributed to aromatic hydrocarbons, becomes more

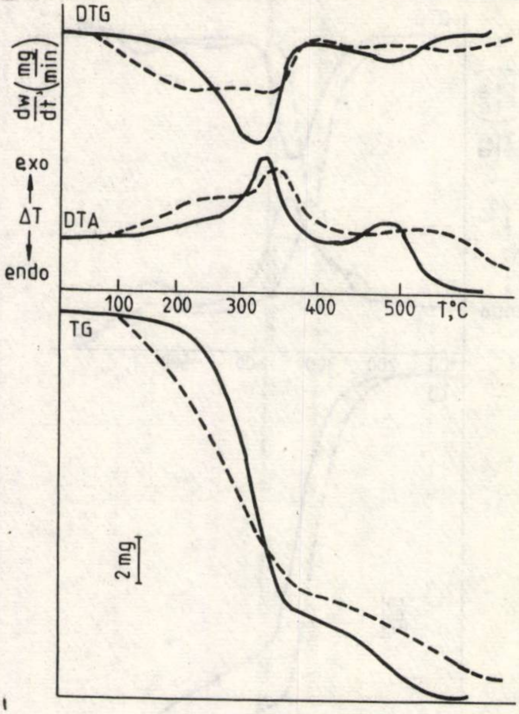

Fig. 2.– Derivatogrammes of the oils obtained from the oily cinder resulted from lamination, through processes of destructive distillation at $T < 400°C$ (in atmospheric air) (- - -) and at $T > 500°C$ (under vacuum) (——).

pronounced, while that from 1 745 cm^{-1}, attributed to the $>C=O$ and –C–O–C– groups acids, ketones, esters, is diminishing (Fig. 5).

By correlating the increase of the initial volatilization–decomposition temperatures with the duration of utilization, an observation should be that, initially compounds with low molecular weight [8] (acids, esters, a.s.o.) are eliminated and aromatic hydrocarbons formed during utilization, through reactions of dehydrocyclization.

On high utilization durations and high temperatures, high molecular weight compounds do appear through polymerization, further on decomposition at high temperatures; this explains the increase of the weight loss corresponding to the two and three decomposition stages.

This observation is supported by the IR (Fig. 5) and H^1-RMN (Fig. 6) spectra given comparatively with those of the global product of the fraction, having boiling point below 160°C, resulted from the distillation of the oil recovered from the oil cinder.

The two specific bands from the IR spectra being sensible to structural modifications, may be employed for drawing of some calibration curves for the estimation

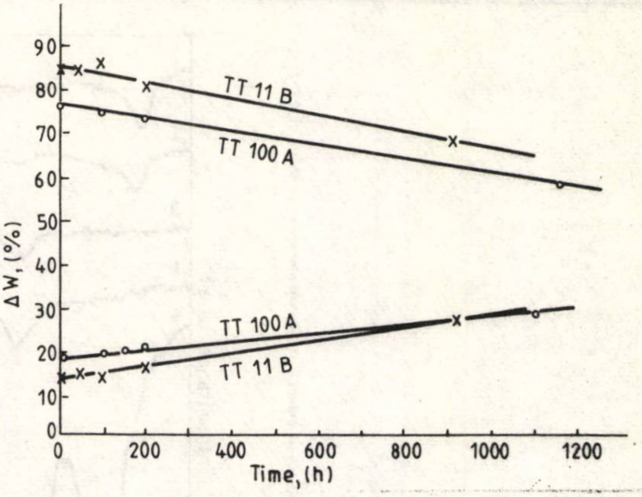

Fig. 3.- Weight losses in the first and second stage of volatilization-decomposition, as depending on the utilization duration of TT 100 A and TT 11 B oils.

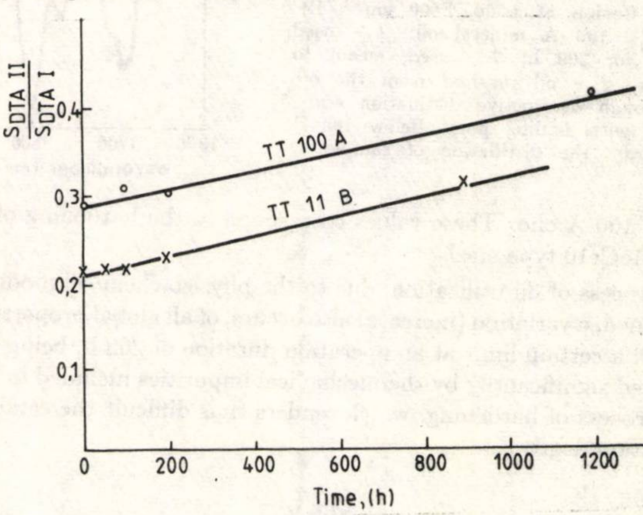

Fig. 4.- Ratio of the peaks'surfaces from the DTA S_{II}/S_I curve, as a function of the utilization duration for TT 100 A and TT 11 B employed in thermal treatments.

of the oil's quality. With a view to diminishing the influence of the oil film's thickness, the absorbance of these bands has been reported to a standard band (from 2 905 cm^{-1}), the ratio obtained being plotted graphically as a function of the oil's duration of utilization (Fig. 7).

Extrapolation of the data presented in Figs. 3, 4 and 7 leads to the maximum utilization durations of the studied oils, i.e. 920 h for the TT 11 B oil and 1 180

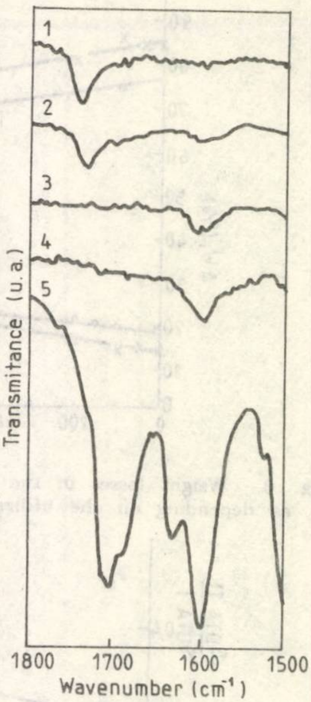

Fig. 5.– Region of 1 500...1 800 cm^{-1} IR spectra: TT 100 A mineral oil: *1* – used; *2* – used for 200 h; *3* – used, meant to regeneration; *4* – oil resulted from the oily cinder, through destructive distillation and *5* – fraction with boiling point below 160°C, resulted from the distillation of sample 4.

h for the TT 100 A one. These values correspond to the hardening of 33MoCr10 type and 20MoCr10 type steels.

In the process of oil utilization, due to the physico-chemical modifications already mentioned, a variation (increase) also occurs, of all global properties (s. Table 1); they reach a certain limit at an operation duration of 200 h, being at the same time influenced significantlly by the mechanical impurities included in the mixture during the process of hardening, which renders thus difficult the establishment of the deterioration degree.

Table 1

Variation of the Characteristics of Oils Employed in Thermal Treatments as a Function of their Duration of Utilization

Characteristic	Oil type	Utilization duration, [h]				
		non-utilized	50	100	150	200
Inflammability point, [°C]	TT 11 B	185	188	190	194	196
	TT 100 A	187	186	194	197	197
Conradson coke, [%]	TT 11 B	0.882	0.7...0.83	1.03...1.08	1.12...1.14	1.025...1.3
	TT 100 A	0.900	0.62...0.66	1.15...1.20	1.12...1.13	1.800...1.86
η, [Pa.S] 100°C	TT 11 B	0.044	0.041	0.043	0.049	0.051
	TT 100 A	0.037	0.049	0.036	0.049	0.047

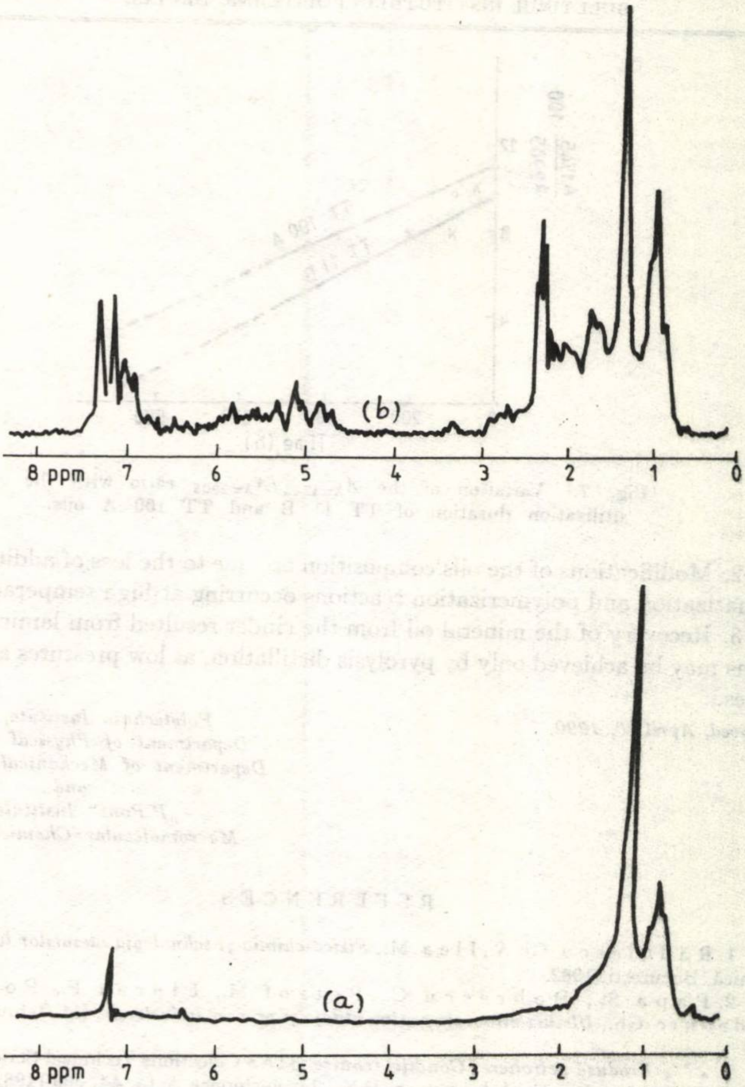

Fig. 6.– H^1-RMN-spectra of used mineral oil employed in thermal treatments (*a*) and of the fraction with a boiling point below 250°C, resulted from its distillation (*b*).

4. Conclusions

1. The efficiency of the thermogravimetry of the differential thermal analysis and of IR spectroscopy has been established for the determination of the used degree of mineral oils induced by thermal treatments.

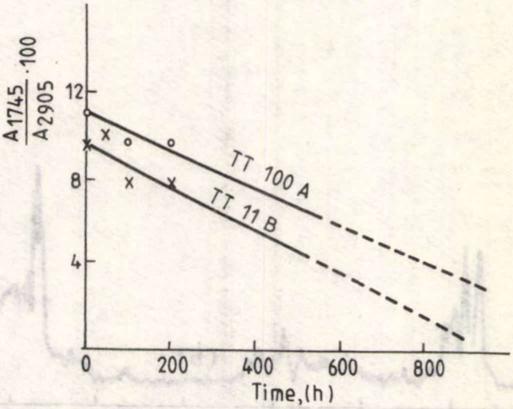

Fig. 7.– Variation of the $A_{\lambda=1745}/A_{\lambda=2905}$ ratio with the utilization duration of TT 11 B and TT 100 A oils.

2. Modifications of the oils'composition are due to the loss of additives and to aromatization and polymerization reactions occurring at high temperatures.

3. Recovery of the mineral oil from the cinder resulted from lamination operations may be achieved only by pyrolysis distillation, at low pressures and temperatures.

Received, April 10, 1990

Polytechnic Institute, Jassy,
Department of Physical Chemistry,
Department of Mechanical Engineering
and
„P.Poni" Institute of
Macromolecular Chemistry, Jassy

REFERENCES

1. Rădulescu Gh.A., Ilea M., *Fizico-chimia şi tehnologia uleiurilor lubrefiante.* Ed. Tehnică, Bucureşti, 1982.
2. Papa St., Dobrescu C., Petrof M., Florea F., Popescu A., Andronic Gh., *Uleiuri minerale pentru utilaje şi procese industriale.* Ed. Tehnică, Bucureşti, 1978.
3. * * * *Produse petroliere. Condiţii tehnice.* STAS Colections Technical Series A, 1965.
4. Corel A.B., Cabbiness D.K., Termochimica Acta, **44**, 363 (1981).
5. Paczuski M., Kardosz K., J. of Thermal Anal., **32**, 1805 (1987).
6. Tiunova I., Thermochim. Acta, **134**, 79 (1988).
7. Levi M., Kramer R., Thermochim. Acta, **134**, 327 (1988).

STUDIUL MODIFICĂRILOR FIZICO-CHIMICE ŞI STRUCTURALE ALE ULEIURILOR MINERALE ÎN CONDIŢII DE UTILIZARE

(Rezumat)

Se pun în evidenţă modificările fizico-chimice şi structurale ale uleiurilor minerale utilizate în diferite procese metalurgice. S-au elaborat două metode rapide de determinare a gradului de uzură

BULETINUL INSTITUTULUI POLITEHNIC DIN IAŞI
Tomul XXXIX (XLIII), Fasc. 1–4, 1993
Secţia II
CHIMIE ŞI INGINERIE CHIMICĂ

D.C. 620.193; 546.621

CORROSION BEHAVIOUR OF ALUMINIUM IN ETHYLENE CARBONATE SOLUTIONS

BY

MARIA APOSTOLESCU, FLORIN BANDRABUR,
ŞT. IVĂŞCAN and VALERIU JUMANCA

1. Introduction

In the spinning bath of acryl polymer the ethylene carbonate in aqueous solution of various concentrations is used. Taking into account the contingency of replacing the stainless steel usually used in the construction of spinning equipement with the more cheaper aluminium, researches have been initiated on its behaviour in ethylene carbonate solutions.

In the first part of the investigations [1] the corrosion behaviour of aluminium (simple and welded) in liquid and gaseous phase was studied, on a laboratory equipment, using the gravimetric analysis.

In the present paper the experimental results on the behaviour to corrosion of aluminium obtained on a micropilot equipment simulating the real conditions in commercial spinning equipments are reported.

The obtained results are given as gravimetric indices. The gravimetric investigations were completed by electrochemical measurements (polarization curves) and kinetic data obtained by means of "Coorater" apparatus.

2. Experimental

The test samples prepared from aluminium sheed (99.5%) were mechanically and chemically worked according to the procedures specific to this material [2].

The solutions of ethylene carbonate were taken directly from various points of the spinning equipment. For each solution the measurements were taken at two temperatures, namely 60±1°C and 90±1°C. The test time for each system was of 500 hours. In Table 1 the characteristics of test solutions are given.

To suppress the decomposition of ethylene carbonate by hydrolysis [3] the solution pH was corrected by adding oxalic acid.

The experimental results obtained by gravimetric procedure in micropilot equipment are depicted in Figs. 1 and 2. The curves in these figures indicate

Table 1

Characteristics of Ethylene Carbonate Solutions

No.	Concentration of ethylene carbonate solution %	State of aggregation at 20°C	pH of solution at 60°C	Density of solution at 60°C, [g/cm^3]
1	22	liquid	4.63	1.05
2	26	liquid	4.64	1.08
3	89	solid	4.81	1.25
4	97	solid	4.89	1.27

a different behaviour of aluminium, in function of concentration and temperature of solutions.

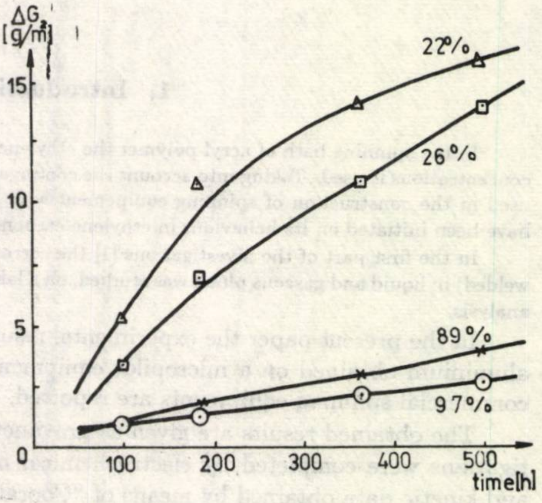

Fig. 1.– Variation of corrosion rate of Al at 60°C, in solutions of ethylene carbonate.

Thus, at the same temperature the corrosion rate in diluted solutions is higher (3...4 times) than that in concentrated solutions. Instead, the temperature influences in a lesser extent. For a temperature increase of 30°C the reaction rate doubles.

The corrosion type as well as its distribution on the test sample surface was followed, as in a previous paper [1], on photographs accomplished with microscope (enlarged by 50 times). The analysis of photographs clearly indicate a pitting corrosion process. With increasing solution concentration the number of pitts on surface unit diminishes, but the pitt is much more developed.

The behaviour of aluminium in solutions of ethylene carbonate was also investigated by electrochemical measurements. The data obtained by means of a "Corrater" apparatus lead to the same conclusion as gravimetric analysis. Thus, at low concentrations of ethylene carbonate the corrosion is almost generalized, the corrosion rate is high, while at high concentrations the pitts are visible with the

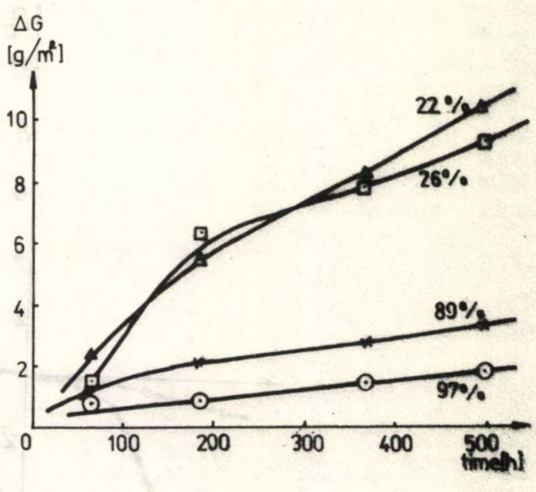

Fig. 2.– Variation of corrosion rate of Al at 90°C, in solutions of ethylene carbonate.

naked eye, being rather seldom but desper.

The potentiostatic curves were plotted for solutions with various pH values (3.5...4.9) corrected by adding oxalic acid) based on data obtained on a potentiostatic of "Radelkis" type. The curves have similar shapes, the differences being caused by the variation of experimental parameters. The anode branch indicates a process of aluminium dissolution, whose rate depends on the pH value, fact also ascertained by the various content of Al^{+3} in tested solutions. At more acid pH a flate region occurs on the polarization curve (Fig. 3) which can be due to a process of formation of aluminium oxide.

The cathode branch indicates a process of hydrogen evolution.

The correlation of all experimental data allows the assumation of following corrosion mechanism:

1. Dissociation of oxalic acid:

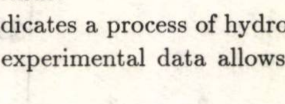

$$\begin{array}{l}\mathrm{COOH}\\ |\\ \mathrm{COOH}\end{array} \rightarrow \begin{array}{l}\mathrm{COOH}\\ |\\ \mathrm{COO^-}\end{array} + \mathrm{H^+}$$

2. Process of electrochemical corrosion:

a) anode $Al \rightarrow Al^{3+} + 3e^-$; b) cathode $3H^+ + 3e^- \rightarrow 3H$

3. Formation of aluminium oxalate, occuring as a gelatinous precipitate, even only after 100 hours of experiment.

To the aggresive character of solutions of ethylene carbonate caused by the oxalic acid, the action adds of carbon dioxyde resulted from the hydrolysis process:

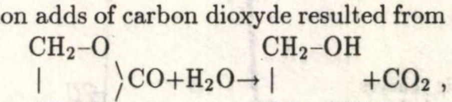

$$\begin{array}{l}\mathrm{CH_2{-}O}\\ |\\ \mathrm{CH_2{-}O}\end{array}\!\!\Big\rangle \mathrm{CO} + \mathrm{H_2O} \rightarrow \begin{array}{l}\mathrm{CH_2{-}OH}\\ |\\ \mathrm{CH_2{-}OH}\end{array} + \mathrm{CO_2}\,,$$

which is hindered by oxalic acid but not suppressed.

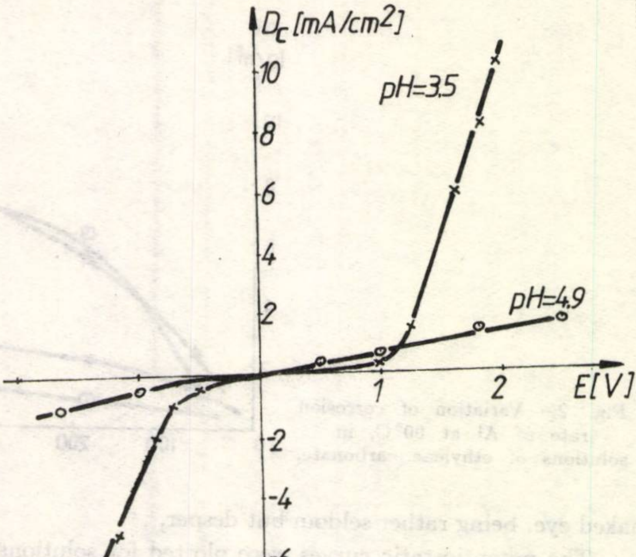

Fig. 3.– Potentiostatic curves for the solution of ethylene carbonate (22%) at 20°C.

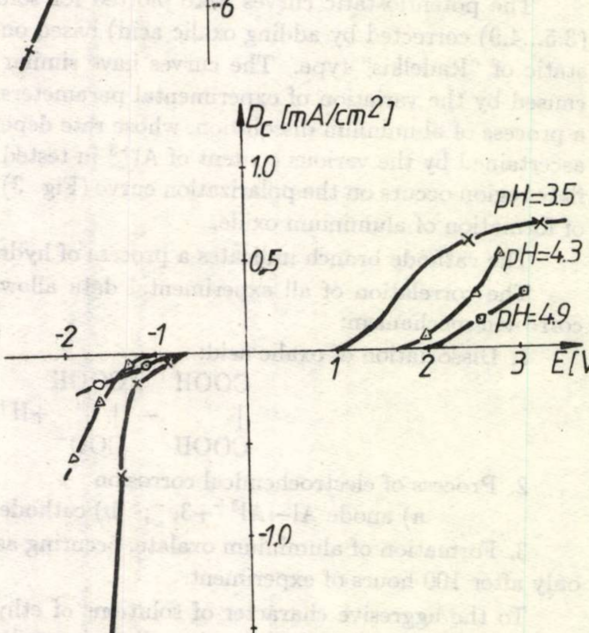

Fig. 4.– Potentiostatic curves for the solution of ethylene carbonate (98%) at 20°C.

3. Conclusions

1. In solutions of ethylene carbonate of 22...97% concentrations and pH = = 4.6...4.9, the aluminium (99.5%) undergoes a process of pitting corrosion.

2. Both the gravimetric and electrochemical measurements lead to the same conclusions on the behaviour of aluminium in solutions of ethylene carbonate.

3. The losser of aluminium are small but due to the corrosion type the danger or perforation occurs and consequently the use of aluminium in the construction of equipment for spinning of synthetic fibers is not recommended.

Received, April 24, 1992

Polytechnic Institute, Jassy,
Department of Inorganic
Chemical Technology

REFERENCES

1. Ivăşcan Şt., Apostolescu M., Bandrabur F., Jumanca V., IIIrd Symp. of Chem. Proc. Eng., Polyt. Inst., Jassy and C.I.C., Piatra-Neamţ, 1983, 123-129.
2. Antohi N., *Reacţia izocianaţilor cu derivaţi ai acidului 6-aminocapronic şi obţinerea de polimeri cu sulf.* Ph.D. Diss., Polyt. Inst., Jassy, 1981.
3. Marinescu A., Adonianţ Gh., Bay E., *Tehnologii electrochimice şi chimice de protecţie a materialelor metalice.* Ed. Tehn., Bucureşti, 1984.

COMPORTAREA LA COROZIUNE A ALUMINIULUI ÎN SOLUŢII DE CARBONAT DE ETILENĂ

(Rezumat)

S-a studiat comportarea aluminiului în soluţii apoase de carbonat de etilenă.

Datele experimentale s-au prelucrat sub formă de indici masici de coroziune şi curbe de polarizare.

În urma analizei datelor experimentale s-a stabilit că procesul de coroziune al aluminiului în soluţii de carbonat de etilenă de concentraţii cuprinse între 22...97% şi pH=4,6...4,9 se manifestă sub formă de coroziune în puncte.

BULETINUL INSTITUTULUI POLITEHNIC DIN IAŞI
Tomul XXXIX (XLIII), Fasc. 1–4, 1993
Secţia II
CHIMIE ŞI INGINERIE CHIMICĂ

C.D. 631.828

ANALYSE DE L'INSTALLATION NORSK-HYDRO D'OBTENTION DES NITROPHOSPHATES

II. UTILISATION DE L'ORDINATEUR DANS L'ANALYSE DU PROCESSUS TECHNOLOGIQUE DE „DÉSAGRÉGATION NITRIQUE"

PAR

CAROLINA HAGIU et RODICA DIACONESCU

1. Introduction

Dans les installations industrielles d'obtention des nitrophosphates, la modification fréquente de la matière première phosphatique détermine une diminution de la capacité de production de l'installation, provoquée par le temps nécessaire au réglage des paramètres technologiques selon les valeurs imposées par la nouvelle sorte de matière première utilisée dont la qualité modifie également celle de l'engrais obtenu. Dans ces conditions une corrélation rigoureuse s'impose entre le nécessaire d'acide azotique introduit et de l'acide de lavage, de sorte que la solution phosphonitrique obtenue après le filtrage (solution-mère) ait une composition chimique constante, ce qui assurerait tant la stabilité des processus suivants du flux technologique que la qualité du produit. La corrélation des débits de phase liquide réactant et des débits des produits intermédiaires et finis avec la masse de roche phosphatique et avec la qualité de celle-ci se réalise par les modèles de bilan de masse pour le processus technologique de désagrégation nitrique.

Dans un travail antérieur [1] on a élaboré les modèles de bilan de masse pour les processus composants et pour le processus technologique de désagrégation nitrique et on a verifié, à partir des données expérimentales industrielles, leur valabilité.

Dans ce qui suit on a effectué, à l'aide d'un ordinateur, une analyse détaillée du processus technologique de désagrégation nitrique, à partir des modèles de bilan de masse.

2. Analyse du processus technologique de „désagrégation nitrique"

2.1. Schéma logique de calcul

Les modèles de bilan de masse pour le processus technologique sont présentés en [1]. Les rapports qui établissent une corrélation entre les débits des produits finis et ceux intermédiaires avec le débit de matière première solide et avec la qualité de celle-ci, représentés dans le schéma bloc du processus technologique de la Fig. 1, sont calculés à l'aide des relations du Tableau 1 [1].

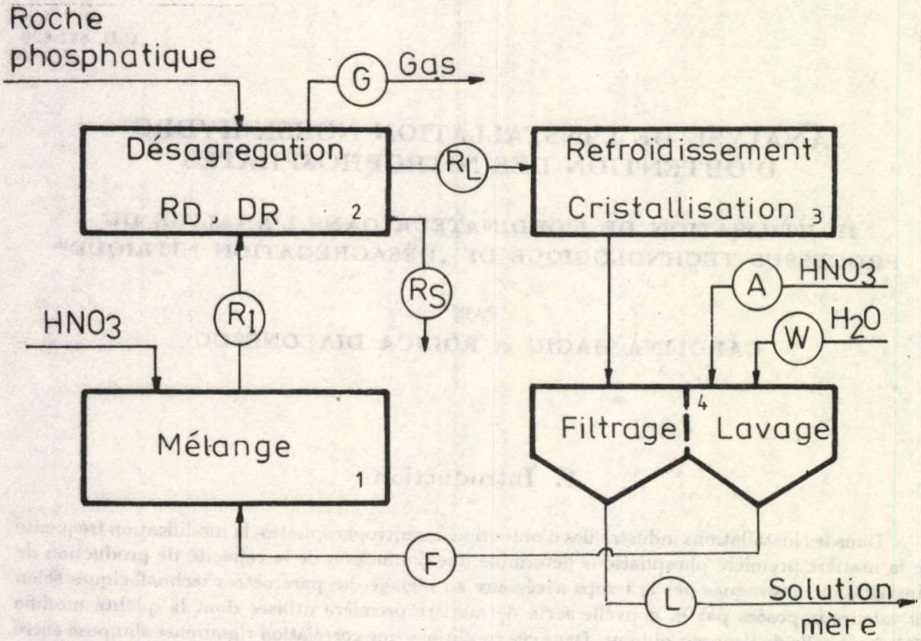

Fig. 1.- Schéma bloc du processus technologique de désagrégation nitrique et des rapports phasiques spécifiques.

Pour l'analyse du processus technologique à l'aide des modèles de bilan de masse on utilise le schéma logique de calcul présenté dans la Fig. 2, pour l'élaboration duquel on a pris en considération les particularités technologiques spécifiques au procédé Norsk-Hydro d'obtention des engrais complexes. Ainsi, pour obtenir des engrais ayant une des plus élevées teneur en P_2O_5 assimilable et une qualité bien déterminée il est nécessaire que le rapport Ca/P, de la solution-mère, soit maintenu constant à une valeur maxima de 0,35; on assure en même temps une teneur constante en eau et implicitement en azote en corrélant la quantité d'eau de lavage avec celle de l'eau liée au $Ca(NO_3)_2 \cdot 4H_2O$, de sorte que la teneur en eau de la solution de désagrégation soit à peu près égale à celle de la solution-mère; c'est en introduisant le test $|\overline{X}_{H_2O[\;]l_2} - \overline{X}^{I}_{H_2O[\;]l}| \leq 0,002$ que l'on assure cette condition dans le schéma logique de calcul. La quantité d'acide azotique de lavage est corrélée avec l'acide frais par la norme d'acide (D_R) en assurant ainsi une teneur constante en azote à la solution de désagrégation et respectivement à la solution-mère.

Tableau 1

Rapports phasiques. Relations de calcul

Nr.	Notation	Définition	Relations de calcul
1	N	$\frac{m^{\text{stoech.}}_{\text{HNO}_3 100\%}}{m^0_{[\,]s}}$	$N = 2,25(\overline{X}^0_{\text{CaO}_{[\,]s}})^T + 3,706\overline{X}^0_{\text{Al}_2\text{O}_{3[\,]s}} +$ $+2,362\overline{X}^0_{\text{Fe}_2\text{O}_{3[\,]s}} + 1,34\overline{X}^0_{\text{K}_2\text{O}_{[\,]s}}$
2	D_R	$\frac{m^{\text{exp}}_{\text{HNO}_3 100\%}}{m^0_{[\,]s}}$	$D_R = 1,2...1,5$
3	L	$m^{\text{I}}_{[\,]l}/m^0_{[\,]s}$	$L = \frac{0,4366\overline{X}^0_{\text{P}_2\text{O}_{5[\,]s}}}{\overline{X}^{\text{I}}_{P[\,]l}}$
4	S	$m^{\text{I}}_{[\,]s^*}/m^0_{[\,]s}$	$S = \frac{0,7143(\overline{X}^0_{\text{CaO}_{[\,]s}})^T - L\overline{X}^{\text{I}}_{\text{Ca}_{[\,]l}}}{\overline{X}^{\text{I}}_{\text{Ca}_{[\,]s^*}}}$
5	G	$m_{[\,]g_2}/m^0_{[\,]s}$	$G = \frac{\overline{X}^0_{\text{CO}_2[\,]s} - L\overline{X}^{\text{I}}_{\text{CO}_2[\,]l}}{\overline{X}_{\text{CO}_2[\,]g_2}}$
6	R_s	$m_{[\,]s_2}/m^0_{[\,]s}$	$R_s = 0,065\overline{X}^0_{A"_{[\,]s}}$
7	R_L	$m_{[\,]l_2}/m^0_{[\,]s}$	$R_L = 1 + R_D - G - R_s$
8	R_D	$\frac{m^0_{[\,]l_1} + m_{f\text{II}}}{m^0_{[\,]s}}$	$R_D = [R_L\overline{X}_{\text{N}_{[\,]l_2}}\overline{X}_{\text{P}f\text{II}} + G\overline{X}_{\text{N}_{[\,]g_2}}\overline{X}_{\text{P}f\text{II}} -$ $-(R_L\overline{X}_{P_{[\,]l_2}} - 0,4366\overline{X}^0_{\text{P}_2\text{O}_5} \times$ $\times(\overline{X}_{\text{N}f\text{II}} - 0,222\overline{X}^0_{\text{HNO}_3})]/$ $/0,222\overline{X}^0_{\text{HNO}_3}\overline{X}_{\text{P}f\text{II}}$
9	F	$m_{f\text{II}}/m^0_{[\,]s}$	$F = \overline{X}_{P[\,]^*_{s_4}}(R_L - L)/\overline{X}_{\text{P}f\text{II}}$
10	A	$m^0_{[\,]l_2}/m^0_{[\,]s}$	$A = D_R/\overline{X}^0_{\text{HNO}_3} - R_D + F$
11	W	$m^0_{[\,]l_3}/m^0_{[\,]s}$	$W = L + S + F - R_L - A$
12	R^0_L	$\frac{m^0_{[\,]l_1}}{m^0_{[\,]l_1} + m_{f\text{II}}}$	$R^0_L = \frac{D_R - A\overline{X}^0_{\text{P}_2\text{O}_5}}{R_D\overline{X}^0_{\text{HNO}_3}}$

Les données initiales et les grandeurs nécessaires pour résoudre à l'aide de l'ordinateur le modèle mathématique sont présentés dans le Tableau 2. Les relations de calcul pour les fractions de masse des composants sont déduites des modèles de bilan de masse qui correspondent aux composants et aux phases où elles interviennent et sont présentées en [1]. La composition de la matière première phosphatique a été exprimée par la fraction de masse du composant utile ($\overline{X}^0_{\text{P}_2\text{O}_5[\,]s}$) et par le rapport entre les fractions de masse du CaO et du P_2O_5; le domaine de la variation de ces derniers a été établi à partir de l'analyse statistique concernant la composition de 20 types de matières premières phosphatiques, qu'on trouve en [2]. En utilisant les mêmes données statistiques on a également établi les fractions de masse des autres composants de la matière première phosphatique.

On a choisi comme valeurs variables la composition des roches phosphatiques (par $\overline{X}^0_{\text{F}_2\text{O}_5}$ et $\overline{X}^0_{\text{CaO}}/\overline{X}^0_{\text{P}_2\text{O}_5}$), la norme d'acide azotique (D_R) et la concentration de l'acide azotique, valeurs qui déterminent, en dernière analyse, le régime technologique.

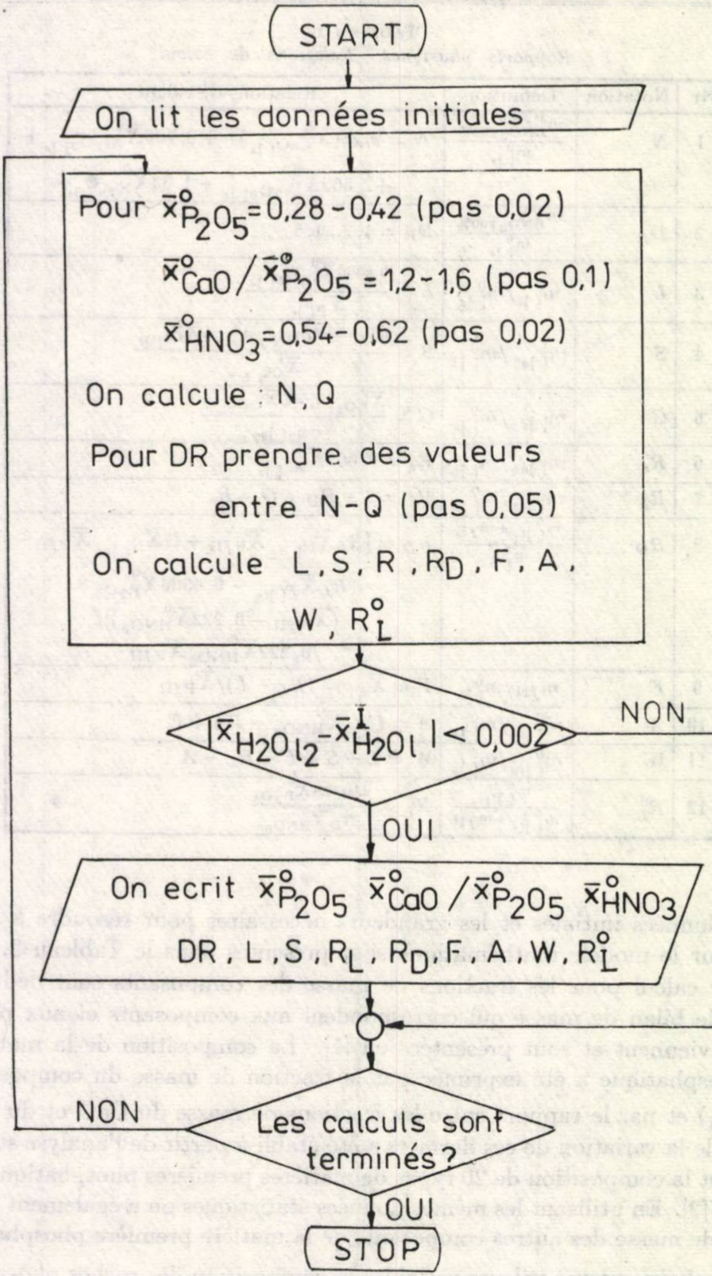
START
On lit les données initiales
Pour $\bar{x}^o_{P_2O_5}$ = 0,28 - 0,42 (pas 0,02)
$\bar{x}^o_{CaO} / \bar{x}^o_{P_2O_5}$ = 1,2 - 1,6 (pas 0,1)
$\bar{x}^o_{HNO_3}$ = 0,54 - 0,62 (pas 0,02)
On calcule : N, Q
Pour DR prendre des valeurs entre N - Q (pas 0,05)
On calcule L, S, R, R_D, F, A, W, R^o_L
$|\bar{x}_{H_2O\,l_2} - \bar{x}^I_{H_2O\,l}| < 0,002$
NON
OUI
On ecrit $\bar{x}^o_{P_2O_5}$ $\bar{x}^o_{CaO} / \bar{x}^o_{P_2O_5}$ $\bar{x}^o_{HNO_3}$
DR, L, S, R_L, R_D, F, A, W, R^o_L
NON
Les calculs sont terminés ?
OUI
STOP

Fig. 2.- Schéma logique de calcul.

Tableau 2

Grandeurs nécessaires au roulage du programme

Phase	Grandeurs nécessaires	Valeurs numériques ou relations de calcul
Matière première phosphatique	$\overline{X}^0_{\mathrm{P_2O_5}}$	0,28...0,42
	$\overline{X}^0_{\mathrm{CaO}}/\overline{X}^0_{\mathrm{P_2O_5}}$	1,2...1,6
	$\overline{X}^0_F$	0,03
	$\overline{X}^0_{\mathrm{CO_2}}$	0,04
	$\overline{X}^0_{\mathrm{Al_2O_3}}$	0,01
	$\overline{X}^0_{\mathrm{Fe_2O_3}}$	0,014
	$\overline{X}^0_{\mathrm{K_2O}}$	0,004
	Inert $\overline{X}^0_{\mathrm{A''}}$	0,057
Acide azotique	$\overline{X}^0_{\mathrm{HNO_3}}$	0,54...0,62
Acide recirculé f_{II}	$\overline{X}_{\mathrm{P}f\mathrm{II}}$	0,0326
	$\overline{X}_{\mathrm{N}f\mathrm{II}}$	0,1025
	$\overline{X}_{\mathrm{Ca}f\mathrm{II}}$	0,035
	$\overline{X}_{\mathrm{A''}f\mathrm{II}}$	0,025
Phase liquide initiale	$\overline{X}^0_{N[\,]l}$	$\overline{X}^0_{N[\,]l} = \overline{X}_{\mathrm{N}f\mathrm{II}} + R^0_L(0,222\overline{X}^0_{\mathrm{HNO_3}} - \overline{X}_{\mathrm{N}f\mathrm{II}})$
Norme d'acide (D_R)	D_R	1,2...1,6
Solution de désagrégation, $[\,]l_2$	$\overline{X}_{N[\,]l_2}$	$\overline{X}_{N[\,]l_2} = [R_D\overline{X}^0_{N[\,]l} - G\overline{X}_{N[\,]g_2}]/R_L$
	$\overline{X}_{P[\,]l_2}$	$\overline{X}_{P[\,]l_2} = [0,4366\overline{X}^0_{\mathrm{P_2O_5}} + F\overline{X}_{\mathrm{P}f\mathrm{II}}]/R_L$
Gaz de désagrégation, $[\,]g_2$	$\overline{X}_{\mathrm{F}[\,]g_2}$	0,0256
	$\overline{X}_{\mathrm{CO_2}[\,]g_2}$	0,1324
	$\overline{X}_{\mathrm{N}[\,]g_2}$	0,0836
Solution mère, $[\,]^{\mathrm{I}}_l$	$\overline{X}^{\mathrm{I}}_{\mathrm{Ca}[\,]l}$	0,35
	$\overline{X}^{\mathrm{I}}_{\mathrm{P}[\,]l}$	0,10
	$\overline{X}^{\mathrm{I}}_{\mathrm{Ca}[\,]l}/\overline{X}^{\mathrm{I}}_{\mathrm{P}[\,]l}$	0,35
Solide humide non-lavé, $[\,]^*_{s_4}$	$\overline{X}_{P[\,]s^*_4}$	0,0179
Fondue de $\mathrm{Ca(NO_3)_2 \cdot 4H_2O}$, $[\,]^*_s$	$\overline{X}_{\mathrm{Ca}[\,]s^*}$	0,1535
	$\overline{X}_{\mathrm{N}[\,]s^*}$	0,0179

2.2. Résultats et discussions

Les résultats obtenus après avoir roulé le programme élaboré selon le schéma logique de la Fig. 2 sont transformés en tableaux et diagrammes. Ils sont partiellement présentés dans les Figs. 3...5.

De l'analyse des données présentées dans ces figures on peut dégager les conclusions suivantes:

a) L'accroissement de la teneur en CaO de la roche phosphatique, mis en évidence par l'augmentation du rapport $\overline{X}^0_{\mathrm{CaO}}/\overline{X}^0_{\mathrm{P_2O_5}}$ pour une concentration

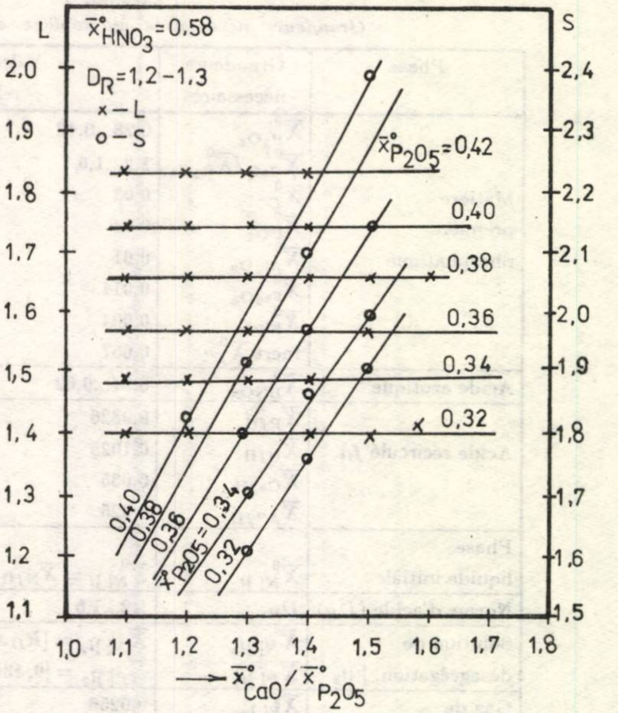

Fig. 3.– Variation des rapports *A* et *W* fonction de la norme d'acide (D_R) et du rapport $\overline{X}^0_{CaO}/\overline{X}^0_{P_2O_5}$.

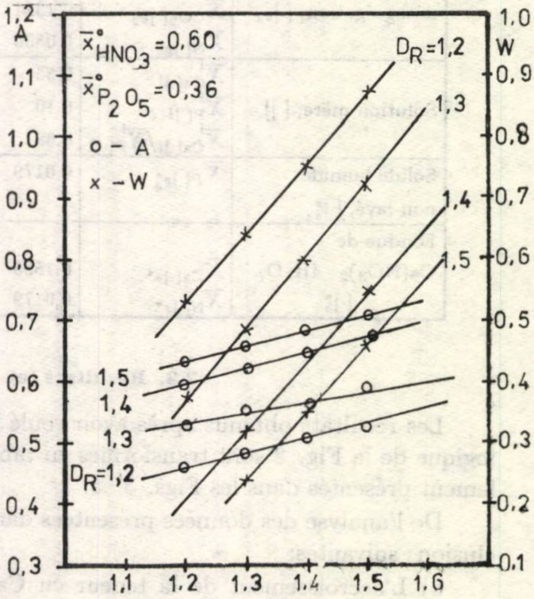

Fig. 4.– Variation des rapports *A* et *W* fonction de la norme d'acide (D_R) et de la teneur en P_2O_5 ($\overline{X}^0_{P_2O_5}$).

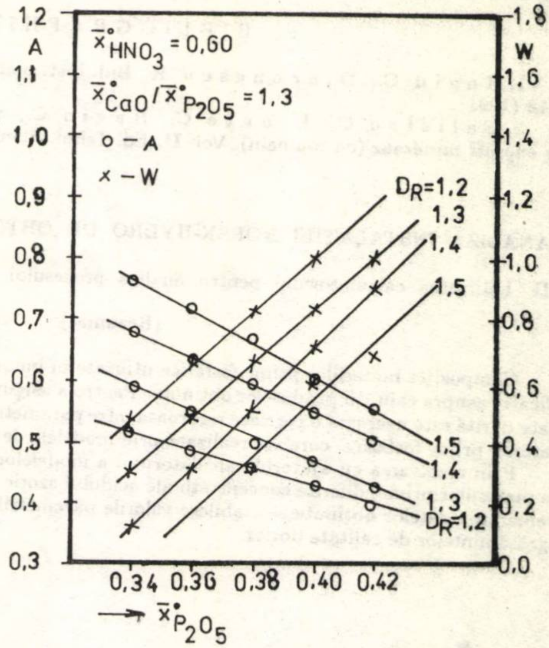

Fig. 5.– Variation des rapports L et S fonction du rapport $\overline{X}^0_{CaO}/\overline{X}^0_{P_2O_5}$ et de la teneur en P_2O_5 ($\overline{X}^0_{P_2O_5}$).

constante de l'acide, détermine l'accroissement des quantités d'acide azotique et d'eau introduites au filtrage et au lavage du $Ca(NO_3)_2{\cdot}4H_2O$. L'accroissement de la norme d'acide azotique (D_R) pour un rapport CaO/P_2O_5 constant détermine l'augmentation de la quantité d'acide de lavage et la diminution de la quantité d'eau.

b) L'accroissement de la teneur en P_2O_5 de la roche phosphatique, pour un rapport constant CaO/P_2O_5 et pour un concentration constante de l'acide azotique, entraîne la diminution de la quantité d'acide de lavage et l'augmentation de la quantité d'eau de lavage. L'accroissement de la norme d'acide azotique (D_R), pour une teneur constante en P_2O_5 et pour un rapport CaO/P_2O_5 constant, détermine l'accroissement de la quantité d'acide de lavage et respectivement, la diminution de la quantité d'eau de lavage.

c) L'accroissement du rapport CaO/P_2O_5 de la roche phosphatique n'exerce aucune influence sur la quantité de solution phosphonitrique obtenue, quelles que soient la norme d'acide et la concentration de l'acide utilisé, mais il provoque une augmentation significative de la masse de $Ca(NO_3)_2{\cdot}4H_2O$; la quantité de solution phosphonitrique obtenue augmente en même temps que la teneur en P_2O_5 de la roche phosphatique.

Reçue le 26 novembre 1991

Institut Polytechnique, Jassy,
Chaire de Technologie chimique
anorganique

BIBLIOGRAPHIE

1. Hagiu C., Diaconescu R., Bul. Inst. polit., Iaşi, **XXXVII (XLI)**, *1-4*, s. II, 41-48 (1991).

2. Calistru C., Leonte C., Hagiu C., Siminiceanu I., *Technologie des engrais minéraux* (en roumain). Vol. **II**, Ed. Tehn., Bucureşti, 1984.

ANALIZA INSTALAŢIEI NORSK-HYDRO DE OBŢINERE A NITROFOSFAŢILOR

II. Utilizarea calculatorului pentru analiza procesului tehnologic „dezagregare nitrică“

(Rezumat)

Compoziţia materiilor prime fosfatice utilizate în industria nitrofosfaţilor influenţează semnificativ asupra calităţii produselor obţinute. Pentru a asigura obţinerea unor îngrăşăminte de calitate dorită este necesară o corelare riguroasă între parametrii procesului tehnologic şi compoziţia materiei prime fosfatice, corelare realizată prin modelele de bilanţ de masă.

Prin rezolvarea cu ajutorul calculatorului a modelelor de bilanţ pentru diferite compoziţii ale materiilor prime, diferite concentraţii ale acidului azotic şi diferite valori ale normei de acid şi prelucrarea datelor obţinute se stabilesc valorile parametrilor tehnologici care asigură obţinerea îngrăşămintelor de calitate dorită.

BULETINUL INSTITUTULUI POLITEHNIC DIN IAŞI
Tomul XXXIX (XLIII), Fasc. 1–4, 1993
Secţia II
CHIMIE ŞI INGINERIE CHIMICĂ

D.C. 546.264; 541.11

A COMPARATIVE STUDY ON THE THERMAL DECOMPOSITION OF SOME NATURAL CARBONATES

BY

AL. SZÉP and GH. MIHĂILĂ

1. Introduction

The dissociation process of the natural carbonates, described by the stoichimetrical equation:

$$MeCO_3 = MeO + CO_2,$$

belongs to the unitary chemical process “adsorption–reaction and formation and growing of germs” [1], [2]. Depending on the carbonate variety, size of the granules subjected to the thermal dissociation and temperature, the overall rate is controlled, either by transformation processes, i.e. chemical reaction and formation and growing of germs, or by diffusional processes, namely transfer of carbon dioxide through crust and its transfer across the film surrounding the solid, heat transfer through crust, etc. [1],...,[4].

In order to verify the influence of carbonate nature over the thermal dissociation mechanism, in what follows the dissociation of four varieties of natural carbonates, as samples of spherical shape, having 5, 10 and 15 mm in diameter, in the temperature range of 958...1 348 K, is studied. On the basis of the direct experimental data, for each raw carbonate, the influence of temperature and granule size over the decarbonation degree and the most probable mechanism is established.

2. Experimental

For this comparative study, we have selected four varieties of raw carbonate, i.e. a Greek magnesite with 96.7% $MgCO_3$, 2.3% $CaCO_3$ and 51.3% ignition loss (IL), a dolomite of Voşlobeni deposit with 47.37% IL, a limestone of Bistriţa deposit with 43.58% IL and an usual marble with 43.49% IL. From each of these four varieties of raw carbonates we fashioned mechanically several spherical samples with diameters of 5, 10 and 15 mm, respectively. The thermal decomposition of each sample was carried out on a thermoanalyzer fully described in a previous paper [5]. All experiments were performed under isothermal conditions and a constant flowrate of the carrier gas.

The decarbonation degree, η, was calculated by means of the relation:

$$\eta = \frac{\Delta m_\tau}{m^0 \overline{X}^0_{\mathrm{IL}}}, \tag{1}$$

where: Δm_τ is the mass variation of the sample at any instant, m^0 – the initial mass of the sample and $\overline{X}^0_{\mathrm{IL}}$ – the total mass fraction of the ignition loss.

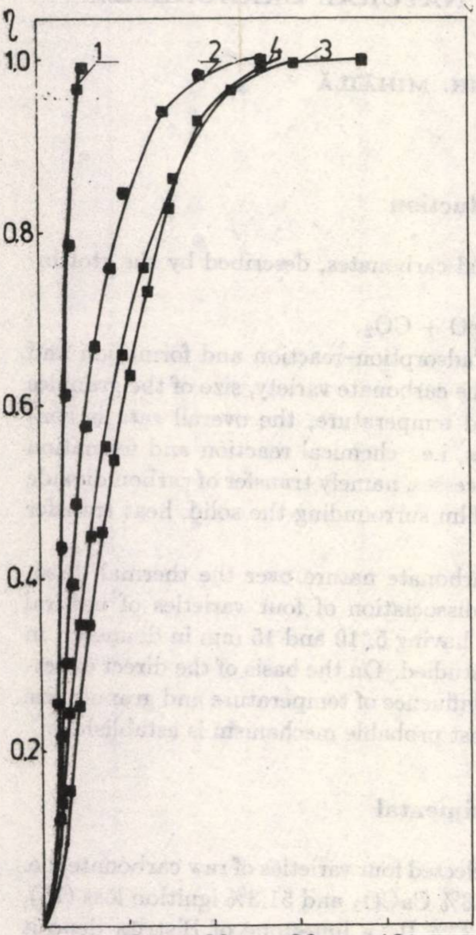

Fig. 1.– Variation of η vs. τ at 1 158 K for spheres with 5 mm in diameter of different carbonates: *1* – magnesite; *2* – dolomite; *3* – limestone; *4* – marble.

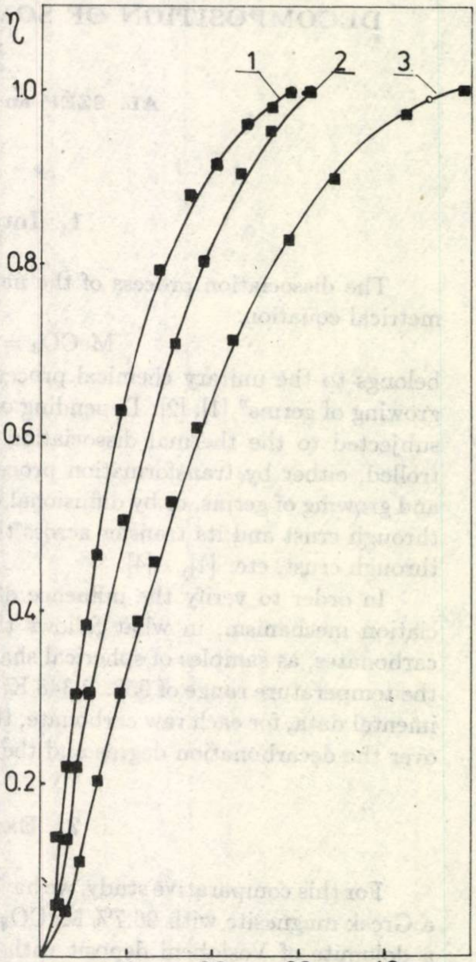

Fig. 2.– Variation of η vs. τ at 1 158 K for spheres with 10 mm in diameter of different carbonates: *1* – dolomite; *2* – limestone; *3* – marble.

The thermogravimetrical measurements allowed to establish the dependence of the decarbonation degree vs. time, τ, (Figs. 1,...,3).

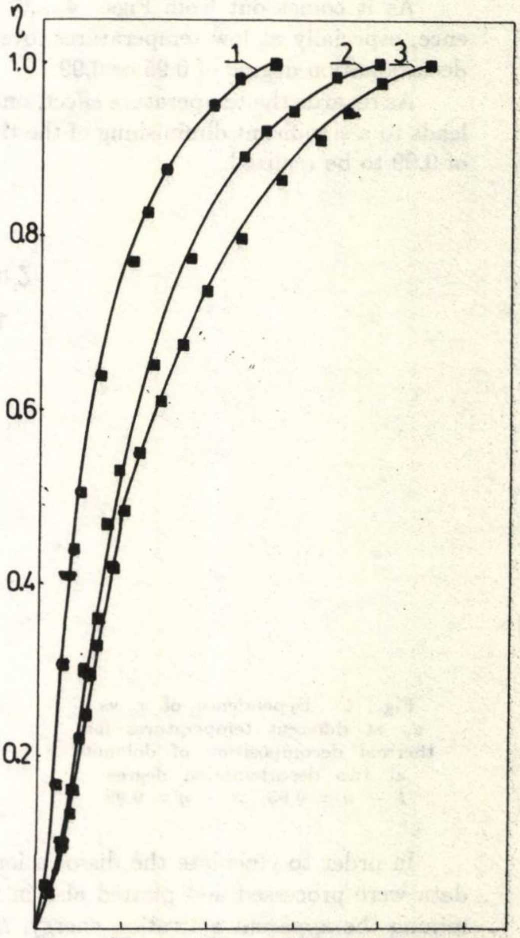

Fig. 3.- Variation of η vs. τ at 1 258 K for spheres with 15 mm in diameter of different carbonates: *1* – dolomite; *2* – limestone; *3* – marble.

Under the conditions mentioned above, as shown in Figs. 1,...,3, variation of η vs. τ depends in an essential manner on the carbonate variety investigated.

3. Discussion

To point out the real influence of the carbonate nature, granule size and temperature over the rate of the thermal decomposition process, the direct experimental data were processed and plotted in the $\tau - d_p$, $\tau - T$ and $\ln(1/\tau) - T^{-1}$ coordinates (Figs. 4,...,6).

As it comes out from Figs. 4,...,6, the granule size has a significant influence, especially at low temperatures, over the time necessary for realization of a decarbonation degree of 0.95 or 0.99.

As regards the temperature effect, one can be seen in Fig. 7 that its increasing leads to a significant diminishing of the time necessary for a decarbonation degree of 0.99 to be realized.

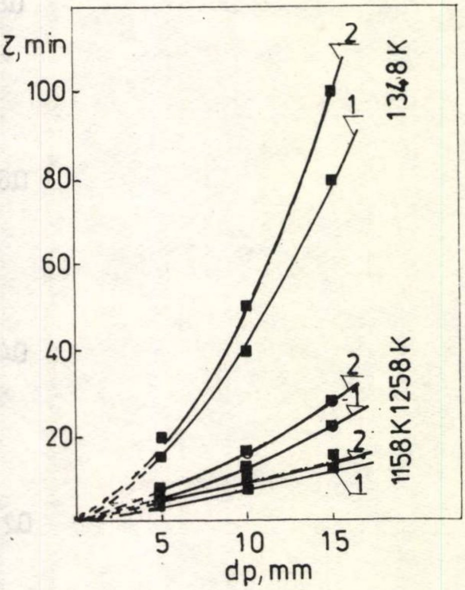

Fig. 4.- Dependence of τ vs. d_p at different temperatures for thermal decomposition of dolomite at two decarbonation degree: *1* - $\eta = 0.95$; *2* - $\eta = 0.99$.

In order to elucidate the dissociation mechanism, the primary experimental data were processed and plotted also in the $\ln(1/\tau)$ vs. T^{-1} coordinates, determining the apparent activation energy, E_a; the obtained values are presented in Table 1. The data of Table 1 show that in all cases, the process develops according with a transformation mechanism, i.e. $E_a \geq 41,900$ J.mol^{-1} (10,000 cal.mol^{-1}). But, in the case of dolomite, these data prove the existence of two transformation mechanisms, due to the two decomposition steps, former specific to dolomite and the latter to calcium carbonate, as previously reported [3]. The dissociation rate of the four carbonates is situated in the following order:

marble < limestone < dolomite < magnesite.

4. Model of the Real Development of the Process

If we assume that the heat transfer and heat utilization are not rate-controlling

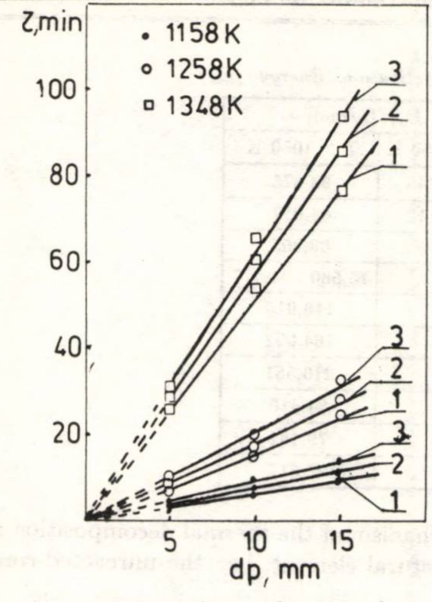

Fig. 5.– Dependence of τ vs. d_p at different temperatures for thermal decomposition of limestone at three decarbonation degree: *1* – $\eta = 0.95$; *2* – $\eta = 0.975$; *3* – $\eta = 0.99$.

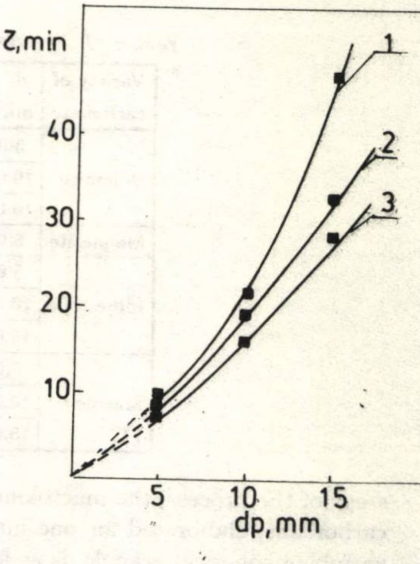

Fig. 6.– Dependence of τ vs. d_p at 1 258 K and $\eta = 0.99$ for thermal decomposition of different carbonates: *1* – marble; *2* – limestone; *3* – dolomite.

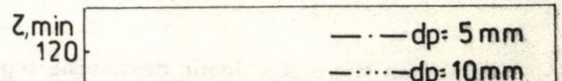

Fig. 7.– Dependence of τ vs. T at $\eta = 0.99$ for spheres of marble (□), limestone (○), dolomite (•) and magnesite (△) with different diameters.

Table 1

Values of the Apparent Activation Energy (E_a)

Variety of carbonate	d_p mm	E_a, [J/mol] $T < 1050$ K	$T > 1050$ K
Dolomite	5.0	252,745	93,675
	10.0	310,112	64,017
	15.0	185,466	63,255
Magnesite	5.0	–	75,580...94,477
Limestone	5.0	–	140,915
	10.0	–	164,092
	15.0	–	210,551
Marble	5.0	–	84,410
	10.0	–	79,181
	15.0	–	92,617

steps of the process, the macrokinetic mechanism of the thermal decomposition of carbonates, elaborated for one macrostructural element, i.e. the unreacted-core-shrinking spherical granule, is as follows:

$$[\text{Thermal dissociation}] - \left[\begin{array}{c}\left[\begin{array}{c}\text{Formation and growing of germs of the}\\ \text{new solid phase}\end{array}\right]\\ \left[\begin{array}{c}\text{Desorption}\\ \text{of CO}_2\end{array}\right] - \left[\begin{array}{c}\text{Transfer of}\\ \text{CO}_2\text{ through}\\ \text{crust}\end{array}\right] - \left[\begin{array}{c}\text{Transfer of}\\ \text{CO}_2\text{ across}\\ \text{the fluid film}\\ \text{surrounding}\\ \text{the solid}\end{array}\right]\end{array}\right.$$

Based on the macrokinetic mechanism represented above, the macrokinetic and mathematic models of the process have been elaborated. These models are set up in Table 2.

Table 2

Macrokinetic and Mathematical Models of one Macrostructural Element

Macrokinetic model	Mathematic model
Thermal dissociation $(-\overline{r}) = k(1-\eta)^{n'}$	$n'=0,\ 1-(1-\eta)^{1/3} = k'\tau$
	$n' = 1,\ -\ln(1-\eta) = k''\tau$
	$n' \neq 1,\ 1-(1-\eta)^{1-n} = (1-n)k'''$
Formation and growing of germs $\overline{r} = k(1-\eta)\tau^{n-1}$	$\eta = 1 - \mathrm{e}^{-k\tau^n}$
Transfer of CO_2 through crust $\overline{q} = D_{\mathrm{ef}_{CO_2}} \frac{\mathrm{d}C_{CO_2}}{dr}$	$1 - 3(1-\eta)^{2/3} + 2(1-\eta) = k^*\tau$
	$(1-\frac{2}{3}\eta) - (1-\eta)^{2/3} = k^*\tau$
	$[1+(z-1)\eta]^{2/3} + (z-1)(1-\eta)^{2/3} - z = k^*\tau$
Transfer of CO_2 across the gas surrounding the solid $\overline{q} = K_{T_{CO_2}}(P^e_{CO_2} - P_{CO_2[\,]_g})$	$\tau = \frac{\rho^* R}{3K_{T_{CO_2}} \Delta P_{CO_2}} \eta$

Representing the kinetical experimental data in the coordinates proper to each model listed in Table 2, we found out that the real process is well enough described by the Avrami – Kolmogorov – Erofeev's equation, i.e.

$$\ln[-\ln(1-\eta)] = \ln k^{+} + n \ln \tau, \tag{2}$$

resulted by double logarithmation of the mathematical model in Table 2, rows 2 and 4.

This fact is also evidenced by the data represented in Fig. 8. In the case of dolomite the equation (2) fits the data only in the decarbonation degree range of 0.00...0.86 and for magnesite, limestone and marble it does up to $\eta = 0.99$.

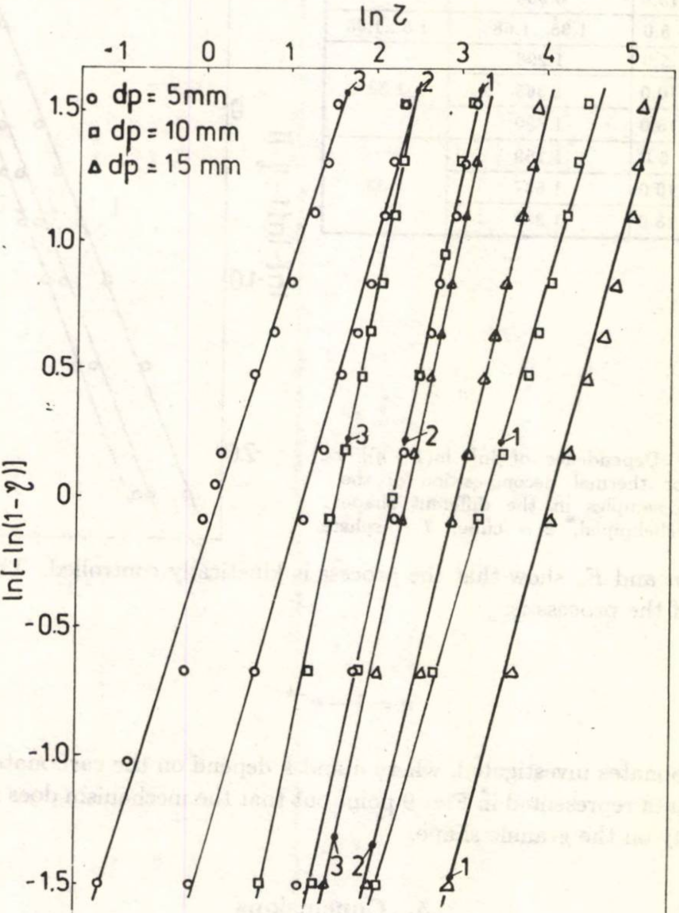

Fig. 8.– Dependence of $\ln[-\ln(1-\eta)]$ vs. $\ln \tau$ for thermal decomposition of marble pheres at different temperature: *1* – 1 158 K; *2* – 1 258 K; *3* – 1 348 K.

The kinetic factor, n, was calculated graphically; its values are set up in Table 3.

Table 3

Values of the Kinetic Factor, n

Variety of carbonate	d_p mm	n Determined value	n Mean value
Dolomite	5.0	1.198	1.00
	10.0	0.928	
	15.0	0.905	
Magnesite	5.0	1.35...1.68	1.5...1.66
Limestone	5.0	1.298	1.33
	10.0	1.365	
	15.0	1.390	
Marble	5.0	1.259	1.33
	10.0	1.537	
	15.0	1.350	

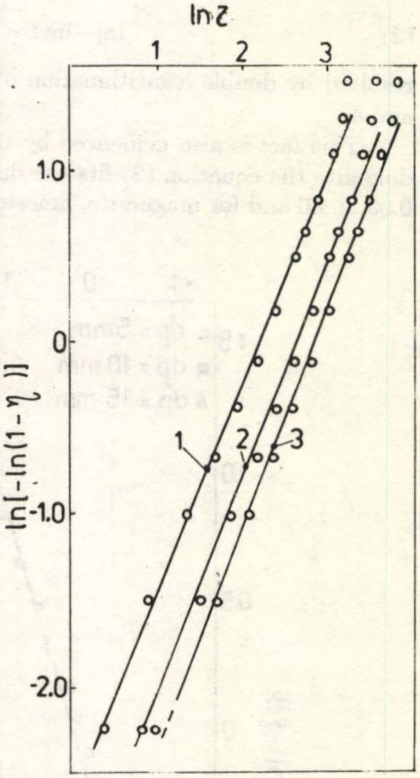

Fig. 9.- Dependence of $\ln[-\ln(1-\eta)]$ vs. $\ln\tau$ for thermal decomposition of the marble samples in the different shape: *1* - parallelipiped; *2* - cube; *3* - sphere.

Both n and E_a show that the process is kinetically controlled. The kinetical equation of the process is:

$$\eta = 1 - e^{-k\tau^n} \tag{3}$$

for all carbonates investigated, where n and k depend on the carbonate variety.

The data represented in Fig. 9 point out that the mechanism does not depend significantly on the granule shape.

5. Conclusions

The obtained results may be summarized as follows:

1. The kinetical study of the thermal decomposition of dolomite, magnesite, limestone and marble have shown that the process is kinetically controlled in the

temperature range of 1 158...1 348 K for spherical granules having 5, 10 and 15 mm in diameter.

2. The process is described by the equation (3), where n and k are depending on the carbonate variety.

3. The kinetical mechanism does not depend significantly on the granule shape.

Notations

$\bar{r}$ – rate of the transformation process, [mol/m^2.s];
$\bar{q}$ – rate of the diffusional process, [mol/m^2.s];
C_{CO_2} – concentration of CO_2, [mol/m^3];
$D_{ef.CO_2}$ – diffusion coefficient of CO_2, [m^2/s];
$P^e_{CO_2}$ – dissociation pressure, [Pa];
$P_{CO_{2[\,]_g}}$ – partial pressure of CO_2 in the gaseous phase, [Pa];
ΔP_{CO_2} – pressure gradient, [Pa];
$K_{T_{CO_2}}$ – transfer coefficient of CO_2 through gaseous film, [mol/m^2.s.Pa];
r – the granule radius, [m];
ρ^* – molar density, [mol/m^3];
k, k', k'', k''' – rate constant of the dissociation process, [mol/m^2.s];
k^* – overall constant of the diffusion process, [s^{-1}];
d_p – diameter of the granule, [mm].

Received, March 24, 1992

Polytechnic Institute, Jassy,
Department of Inorganic
Chemical Technology

REFERENCES

1. Calistru C., Leonte C., *Tehnologia substanţelor anorganice.* EDP, Bucureşti, 1972.

2. Ifrim L., Calistru C., *Procesul chimic unitar adsorbţie-reacţie-formare şi creştere de germeni.* Inst. polit., Iaşi, 1986.

3. Szép Al., Mihăilă Gh., Leonte C., Vuţă Gh., Rev. Chim. (Bucharest), **39**, 32 (1988).

4. Szép Al., Mihăilă Gh., Smocot R., Ivaniciuc M., Bul. Inst. polit., Iaşi, **XXXVII** (**XLI**), *1-4*, s. II, 37 (1991).

5. Calistru C., Mihăilă Gh., An. Şt. Univ. „Al.I.Cuza“, Iaşi, **18**, 97 (1972).

STUDIUL COMPARATIV AL PROCESULUI DE DESCOMPUNERE TERMICĂ A UNOR CARBONAŢI NATURALI

(Rezumat)

S-a cercetat descompunerea termică a dolomitei, magnezitei, calcarului şi a marmurei, sub formă de granule sferice cu diametrul de 5, 10 şi 15 mm, în condiţii izoterme, folosind metoda termogravimetrică. S-a realizat modelarea macrocinetică şi matematică a procesului, desfăşurat într-un element macrostructural – granula cu miez nereacţionat. Prin reprezentări grafice ale datelor experimentale în coordonate specifice modelelor elaborate, s-a găsit că procesul se desfăşoară după un mecanism de transformare, al cărui model matematic este $\eta = 1 - e^{-k\tau^n}$, în care k şi n depind de natura carbonatului studiat. Forma geometrică a granulelor nu influenţează în mod semnificativ mecanismul macrocinetic al procesului de descompunere termică a carbonaţilor.

BULETINUL INSTITUTULUI POLITEHNIC DIN IAŞI
Tomul XXXIX (XLIII), Fasc. 1–4, 1993
Secţia II
CHIMIE ŞI INGINERIE CHIMICĂ

D.C. 544.844; 546.13; 54-92

HIGH PERFORMANCE LIQUID CHROMATOGRAPHY OF CHLORIDE IN POLYMERS

BY

MARCEL IONEL POPA

1. Introduction

Macromolecular compounds are widely used in enzyme and drug coupling. They show the advantage of being easily biodegradable and biocompatible without giving toxic compounds after digestion. At the same time they can offer an adequate microsystem for enzyme and drug actions requiring the presence of metallic ions and a certain water concentration [1],...,[6].

For the medical use is necessary the knowledge of the caracteristics and the purity of the polymers. In the synthesis reaction different prodrugs uses compounds which contain chloride.

A simple and rapid method for separation and determination of chloride from the new products is based of the high performance liquid chromatography.

2. Experimental

a) *Apparatus.* A high-pressure liquid chromatograph Varian model 5020, equipped with column IC-PakA 50×4.4 mm and conductivity detector at range 500 μSFS was used for detection of chloride.

b) *Sample Preparation.* Weight 50 mg of polymer into a 10 ml volumetric flask and then extracted in water at 60°C for 30 min. The solution was filtred by Arcodisc 0.4 μm before injection. Volum injection was 20 μl.

c) *Eluent.* A tampon sodium borate/gluconate 2%, n-butanol 2%, acetonitril 12%, water 84% was used.

d) *Mobile Phase Preparation.* To an one liter volumetric flask add: 19 g sodium gluconate, 18 g acid boric, 25 g sodium tetraborate decahydrate. Add approximately 500 ml water and mix thoroughly until dissolved, then add 250 ml glicerin. Fill to the mark with water and mix thoroughly. Concentrate may be stored for up to six month before requiring replacement.

To prepare sodium borate/gluconate eluent, place approximately 500 ml water into an one liter volumetric flask and to this add: 20 ml borate gluconate, 20 ml n-butanol, 120 ml acetonitrile, then fill the flask to the mark with water and mix thouroughly. Filter through a 0.22 μm Durapore membrane.

3. Results and Discussion

The analysis of ions in real samples is often complicated by the presence of interferences in the sample matrix. Typically these matrices contain a major constituent that affects the quality of separation and detection of the component of interest. Generally, these problems are caused by pH, high or low concentrations, organics, coelution or reactivity.

The first step for successful analysis of real samples is to qualify the sample both in terms of analytes interest and sample matrix.

The effects of sample pH can be seen both in the chromatographic analysis and in the sample itself.

Without any sample preparation, high and low pH samples may cause perturbations and drift in the chromatographic baseline which may interfere with the analytes of interest. This is of particular concern when analysing for anions using standard borate/gluconate eluent.

One of the most common problems encoutered real samples represents extremes in ionic concentrations. Exceedingly high levels of total ionic species may result in column over loading and degradation of the analytical separation. Dilution of the sample will often eliminate this problem. A more common situation is the presence of very high levels of ion species in the presence of very levels of the analytes of interest. In these cases, dilution may lower the analyte levels below the detection limits and the high level species may interfere with the analytes of interest. These types of problemes are often encoutered when analysing samples such as brines.

Samples with very clean matrices, such as high purity water samples, may exhibit extremely low levels of ionic species. The analytes of interest in these samples may be below the normal detection limits for direct injection. In these cases, the sample must either be concentrated in some manner, or a more selective and sensitive detection method must be used.

The presence of organic compounds may interfere with the analysis of inorganic ions. If the eluent does not contain any organic modifiers, very hydrophobic organic compounds in the sample matrix may adsorb or bind into the column packing. This can cause a loss in column capacity resulting in a general decrease in resolution. Although hydrophilic organic compounds will usually eluate off the column in most, ion separation, they may interfere with analytes of interest. Certain organic compounds can act as chelates to bind ions in the sample matrix.

Coelution of components in the sample can range from slight overlapping of analyte peaks where sufficient quantification may still be carried out, to the point case where two or more analyte peaks show no separation and overlap completely. This can make accurate detection and quantification difficult, if not impossible. Coelution of analytes can occur due to too strong an eluent, inappropriate column selectivity, or high levels of one species which another closely eluting analyte. Depending on the cause of the coelution, various method modification should be considered such as, sample preparation, chemistry modification, or a change in the detections mode.

Many ionic species are reactive and undergo electrochemical reactions in solution. Care must be taken to ensure that these species remain unchanged troughout the sample preparation and analysis procedures so thay accurate results will be obtained.

By liquid chromatography it is possible separation directly of chloride and other ions. In Fig. 1 the chromatogram of mixture standard containing chloride, bromide and sulphate is presented.

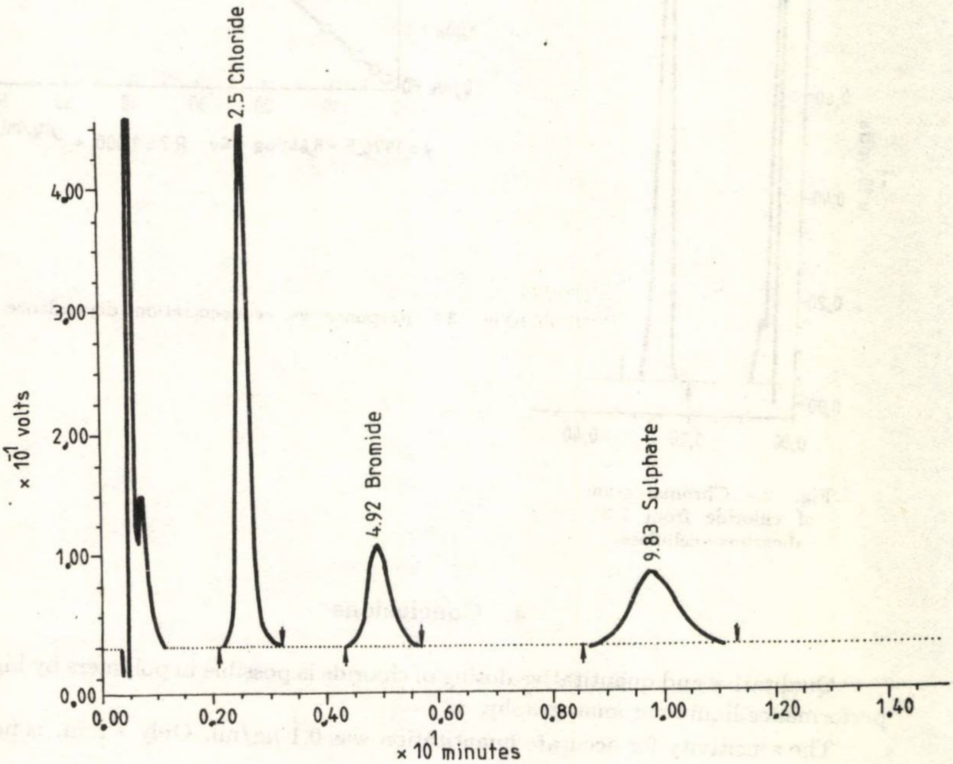

Fig. 1.– High pressure liquid chromatogram for a standard mixture of chloride, bromide and sulphate.

The concentration of chloride in 2,3 dicarboxy-cellulose (Fig. 2) used in medicine was determined by measuring the peak area and comparing the value with a calibration curve prepared using standard of known concentration.

Linearity was observed in the concentration range of 0.1 to 50 μg/ml (Fig. 3). The consecutive injections of a mixture gave a percent relative deviation <1% for all components.

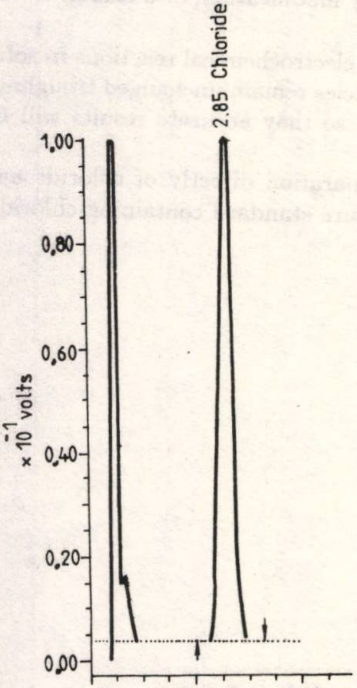

Fig. 2.– Chromatogram of chloride from 2,3 dicarboxy-cellulose.

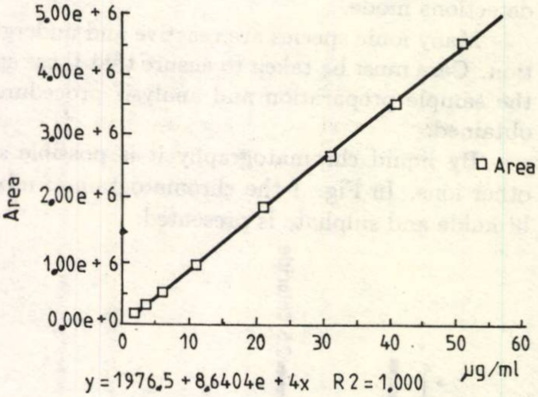

Fig. 3.– Response vs. concentration dependence.

4. Conclusions

Qualitative and quantitative dosing of chloride is possible in polymers by high-performance liquid chromatography.

The sensitivity for accurate quantitation was 0.1 μg/ml. Only 7 min. is need for each sample.

This method is specific, sufficiently sensitive and may useful for purity control polymers used in medicine.

Received, March 24, 1993

Polytechnic Institute, Jassy
Department of
Physical Chemistry

REFERENCES

1. Simionescu Cr., Popa M.I., Dumitriu S., Z. Naturforsch., **39b**, 387 (1984).

2. Simionescu Cr., Popa M.I., Dumitriu S., Biomaterials, **118** (1986).

3. DellaValle F., Romeo A., Eur. Patent Appl. EP *216453*, April 1, 1987.

4. Rego A., Nelson B., J. Pharm. Sci., **71**, 1219 (1982).

5. Dumitriu S., Popa M.I., Colloid Poly. Sci., *267*, 595 (1989).

6. Hunt J.A., Joshi H.N., Stella V.J., Topp E.M., J. of Control. Release, **12**, 159 (1990).

CROMATOGRAFIA ÎN FAZĂ LICHIDĂ DE ÎNALTĂ PERFORMANŢĂ A CLORULUI DIN POLIMERI

(Rezumat)

Se prezintă o metodă rapidă şi precisă de dozare a ionilor de clor prin cromatografie în fază lichidă de înaltă performanţă.

Aceşti ioni, alături de ionii de brom şi sulfat, rămân în probele de polimeri în procesele de modificare în vederea realizării de noi medicamente.

Cromatografia în fază de înaltă performanţă poate fi aplicată cu succes la identificarea şi dozarea acestor ioni.

Sensibilitatea metodei este sub 0,1 μg ioni de clor pe 1 mg probă.

BULETINUL INSTITUTULUI POLITEHNIC DIN IAŞI
Tomul XXXIX (XLIII), Fasc. 1-4, 1993
Secţia II
CHIMIE ŞI INGINERIE CHIMICĂ

D.C. 661.183.48; 66.097.4

ACIDITY AND CATALYTIC ACTIVITY OF DEALUMINATED MORDENITES

BY

I. SĂNDULESCU, P. ONU, V. POPA and D. GÂNJU

1. Introduction

Scientific and practical interest for zeolite catalysts are determined by high conversion and selectivity, reduced reaction temperatures and another advantages. Catalysts based on mordenites have a higher Brönsted acidity and important uses in the field of catalysis. Selectivity and catalytic activity of this zeolite could be changed between certain limits by ion-exchange with different cations by modification of molar ratio ($SiO_2/Al_2O_3 = m$) or through dealumination method [1],...,[4]. Brönsted acidity may be changed by modification module (m), too. The number of acidic sites of catalysts could be determined by adsorbtion in certain conditions of different organic bases, for examples n-butylamine, and the distribution of acidity strength by thermogravimetric desorbtion of some organic compounds [5].

In this paper are presented experimental dates about acidity of certain dealuminated mordenites and the influence of it in the disproportionation of toluene and isomerization of o-xylene reactions.

2. Experimental Data

Using a mordenite, with oxide formula $10.8\ SiO_2.Al_2O_3.Na_2O.6.4\ H_2O$, by thermal treatment with 6N HCl solution, at different contact times [1], have been obtained dealuminated mordenites with different modules (m): HM-1($m = 18$); HM-18($m = 48.5$) and HM-26($m = 54.1$). The acidity of the samples and distribution of acidity strength have been estimated by adsorbtion and thermogravimetric desorbtion of n-butylamine. For this purpose have been used a Du Pont 1090 thermal analyser. Desorbtion was done until 500°C temperature. From n-butylamine adsorbtion at room temperature have been calculated the number of acidic sites and from the weight loss, as a effect of heating, was calculated the distribution of acidic strength of the partialy dealuminated mordenites dreated by hydrothermal treatment.

The mordenite samples have been tested in the disproportionation of toluene and isomerization of o-xylene reactions. Catalytic reactions were carried out under normal pressure using a continuous flow reactor and reaction products were analysed by GC.

All reactions were done at 250°...400°C and 1.0...5.0 h^{-1} space velocity. Every test was of 2 h long, after that the samples was regenerated. For every dealuminated mordenite and for all catalytic tests the same sample were used.

3. Results and Discussion

Practical results about acidity of dealuminated mordenites and distribution of acidic strength of its are presented in Table 1.

Table 1
Acidity of the Partialy Dealuminated Mordenites

Samples	Acidic sites $\times 10^{20}$	Nr. of acidic sites $\times 10^{20}$			
		<200°C	200°...300°C	300°...400°C	>400°C
HM-1	5.76	2.09	0.81	2.04	0.79
HM-18	6.16	3.69	0.70	0.96	0.88
HM-26	5.28	3.16	0.85	0.68	0.57

Taken into account the practical results, mordenite samples were tested in carboniogenic reactions concerning the disproportionation of toluene and isomerisation of *o*-xylene [5],...,[12]. For HM-1 (Fig. 1), at 375°C, there is a higher concentration of medium acidic sites and for the same temperature on the curve of toluene disproportionation there is a maximum too. In this reaction the soft acidic sites did not action, and strongly sites at higher temperatures produce secondary reaction. In the case of *o*-xylene isomerization (Fig. 2), the maximum conversion there is at low temperatures, about 280°C. So that, at low temperature takes place *o*-xylene isomerization reaction with participation of soft sites of 2.17×10^{20} concentration, while the toluene disproportionation reaction takes place on medium and strongly acid sites of 1.64×10^{20} concentration. The curves have the same shape for HM-18 and HM-26, but the maximum position of its there is a little up or down, depending on the concentration of the acidic sites from the samples. For example in the case of HM-26 sample (Fig. 3), the maximum for toluene disproportionation appears in the field of higher temperature reactions (370°...380°C), which confirm that in this reaction take place strongly and medium acidic sites. In this case the maximum of disproportionation reaction is under 23%, being in accordance to small number of the strongly acidic sites and medium strength of this catalysis. If we are take into account toluene conversion in disproportionation reaction and *o*-xylene conversion in isomerization reaction (Fig. 4) at 330°C we found out a approximately increasing line of its with the increasing of acidic sites which could be actively at reaction temperature. The disproportionation reaction gives higher conversions because it takes place only on strongly acidic sites.

For *o*-xylene, at the same temperature, besides of isomerization reactions take place and transalkylation reactions which are given benzene, toluene polymethyl-

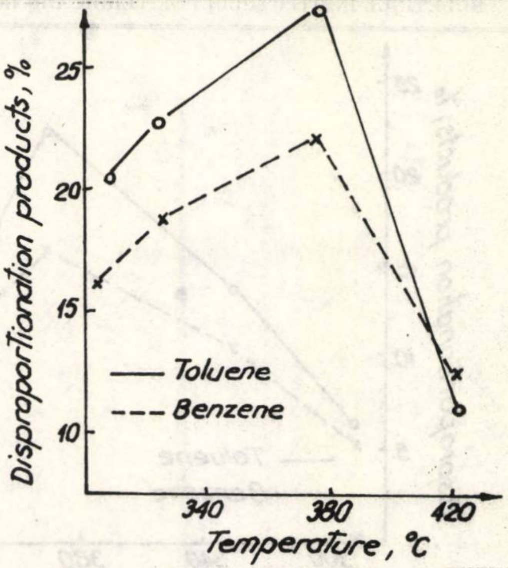

Fig. 1.– Disproportionation of toluene on HM-1.

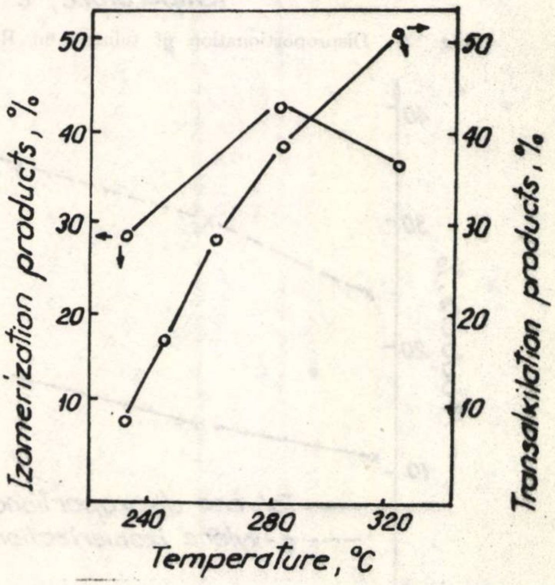

Fig. 2.– Isomerization of *o*-xylene on HM-1.

benzenes and the content of its is over than 20%. Dependence of the toluene transformation degree through disproportionation reaction and *o*-xylene isomerization appears very well if we consider both reaction temperature and number of the acidic sites, which take place in all of these reactions. From Fig. 5 we can deduce

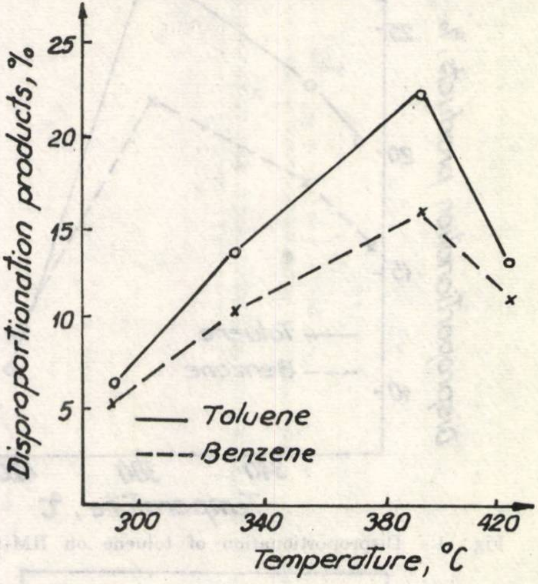

Fig. 3.– Disproportionation of toluene on HM-26.

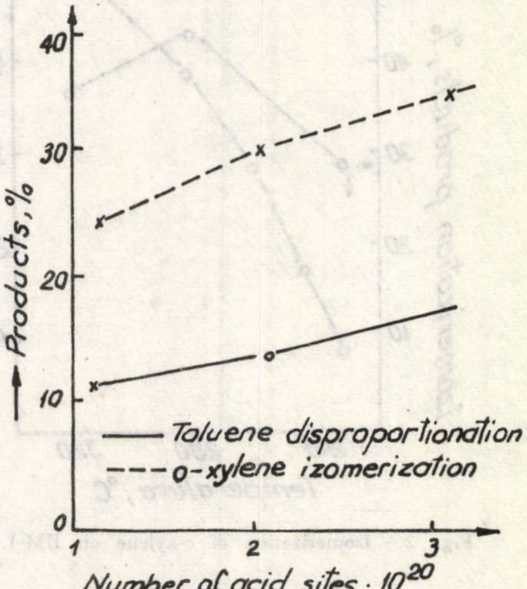

Fig. 4.– Disproportionation of toluene and *o*-xylene isomerization on HM-26, at 33°C.

that at low temperatures on acidic sites takes place *o*-xylene isomerization, with a conversion depassing 45%, while the toluene disproportionation don't exceed 20%. It is possible to conclude that small temperatures are not enough for desorbtion and reorganization of the toluene molecules on strongly acidic sites. Increasing of the reaction temperature determines a decreasing of acidic sites number which take place at reaction and an activation of strongly acidic sites too. In this temperature field predominant are transalkylation reactions, either toluene reaction for which at 375°C conversion is about 50% or 20% for *o*-xylene isomerization, while the disproportionation exceeds 40%.

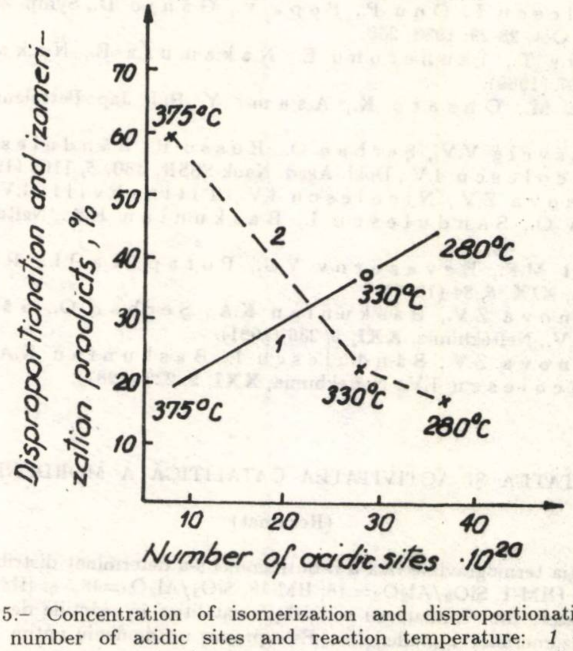

Fig. 5.– Concentration of isomerization and disproportionation products vs. number of acidic sites and reaction temperature: *1* – *o*-xylene isomerization (*p* + *m*-xylene); *2* – toluene disproportionation (benzene+xylene).

4. Conclusions

If the distribution of the acidic strength of mordenite catalysts is known, the optimum field of the reaction for certain catalytic process may be found. Also, it is possible to consider that in the case of certain catalytic process on an acidic catalyst, the fundamental parameters are determinated by the acidic strength distribution, type of reaction, strength of reactants connections with catalyst and by reaction temperature.

Received, June 20, 1991

University of Bucharest
and
Polytechnic Institute, Jassy,
Department of General Chemistry

REFERENCES

1. Onu P., Gânju D., Ababi V., Rev. Chimie, **34**, *4*, 314 (1983).

2. Onu P., Gânju D., Săndulescu I., Symp. Zeolites in Modern Technology, Jassy, Oct. 28-29, 1983, 258.

3. Fernandez C., Vedrine J.C., Grosmangin J., Szabo G., Zeolites, **6**, 484 (1986).

4. Kalló D., Minakev Kh.M., *Catalysis on Zeolites*. Akadémiai Kiadó, Budapest, 1988, 205.

5. Săndulescu I., Onu P., Popa V., Gânju D., Symp. Zeolites in Modern Technology, Jassy, Oct. 28-29, 1983, 250.

6. Amemiy T., Tsunetonu E., Nakamura E., Nakazova T., Org. Chem., **34**, *10*, 3107 (1969).

7. Okada M., Obsato K., Asami Y., Bull. Jap. Petroleum Inst., **13**, *1*, 45 (1971).

8. Berentsveig V.V., Şerban O., Russu R., Săndulescu I., Gryaznova Z.V., Nicolescu I.V., Dokl. Akad. Nauk SSSR, **230**, *5*, 1102 (1976).

9. Griaznova Z.V., Nicolescu I.V., Titinshvili G.V., Şerban O., Občinikova O., Săndulescu I., Baskunian K.A., Neftekhimia, **XVII**, *4*, 531 (1977).

10. Sovčit M.F., Egyazarov Y.G., Potapova I.L., Romanovsky B.V., Neftekhimia, **XIX**, *6*, 84 (1979).

11. Griaznova Z.V., Baskunian K.A., Şerban O., Săndulescu I., Nicolescu I.V., Neftekhimia, **XXI**, *2*, 236 (1981).

12. Griaznova Z.V., Săndulescu I., Baskunian K.A., Şerban O., Russu R., Nicolescu I.V., Neftekhimia, **XXI**, *2*, 226 (1981).

ACIDITATEA ŞI ACTIVITATEA CATALITICĂ A MORDENIŢILOR

(Rezumat)

Prin desorbţia termogravimetrică a n-butilaminei s-a determinat distribuţia tăriei acide a câtorva mordeniţi (HM-1, $SiO_2/Al_2O_3 = 18$; HM-18, $SiO_2/Al_2O_3 = 48{,}5$ şi HM-26, $SiO_2/Al_2O_3 = 54{,}5$). Rezultatele sunt corelate cu activităţile catalitice în reacţiile de disproporţionare a toluenului şi de izomerizare a o-xilenului. Este propus un domeniu optim al temperaturii de reacţie în raport cu tăria centrilor acizi.

BULETINUL INSTITUTULUI POLITEHNIC DIN IAŞI
Tomul XXXIX (XLIII), Fasc. 1–4, 1993
Secţia II
CHIMIE ŞI INGINERIE CHIMICĂ

D.C. 547.476.6; 66.022

INVESTIGATIONS CONCERNING THE OBTAINMENT OF HIGH PURITY MONOMETHYLADIPATE

BY

NATALIA HURDUC, LUCIA ODOCHIAN,
C. LUCA, ELENA MIHAI and ELENA IONESCU

1. Introduction

In a previous paper [1] we have presented a genuine method for the synthesis of monomethyladipate from adipic acid and dimethyladipate, in melt, by employing the *p*-toluenesulfonic acid as catalyst [2].

Having in view the importance of the monomethyladipate in high yield synthesis of the sebacic acid, in the present paper the separation of monomethyladipate from the reaction mixture, its high purification and its characterization by suitable physical and chemical methods are studied.

2. Experimental

For the separation of the monomethyladipate from the reaction mixture by the above mentioned synthesis method [1] the substance has been cooled, two phases being thus separated: a solid and a liquid one, further characterized by the following analysis methods:

a) *Thermogravimetric Analysis*, performed on a Paulik-Paulik-Erdey type derivatograph (MOM Budapest), assuring the simultaneous recording of the following curves: thermogravimetric (TG), derivated thermogravimetric (DTG), differentiated thermal (DTA) as well as of the temperature curve (T). For the obtainment of comparable data, the same working conditions have been applied: heating rate – 12°C/min, sample weight – 20 mg, control material – Al_2O_3 calcinated at 1200°C, atmospheric air.

b) *IR Spectrophotometric Analysis* employed a Perkin–Elmer absorption spectrophotometer, the substances being placed on KBr pellets.

Nuclear magnetic resonance spectrophotometry (RMN) recorded the spectra in $CHCl_3$ used as solvent, at a temperature of 55°C, by employing a Jeol C-60-type spectrometer with a frequency of 60 MHz.

c) *Refractometric Analysis* employed an Abbé refractometer with a precision of 0.001.

d) *Cryoscopic Analysis* was made with a VEB (K) type cryoscope (Leipzig 22), by employing benzene as solvent.

3. Results and Discussion

The two phases obtained by cooling the reaction mixture, as well as the adipic acid and pure dimethyladipate have been subjected to thermogravimetric analysis.

The identity of TG, DTG and DTA curves, observed from the thermogrammes of the adipic acid (Fig. 1) and of the solid phase (Fig. 2) leads to the conclusion that the solid phase represents the pure non-reacted adipic acid.

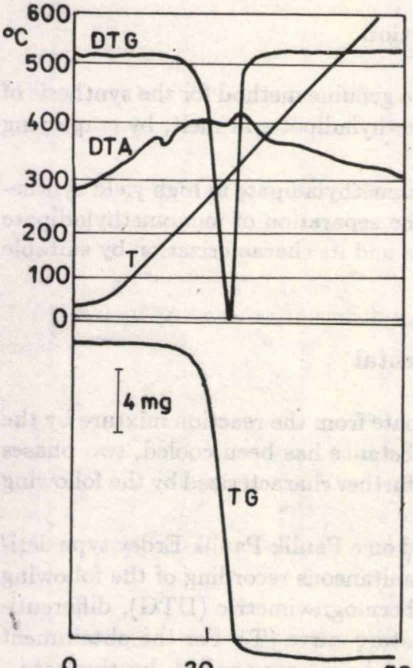

Fig. 1.– Thermogramme of the pure adipic acid.

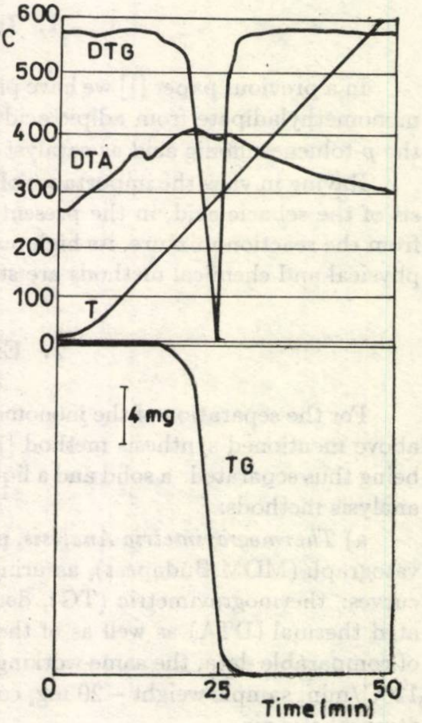

Fig. 2.– Thermogramme of the solid phase.

The thermogrammes of the pure dimethyladipate (Fig. 3) and of the liquid

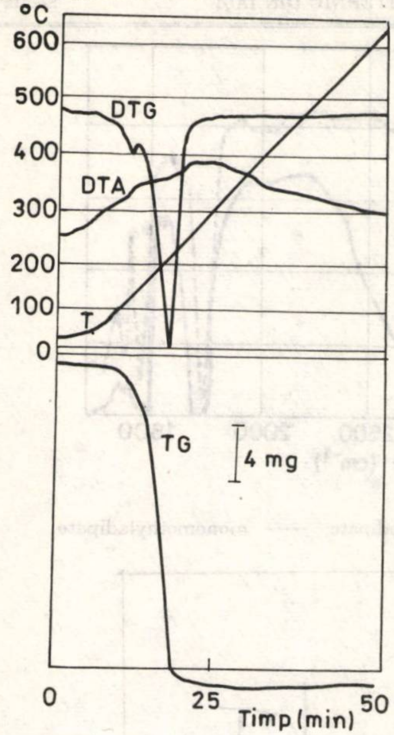

Fig. 3.– Thermogramme of the pure-dimethyladipate.

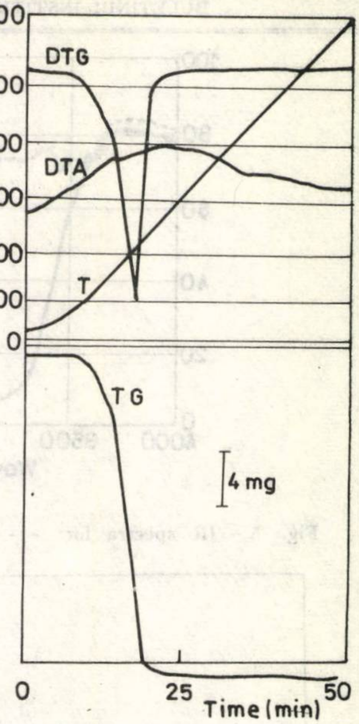

Fig. 4.– Thermogramme of the liquid phase.

phase (Fig. 4) are not identical, which suggests that the liquid phase is a mixture. In order to check this result, the liquid phase has been characterized by density and refraction indices. Table 1 presents these characteristics, as compared with those of the pure monomethyladipate and dimethyladipate [3].

Table 1
Physico-chemical Characteristics of the Liquid Phase

Compound analyzed	d_{20}	n_D^{20}
Dimethyladipate	1.063	1.4285
Monomethyladipate	1.081	1.4401
Liquid phase	1.082	1.4335

The analysis of such data confirms that the liquid phase is a mixture. For the separation of the compounds, the liquid phase has been subjected to fractionated distillation, in vacuum, two fractions being thus obtained.

Table 2 presents the separation conditions of the two fractions (T_f, °C/mm Hg) and the refraction indices (n_D^{20}) corresponding to two synthesis samples, as compared with those of pure dimethyladipate and monomethyladipate, the conclusion being that fraction *I* is pure dimethyladipate, while fraction *II* – pure monomethyladipate.

As the refraction index, density, molar weight and molar refraction may consti-

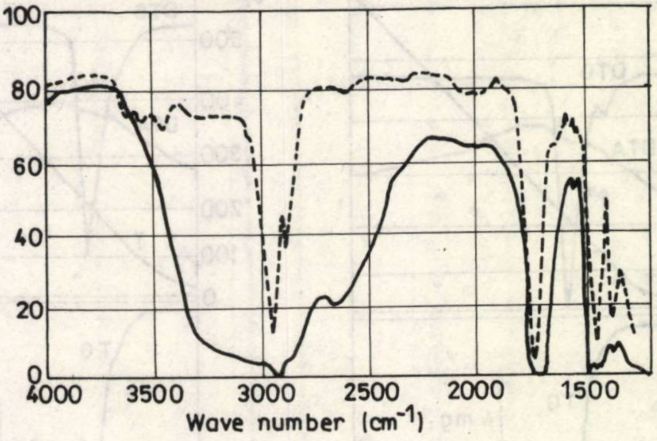

Fig. 5.– IR spectra for: - - - dimethyladipate; —— monomethyladipate.

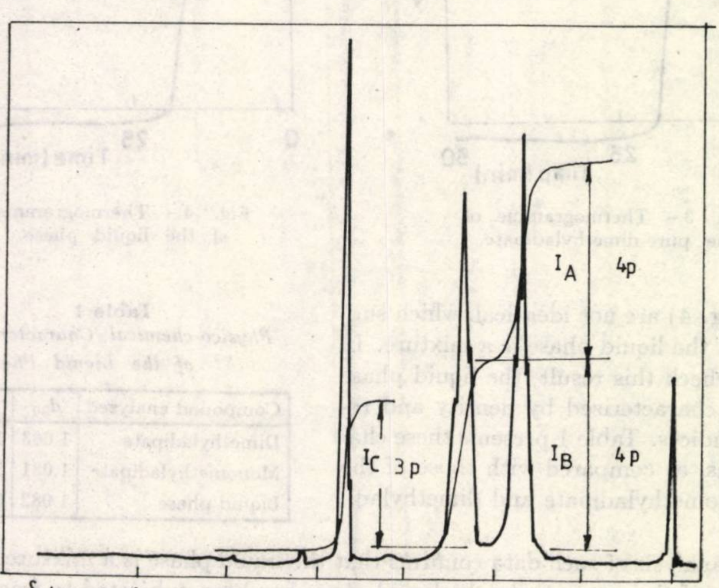

Fig. 6.– The RMN spectrum for fraction *II* (monomethyladipate).

tute a criterion of a substance's purity, they have been employed for the characterization of the monomethyladipate separated through fractionation under vacuum.

Table 2

Refraction Indices at 20° C

Fractionated sample	Compound analyzed	T_f °C/mm Hg	n_D^{20}
I	Dimethyladipate	110/14	1.4285
	Monomethyladipate	162/10	1.4401
I	Fraction *I*-1	90...95/3...4	1.4285
	Fraction *I*-2	142...148/2.5...3	1.4401
II	Fraction *II*-1	90...98/3...4	1.4285
	Fraction *II*-2	142...148/3	1.4400

Table 3, presenting these values for the monomethyladipate we have separated, along with the theoretical values, evidences the good agreement between them, which is indicative of its high degree of purity.

Table 3

Refractometric Characteristics of the Monomethyladipate

Monomethyladipate	M*)	n_D^{20}	d_{20}	R_M
Theoretically	160.17	1.4401	1.081	38.97
Experimentally	160.17	1.4402	1.080	39.05

*) The molar weight has been determined from cryoscopic data.

The IR and the RMN spectra recorded lead to the same conclusion. Thus, Fig. 5 plots graphically the IR spectra of pure dimethyladipate as well as of fraction *III*, where is to be observed a wide band within the 2 500...3 500 cm^{-1} domain, corresponding to the associated carboxyl, resulted in accordance with the theoretical spectrum [4], [5], which confirms that this fraction is a pure monomethyladipate.

The same result is supported by the RMN spectrum, presented in Fig. 6 for fraction *II*.

The performed physical and chemical analyses confirm the separation of the monomethyladipate with a high degree of purity (99.98%) on condition that the fractionation conditions (pressure of 3...4 mm Hg and temperature interval 142°...148°C) should be strictly applied.

Also, under the synthesis and separation employed conditions, both the adipic acid and the pure dimethyladipate may be recovered, thus offering the possibility of their re-introduction into the process of synthesis.

Received, June 11, 1990

Polytechnic Institute, Jassy,
Department of Physical Chemistry
and
Research Center for Synthetic
Fibres, Săvineşti

REFERENCES

1. Hurduc N., Odochian L., Luca C., Mihai E., Ungureanu Şt., Ionescu E., Romanian Patent, Nr. *93557* (1987).

2. Hurduc N., Odochian L., Luca C., Mihai E., Ionescu E., Bul. Inst. polit., Iaşi, **XXXVI** (**XL**), *3-4*, s. II, 35 (1990).

3. * * * E.G.A. Catalog, Handbook, 1981/1982.

4. Mullikam R.C., Pitzer K.S., J. Amer. Chem. Soc., **80**, 3515 (1958).

5. Flett M.St., J. Chem. Soc., 962 (1951).

CERCETĂRI PRIVIND OBŢINEREA MONOMETILADIPATULUI DE ÎNALTĂ PURITATE

(Rezumat)

Se prezintă rezultatele unui studiu privind separarea şi purificarea monometiladipatului din amestecul de reacţie obţinut printr-o metodă originală din dimetiladipat şi acid adipic în topitură în prezenţa acidului *p*-toluensulfonic drept catalizator.

Monometiladipatul separat a fost caracterizat utilizând următoarele metode fizico-chimice: metoda termogravimetrică, spectrometria IR, spectrometria magnetică nucleară (RMN), refractometrie, densitate şi criometrie, metode care indică un înalt grad de puritate, de 99,98%.

BULETINUL INSTITUTULUI POLITEHNIC DIN IAŞI
Tomul XXXIX (XLIII), Fasc. 1-4, 1993
Secţia II
CHIMIE ŞI INGINERIE CHIMICĂ

D.C. 542.936; 547.593; 54-92

FERROCENE POLYMERS AS CATALYSTS IN THE DEHYDRATION REACTION OF CYCLOHEXANOL

BY

I. MAZILU and LUCIA TĂTARU

1. Introduction

Since the dehydration of alcohols is a reaction which can proceed in either homogeneous or heterogeneous catalysis, in the presence of Lewis acids or strong mineral ones [1] it might be suitable for studying the correlation between physical properties and catalytic action for certain polymers containing ferrocene nuclei.

Thus the catalytic properties have been studied of ferrocene polymers which contain double bonds on the macromolecular chain and show signal in ESR spectrum as well as of those thermally treated [2]...[4].

In previous papers the behaviour of some ferrocene polymers as redox initiators in polymerization reaction was discussed [5].

In what follows the studies on their possible applications, their testing as catalysts in dehydrating the cyclohexanol to cyclohexene was considered to be of interest.

2. Experimental

The dehydration reaction of the cyclohexanol was accomplished in two ways:

I. In solid–liquid heterogeneous catalysis. The cyclohexanol in which the finely powdered catalyst was introduced was heated under stirring and refluxing. From time to time samples have been taken and analyzed chromatographically.

II. In gas–solid heterogeneous catalysis. The procedure implies the passing of cyclohexanol vapours through a column filled with catalyst on glass support and heated at temperatures between 160°...250°C.

The yields were followed by means of gas-chromatography. The analyses were done on a "GAS CHROMATOGRAPH C.G.H.F. 18-3" apparatus, at a temperature of 163°C with 2 μl sample, 160 mA and sensitivity 4. The hydrogen was used as carrier gas; the 2 m long column was filled with CARBOWAX 20 M.

3. Results and Discussion

The catalytic action of the following ferrocene polymers has been tested:

a) Poly-*p*-ferrocenylphenylacetylene of *A* type, obtained by condensing the *p*-ferrocenylphenylacetophenone in the presence of acetalic salts (structure I) [6].

b) Poly-*p*-ferrocenylphenylacetylene of *B* type obtained by thermal polymerization at 200°C of the *p*-ferrocenylphenylacetylene, (structure II) [7], and a polymer of *C* type (structure III), obtained by temperature action on the α-chloro-β-formyl-*p*-ferrocenylstyrene [8].

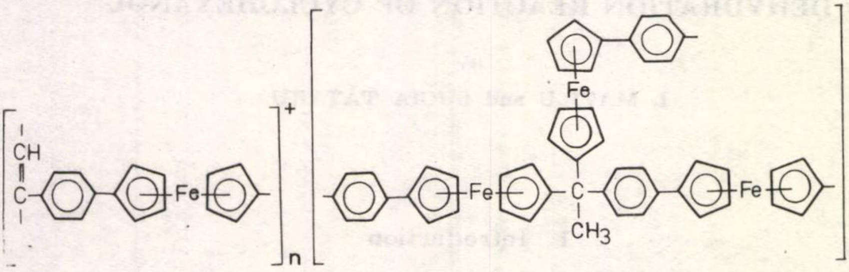

(I)

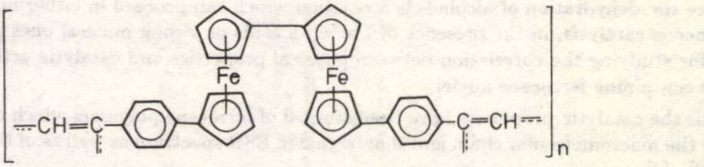

(II)

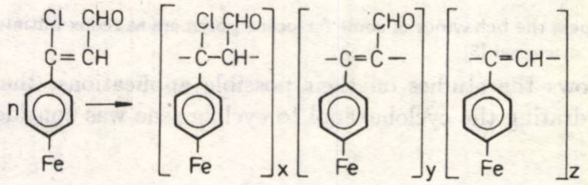

(III)

All the tested polymers are dark brown powders, insoluble in common organic solvents and infusible up to 350°C. The polymers of *A* and *B* type give ESR signal, having a paramagnetic particle concentration of about 10^{17} spin/g. The former has an electric conductivity of 10^{-11} ohm^{-1}cm^{-1}.

Although the polymers of *B* and *C* type have alternate units along the main chain they do not exhibit semiconducting properties, probably due to sterical hindrances caused by bulky substituents which disturb the molecule planarity and prevent the conjugation from extending [7], [8].

By taking into account the structure and properties of these polymers the mechanism of the heterogeneous catalysis might be considered to proceed through a reversible electron transfer between reagent and catalyst which could be promoted by an alternate bond system in the catalyst molecule. A similar mechanism was proposed by Paushkin for dehydration of the dimethylvinylcarbinole in the presence of ferrocene pyropolymers [9].

3.1. Solid–Liquid Heterogeneous Catalysis

In this procedure the increase of yield in dehydrated product depends mainly on the reaction duration. In Fig. 1 the yield versus the reagent–catalyst contact time is plotted.

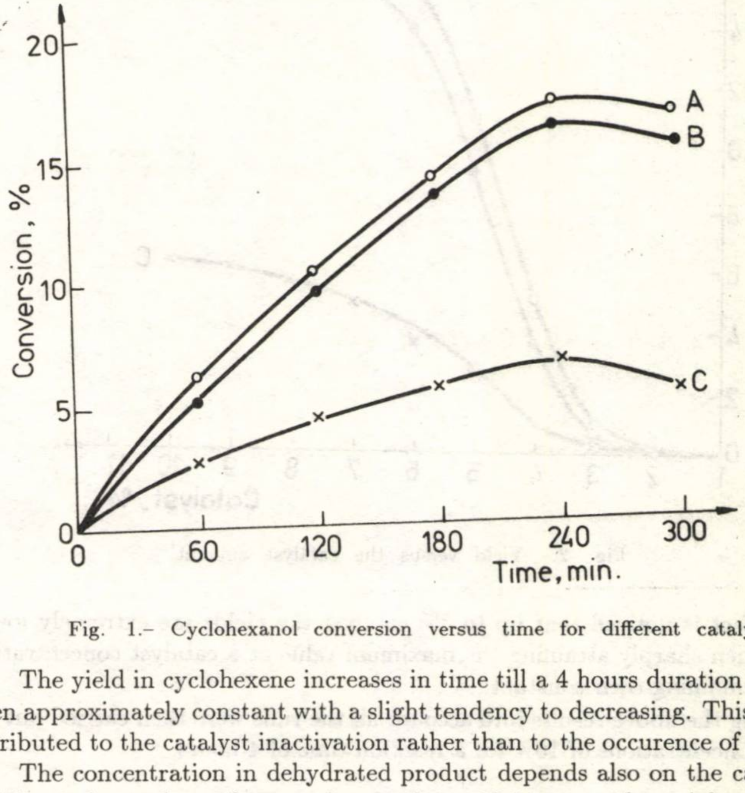

Fig. 1.– Cyclohexanol conversion versus time for different catalysts.

The yield in cyclohexene increases in time till a 4 hours duration and remains then approximately constant with a slight tendency to decreasing. This fact may be attributed to the catalyst inactivation rather than to the occurence of by products.

The concentration in dehydrated product depends also on the catalyst used. In Fig. 1 close values of conversion attaining 17.51 are evidenced for the *A* and *B* catalysts and lower ones for the *C* one.

The weaker catalytic activity of the *C* type polymer is probably due to the lack of electric and paramagnetic properties. The ferrocene polymers are mentioned in literature to show redox properties which increase the rate of the electron exchanges. Consequently, these polymers are active in the dehydration reactions although their content in paramagnetic particles is lower (less than 10^{-17} spin/g) and the alternate double bonds are absent.

All the polymers tested in the present paper contain the redox system ferrocene–ferricinium (Fe^{2+} - Fe^{3+}) whose catalytic action is enhanced with the polymers *A* and *B* by their electric and magnetic properties. The experimental data support the above statement.

The catalyst concentration also influences the yield of the dehydration reaction.

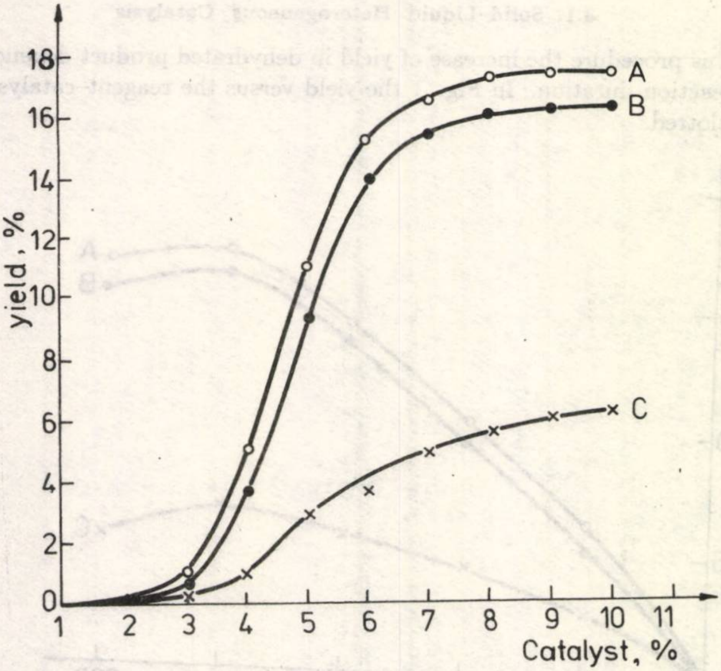

Fig. 2.– Yield versus the catalyst amount.

The fact is noticed that up to 3% catalyst the yields are extremely low and increase then sharply attaining the maximum value at a catalyst concentration of 8% and remaining then constant.

Taking the above results into account all the runs were then carried out using catalyst concentrations of 10% for a reaction time of 4 hours.

3.2. Solid–Gas Heterogeneous Catalysis

In this case the reaction temperature is the essential factor in determining the cyclohexene yield increase. In Fig. 3 the yield dependence vs. the temperature is depicted for the three types of catalysts.

In all cases the yield values lower than in the first procedure were noticed. The yield is seen to increase with increasing temperature up to 230°C above which begins to decrease. In this case the decrease in dehydrated product concentration is due to both catalyst inactivation and occurence of the by products in the reaction medium in greater amounts with increasing temperature. These by products consist mainly of oxydation products as found chromatographycally (Fig. 4).

It can be seen that with the first procedure small amounts (1...2.5%) of cyclo-

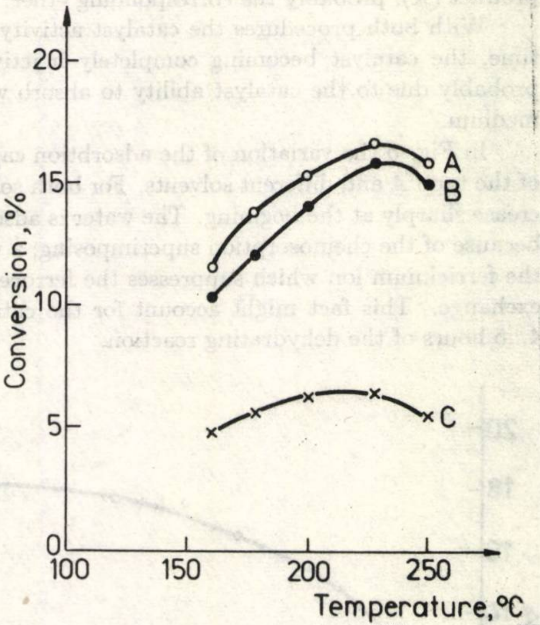

Fig. 3.– Correlation yield–temperature for the three catalysts (*A*, *B*, *C*).

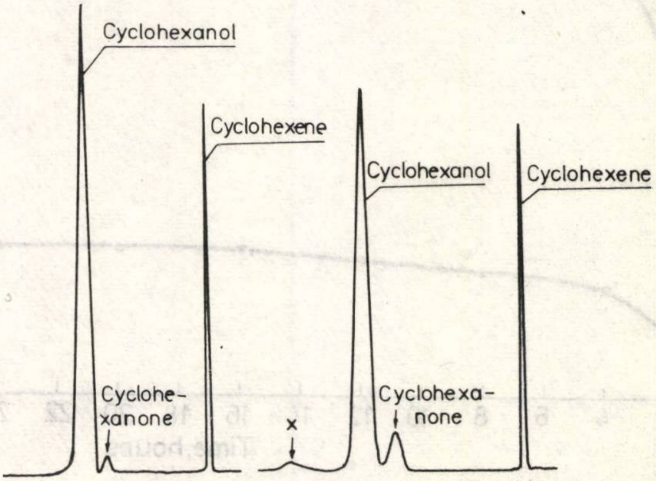

a *b*

Fig. 4.– Chromatogram of the reaction products obtained by cyclohexanol dehydration: *a* - obtained by procedure I, reaction time 4 hours, catalyst 10%; *b* - obtained by the procedure II at 230° C.

hexanone occur, while with the second one these amounts increase with temperature attaining a concentration of 5...6% at 230°C.

Along with cyclohexanone small traces were detected of a new unidentified product (X), probably the corresponding ether.

With both procedures the catalyst activity decrease with increasing reaction time, the catalyst becoming completely inactive after 4...5 hours. This fact is probably due to the catalyst ability to absorb water or reagent from the reaction medium.

In Fig. 5 the variation of the adsorbtion capacity is depicted, for the catalyst of the type *A* and different solvents. For both solvents the adsorbtion is seen to increase sharply at the begining. The water is adsorbed much stronger than benzene because of the chemosorption superimposing; a water molecule is thus attached to the ferricinium ion which suppresses the ferrocene–ferrocinium reversible electron exchange. This fact might account for the catalyst inactivation during the first 4...5 hours of the dehydrating reaction.

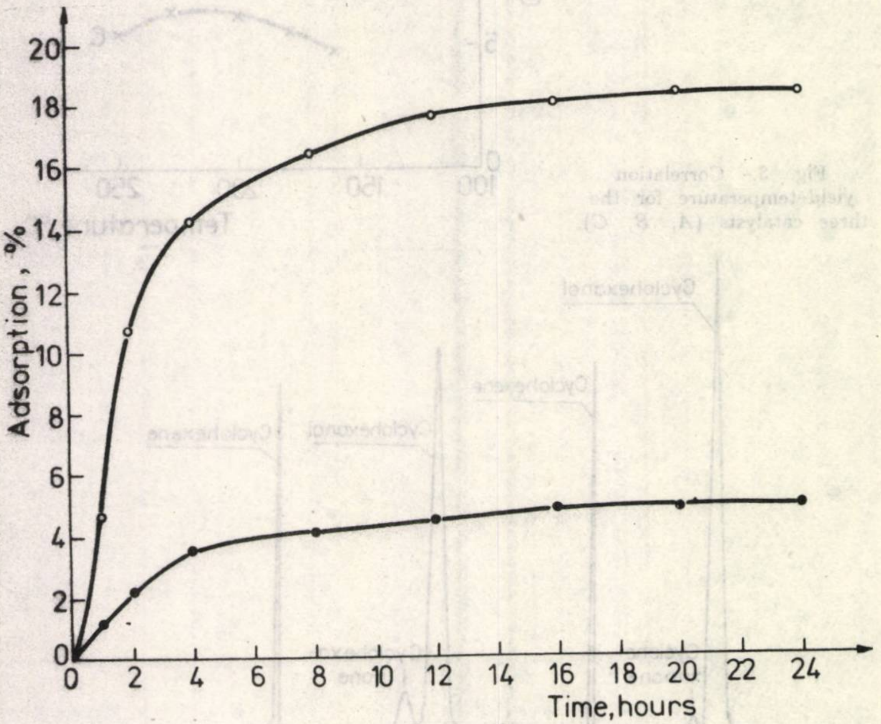

Fig. 5.– The adsorption capacity versus time; *1* – polar solvent (water); *2* – unpolar solvent (benzene).

The above assumptions are also supported by the possibility of reactivating the inactive polymers by heating them at 150°C in air when the desorption takes place. Besides, the IR spectra and elemental analysis data evidence that by these polymers, their structure and constitution at the end of the catalytic process remain unchanged.

In literature the possibility of treating the polymers thermally is mentioned in order to improve their catalytic properties. This phenomenon is caused by the increase in percentage of ferricinium states in the catalyst polymer [9],[10]. In our case, the ferricinium states in the catalyst structure are preponderant and consequently the thermal treatment does not enhance the catalytic activity. The experimental results confirm the above statements, the obtained yields with all the thermally treated polymers being generally low.

Received, March 31, 1993

Polytechnic Institute, Jassy,
Department of
Organic Chemistry

REFERENCES

1. Helmkamp G.K., Johnson jr. H.W., *Selected Experiments in Organic Chemistry*. W.H. Freeman and Comp., San Francisco and London, 1968, 85.
2. Paushkin Ya.M., Burova L.M., Amwlehina L.N., Alekseev S.N., Dokl. Akad. Nauk, SSSR, **148**, 2 (1968).
3. Paushkin Ya.M., Burova I.M., Sladkov A.M., Nepakiath V.P., Kudryavtzeva Y.P., Korshak V.V., Dokl. Akad. Nauk, SSSR, **180**, 622 (1968).
4. Voronina M.A., Vishnyakova T.P., Paushkin Ya.M., Božilova M.A., Aliev L.A., Vysokomol. Soed., **11**, 882 (1969).
5. Simionescu Cr., Mazilu I., Rev. Roum. Chim., **22**, *5*, 753 (1977).
6. Simionescu Cr., Lixandru T., Tătaru L., Mazilu I., J. Organomet. Chem., *73*, 375 (1974).
7. Simionescu Cr., Lixandru T., Mazilu I., Tătaru L., J. Organomet. Chem., *113*, 23 (1976).
8. Simionescu Cr., Lixandru T., Tătaru L., Mazilu I., Cocîrlă I., J. Organomet. Chem., *102*, 219 (1975).
9. Paushkin Ya.M., Vth. Internat. Conf. on Organomet. Chem., Moscow, 1971, **II**, 577.
10. Paushkin Ya.M., Vishnyakova T.P., Lunin A.F., Nizova S.A., *Organičeskie polymernie polyprovodniki*. Khimia, Moskva, 1971, 169-208.

POLIMERI FEROCENICI CATALIZATORI ÎN REACŢIA DE DESHIDRATARE A CICLOHEXANOLULUI

(Rezumat)

Au fost testaţi, drept catalizatori în reacţia de deshidratare a ciclohexanolului, o serie de polimeri ferocenici. Reacţia a fost efectuată în cataliză heterogenă solid–lichid şi solid–gaz. A fost studiată influenţa diferiţilor factori asupra randamentului în produsul de deshidratare.

În timpul reacţiei catalizatorul este dezactivat, dar el poate fi reactivat prin încălzire la 150°C, în aer.

BULETINUL INSTITUTULUI POLITEHNIC DIN IAŞI
Tomul XXXIX (XLIII), Fasc. 1–4, 1993
Secţia II
CHIMIE ŞI INGINERIE CHIMICĂ

D.C. 66.095.192; 547.551.42.

KINETIC STUDY ON SAPONIFICATION OF METHYL 2-CHLORO-DIMETHYLAMIDOSULPHONYL-PHENOXYACETATE

BY

CORNELIU ONISCU, EUGEN HOROBA,
DAN CAŞCAVAL and ADINA DUMITRAŞCU

1. Introduction

In previous papers [1],...,[4] the synthesis of new compounds with physiological activity were reported, namely derivatives of sulphonamidated halogen phenoxyacetic acids, showing a complex action of the energizing of the nervous rell, antidepressive and anticonvulsant action in the "petit-mal" diseases, a new class of chemical compounds of lower toxicity being thus introduced in therapeutics. In the previous papers some stages involving in the synthesis of these products were studied.

In the present paper a kinetic study of the saponification of methyl 2-chloro-dimethylamidosulphonyl-phenoxyacetate is presented and the rate constant and the energy of activation determined.

2. Kinetic Analysis

The energizing drugs coming from the 2-chloro-phenoxyacetic acid are synthesized by the following reaction scheme:

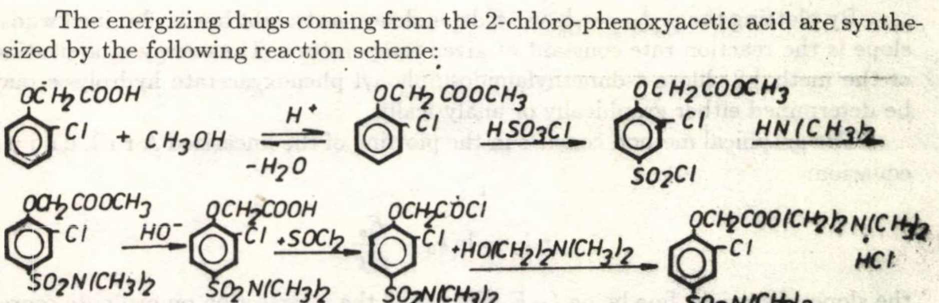
OCH2COOH
Cl
+ CH3OH
H+
-H2O
OCH2COOCH3
Cl
HSO3Cl
OCH2COOCH3
Cl
SO2Cl
HN(CH3)2
OCH2COOCH3
Cl
SO2N(CH3)2
HO-
OCH2COOH
Cl
SO2N(CH3)2
+SOCl2
OCH2COCl
Cl
SO2N(CH3)2
+HO(CH2)2N(CH3)2
OCH2COO(CH2)2N(CH3)2
Cl
HCl
SO2N(CH3)2

The hydrolysis of the methyl 2-chloro-4-dimethylamidosulphonyl-phenoxyacetate is particularly important since the hydrolysis of the amidosulphonyl group and, hence, the cancellation of the biological action is also possible during this stage.

The kinetic study of the hydrolysis of methyl-2-chloro-4-amidosulphonyl-phenoxyacetate with kalium hydroxyde was performed under the following conditions: a) ester/KOH mole ratio = 1:1; b) the reagents were used as methanolic solutions (85% methanol, 15% water, by vol.); c) temperatures: 14°, 27°, 37°and 48°C.

The process development was followed by the reaction freezing, the addition of an amount of HCl taken in excess toward the KOH amount and potentiometric titration with a 2.15×10^{-3} M KOH solution.

For the hydrolysis reaction:

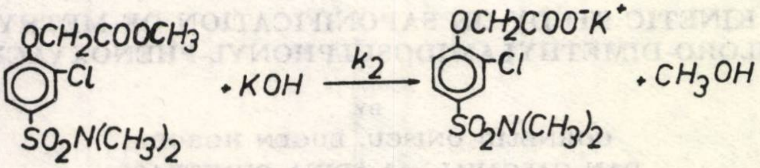

the second order reaction rate [5] is described by the equation:

$$\frac{\mathrm{d}C_x}{\mathrm{d}\tau} = k_2(C_0 - C_x)^2,$$

where: C_x – concentration of the forming kalium salt, [mol/l]; C_0 – initial concentration of the reagents, [mol/l]; k_2 – reaction rate constant, [l/mol.s]; τ – time, [s].

By the integration of the rate equation:

$$\int_0^{C_{xf}} \frac{\mathrm{d}C_x}{(C_0 - C_x)^2} = \int_0^{\tau_f} k_2\,\mathrm{d}\tau$$

the following relation

$$\frac{1}{C_0 - C_{xf}} - \frac{1}{C_0} = k_2\tau_f$$

is obtained.

By plotting the $\frac{1}{C_0-C_x} - \frac{1}{C_0}$ vs. τ dependence, a straight line is obtained whose slope is the reaction rate constant at given temperature. The energy of activation of the methyl-2-chloro-4-dimethylamidosulphonyl phenoxyacetate hydrolysis may be determined either graphically or analytically.

The graphical method consists in the plotting of the linearized Arrhenius equation:

$$\ln k_2 = \ln k_0 - \frac{E_a}{RT},$$

the slope of straight line being $(-E_a/R)$, while the intersection on ordinate represents the preexponential factor (k_0).

According to the analytical method, two values of rate constant for two different temperatures are chosen and two equations with E_a and K_0 obtained.

3. Results and Discussion

The experimental results are depicted in Figs. 1...4.

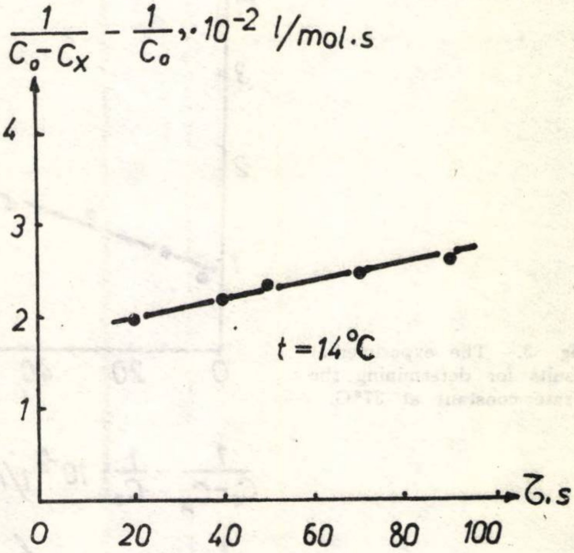

Fig. 1.– The experimental results for determining the rate constant at 14°C.

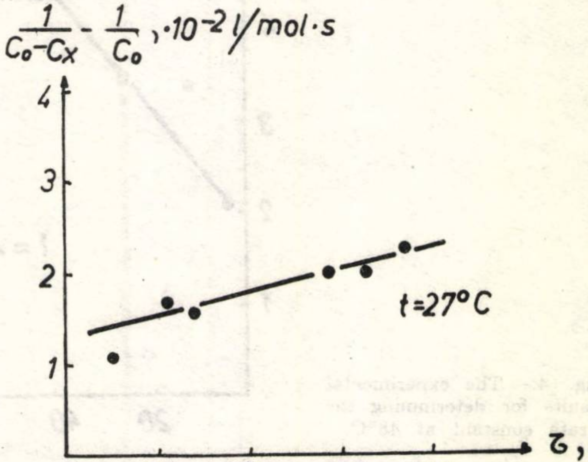

Fig. 2.– The experimental results for determining the rate constant at 27°C.

The rate constants at different temperatures are listed in Table 1.

The energy of activation was calculated by means of both methods. By means of the graph in Fig. 5 the E_a value was estimated namely:

$$E_a = 33.26 \text{ Kj/mol}.$$

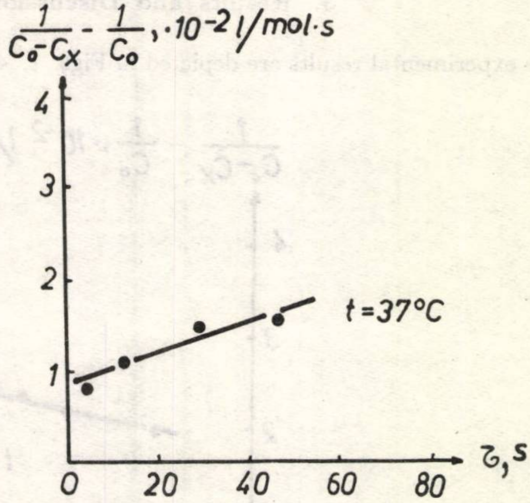

Fig. 3.– The experimental results for determining the rate constant at 37°C.

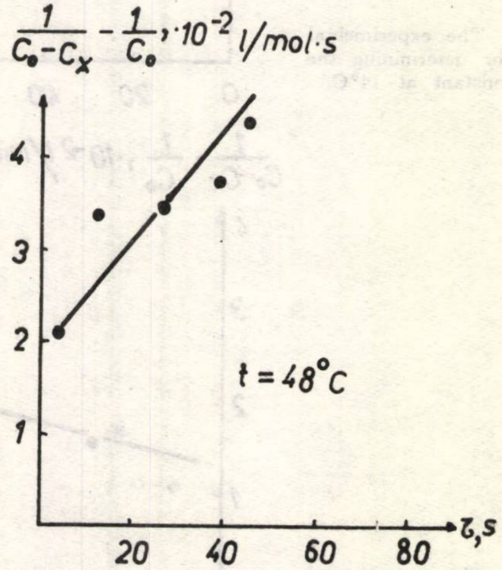

Fig. 4.– The experimental results for determining the rate constant at 48°C.

Table 1

The Rate Constants at Different Temperatures

Temperature, [°C]	14	27	37	48
$k_2 \times 10^2$, [l/mol.s]	2.08	3.33	4.44	8.33

The energy of activation of 31.02 Kj/mol and preexponential factor of 9.04×10^3 l/mol.s were obtained analytically.

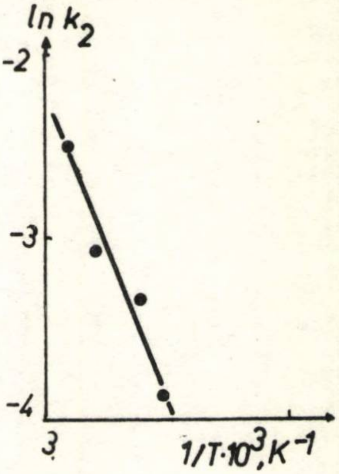

Fig. 5.– The graph for determining the energy of activation.

These values may be used for the modelling of the technological process in order to chose the optimum conditions of hydrolysis of methyl-2-chloro-4-dimethylamidosulphonyl phenoxyacetate.

Received, June 3, 1992

Polytechnic Institute, Jassy,
Department of
Organic Industries

REFERENCES

1. Oniscu C., Horoba E., Rev. Chim., **37**, *3*, 211 (1986).
2. Oniscu C., Botez C., Bul. Inst. polit., Iaşi, **18**, *3-4*, 119 (1972).
3. Oniscu C., Horoba E., Rev. Chim., **35**, 7 (1984).
4. Oniscu C., Botez C., Bul. Inst. polit., Iaşi, **15**, *3-4*, 63 (1969).
5. Neniţescu C.D., *Chimie organică*. EDP, Buc., 1974.

STUDIUL CINETIC AL REACŢIEI DE SAPONIFICARE A 2-CLOR-4-DIMETILAMIDOSULFONIL FENOXIACETATULUI DE METIL

(Rezumat)

Se prezintă un studiu cinetic al reacţiei de saponificare a 2-clor-4-dimetilamidosulfonil fenoxiacetatului de metil cu hidroxid de potasiu. S-au determinat constantele de viteză ale reacţiei de hidroliză la temperaturi diferite şi energia de activare a procesului, împreună cu factorul preexponenţial. Energia de activare s-a determinat grafic şi analitic.

BULETINUL INSTITUTULUI POLITEHNIC DIN IAŞI
Tomul XXXIX (XLIII), Fasc. 1–4, 1993
Secţia II
CHIMIE ŞI INGINERIE CHIMICĂ

C.D. 668.8; 661.727

UNE NOUVELLE CATÉGORIE DE COLORANTS AZOÏQUES

PAR
SAVEL IFRIM

1. Introduction

Les colorants azoïques peuvent être obtenus, facilement, par copulation des sels de diazonium des amines aromatiques primaires avec différents composants de copulation. Les cations de diazonium étant des réactifs électrophiles, l'opération de copulation passe par une réaction de substitution électrophile sur le noyau aromatique du composant de copulation.

Les colorants azoïques présentent une gamme chromatique très vaste avec de belles nuances, à partir de jaune, orange et rouge jusqu'à vert, bleu et noir. Ils teintent les fibres cellulosiques et également les fibres protéiques, comme les fibres de laine et de soie naturelle; on réalise facilement les teintures avec ces colorants. Ces propriétés des colorants azoïques justifient leur fabrication et utilisation dans la technique en grandes quantités par rapport aux autres classes de colorants organiques. On peut apprécier que 50% des colorants synthétiques utilisés dans la pratique sont azoïques.

La liaison des colorants avec les fibres textiles se réalise par forces van der Waals, par liaisons hydrogène et par liaisons électrostatiques; dans le cas des colorants azoïques réactifs apparaissent des liaisons covalentes. La nature des interactions entre colorants et fibres textiles dépend des groupements fonctionnels se trouvant dans la structure chimique des colorants, mais aussi de la structure chimique des fibres textiles.

Parmi les groupements organiques se trouvant dans la molécule des colorants azoïques on peut indiquer ceux hydroxyles, aminiques, carboxyliques, sulfoniques, etc. Ce sont des groupements auxochromiques. On ne connaît pas des colorants organiques ayant dans leur structure chimique des groupements aldéhydiques comme groupements auxochromiques.

Le but de ce travail est de prouver qu'on peut synthétiser des colorants azoïques dont les molécules auront, à côté des autres groupements auxochromiques, également des groupements aldéhydiques ayant un rôle semblable. Les premiers résultats obtenus dans ce domaine ont été publiés dans une Note précédente [1].

2. Partie théorique

L'action auxochromique des groupements organiques se manifeste quand ils sont liés au noyaux aromatiques, ayant lieu à la fois une intensification de la couleur du chromogène. Ce phénomène peut être expliqué par la conjugaison des électrons libres, existant sur les atomes des groupements auxochromiques avec les électrons π des noyaux aromatiques [2]. En conséquence la présence des auxochromes détermine un déplacement de l'absorbtion de la lumière vers le rouge. Par exemple le benzène est incolore pour l'oeil humain, mais dans l'ultraviolet il a un spectre caractéristique, ayant une bande d'absorption maxima à 180 mμ. Si on introduit sur le noyau du benzène un groupement aldéhydique, le spectre ultraviolet de l'aldéhyde benzoïque résulté a l'absorption maxima pour λ=280 mμ.

Pour autres molécules l'introduction d'un groupement aldéhydique détermine un changement plus important de l'absorption de la lumière de sorte que le produit, initialement incolore, devient coloré pour l'oeil humain. Ainsi le phénol, récemment distillé, se présente sous forme de cristaux incolores; comme phénoxyde il reste aussi incolore, mais si on introduit un groupement aldéhydique en position *ortho*, apparait le sel de sodium de l'aldéhyde salicylique, coloré en jaune.

Le fait que le groupement aldéhydique détermine le changement de la lumière vers les longueurs d'onde plus grandes, donc vers le domaine visible, peut être prouvé également par d'autres exemples; ainsi l'anisole est incolore, tandis que l'aldéhyde anisique est jaunâtre.

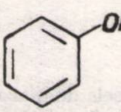

incolore

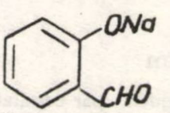

jaune

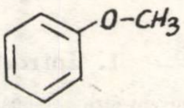

incolore

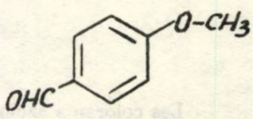

jaunâtre

Les propriétés auxochromiques du groupement aldéhydique se manifestent aussi par ses réactions chimiques. Le groupement aldéhydique est une fonction chimique réactive, réactivité expliquée par l'effet mésomère:

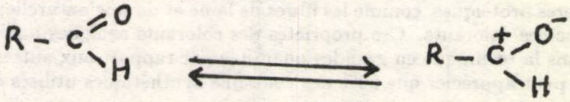

Due à son réactivité, le groupement aldéhydique peut condenser avec les groupement aminiques primaires libres en résultant des bases de Schiff; de même il peut réagir avec les groupements alcooliques en donnant des hémiacétals et des acétals. Telles réactions apparaissent également entre les groupements aldéhydiques et les groupements fonctionnels libres se trouvant dans la structure chimique des fibres textiles, comme les fibres protéiques et cellulosiques.

Dans la littérature de spécialité il y a plusieurs recherches qui reflètent l'interaction des fibres de laine avec les aldéhydes [3]...[6]. Ainsi les groupements aminiques, guanidiniques, thioliques, alcooliques, amidiques, carboxyliques, phénolique se trouvant dans la structure de la kératine, peuvent réagir avec le groupement aldéhydique [7].

En acceptant que le groupement aldéhydique d'un produit organique réagit avec les groupements aminiques libres de la kératine de la laine, on peut former des bases de Schiff ou bien des nouvelles liaisons transversales, déterminant la réticulation des macromolécules polypeptidiques de la kératine, selon le schéma:

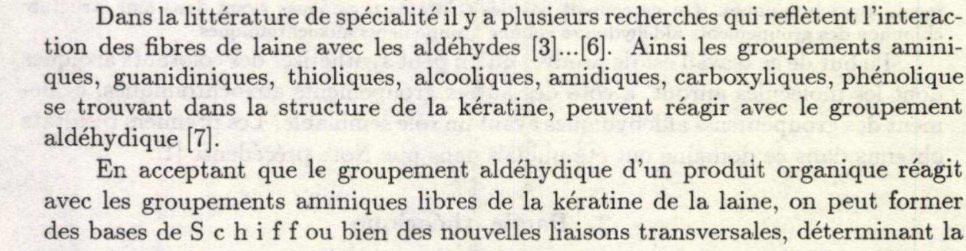

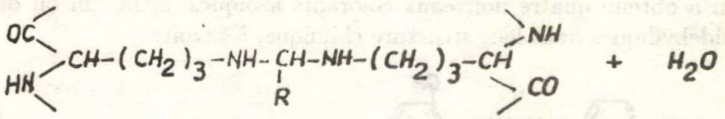

Si le groupement aldéhydique se trouve greffé sur la molécule d'un colorant, il va réagir d'une façon analogue avec les groupements fonctionnels libres de la macromolécule de la kératine ou avec les groupements hydroxyles de la cellulose, en résultant des liaisons covalentes entre les fibres textiles et ces nouveaux colorants.

Les groupements aldéhydiques peuvent parvenir dans les structures chimiques des colorants azoïques par leur présence soit dans la molécule du composant de copulation, soit dans la molécule du composant diazotable. On comprend facilement qu'on peut obtenir des colorants azoïques ayant un seul groupement aldéhydique ou deux. Dans quelques travaux antérieurs nous avons indiqué la possibilité d'obtenir de tels colorants azoïques. Ainsi par tétrazotation des *para*-diamines et copulation des leurs sels de tétrazonium avec certains aldéhydes on peut obtenir des colorants disazoïques ayant deux groupements aldéhydiques dans leurs molécules. Compte tenu de cette possibilité nous avons tétrazoté la benzidine, l'*ortho*-dianisidine, l'*ortho*-tolidine, l'acide benzidin-2,2'-disulfonique et l'acide 4,4'-diaminostilben-2,2'-disulfonique et par copulation des sels de tétrazonium obtenus avec l'aldéhyde salicylique en milieu alcalin, nous avons obtenus cinq nouveaux colorants disazoïques, ayant deux groupements aldéhydiques dans leurs molécules [8]. Ces colorants ont une structure chimique symétrique, étant constitués de deux parties identiques.

En continuant les recherches dans cette direction, dans un autre travail [9], nous avons synthétisé d'autres colorants monoazoïques, ayant dans leurs molécules un ou deux groupements aldéhydiques. Dans ce but nous avons diazoté le *para*-aminobenzaldéhyde et son sel de diazonium a été copulé avec l'aldéhyde salicylique, l'aldéhyde *para*-hydroxybenzoïque, l'acide γ, l'acide *I* et l'acide *H*.

Avec ces colorants on a teinté la laine et le cotton, en résultant de très belles nuances, qui sont stables à l'ébulition à l'eau ou à l'extraction avec la pyridine.

Il est nécessaire de mentionner qu'il n'y a pas dans la littérature qu'une seule recherche scientifique [10] qui indique la possibilité d'obtenir des colorants azoïques, ayant dans la structure chimique de la molécule un groupement aldéhydique, mais l'auteur de cette recherche n'a pas connu notre travail publié en 1969 [1].

3. Partie expérimentale

La présente investigation est orientée vers la même direction des recherches antérieures [1], [8], [9] et elle a comme but de synthétiser de nouveaux colorants azoïques, ayant des groupements aldéhydiques dans leurs molécules. On a utilisé comme composants diazotables p-aminobenzaldéhyde et p, p'-diaminostilbène et comme composants de copulation α- et β-naphtol, azonaphtol O.T. et l'aldéhyde salicylique. On a obtenu quatre nouveaux colorants azoïques, ayant un ou deux groupements aldéhydiques dans leur structure chimique, à savoir:

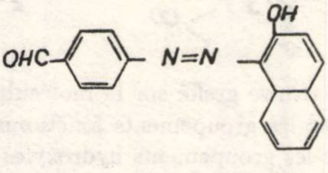

(I)

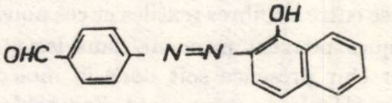

(II)

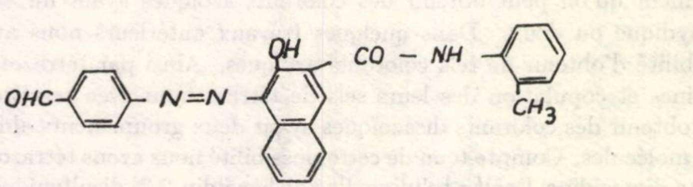

(III)

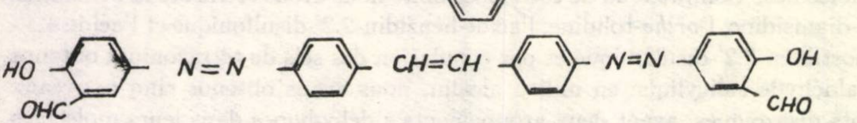

(IV)

On obtient le colorant (I) (4-formil-phényl-azo-2′-hydroxynaphtalène) par la diazotation du *p*-aminobenzaldéhyde et la copulation de son sel de diazonium avec β-naphtol, en milieu alcalin. On introduit 4 g *p*-aminobenzaldéhyde dans un verre Berzelius, on y ajoute 20 ml HCl d=1,19 et 50 ml de l'eau distillée. On refroidit à la glace jusqu'à la température de 2°...3°C, ensuite on introduit une solution aqueuse de 2,5 g azotite, refroidie aussi à 2°...3°C; de cette façon a lieu la diazotation. Dans un autre verre Berzelius, contenant une solution aqueuse de 1,3 g hydroxyde de sodium, on dissout 4,7 g β-naphtol et on refroidit de même à la glace. On introduit sous agitation la solution de diazonium dans la solution alcaline de β-naphtol. Il résulte un colorant rouge, qui par repos change la couleur vers rouge-foncé. Ce colorant se dissout dans une solution aqueuse de carbonate de sodium et précipite avec l'acide chlorhydrique.

Le colorant (II) (4-formil-phényl-azo-1′-hydroxy-naphtalène) a été synthétisé par copulation du *para*-aminobenzaldéhyde avec α-naphtol, dans un milieu alcalin. Les quantités des réactifs utilisés sont les mêmes que dans la premier cas. Le colorant ainsi obtenu est rouge-foncé, soluble en milieu alcalin, d'ou il précipite en présence de l'acide chlorhydrique.

On obtient le colorant (III) (4-formil-phényl-azo-tolylamide de l'acide 2′-hydroxy-3′-naphtoïque) par copulation du *p*-amino-benzaldéhyde diazoté avec azonaphtol O.T., en milieu alcalin. On a diazoté également 4 g *p*-amino-benzaldéhyde, qui par copulation avec la quantité correspondante de azonaphtol O.T. dissous dans une solution de hydroxyde de sodium, détermine la formation d'un colorant très beau, brique-rougeâtre. Ce colorant est soluble dans l'eau.

Le quatrième colorant, p-p'-bis (3-formil-4-hydroxy-fenil-azo)-stilbène, on l'obtient par tetrazotation du p, p'-diamino-stilbène et copulation du sel de tétrazonium resulté avec l'aldéhide salicylique, en milieu alcalin. On a soumis à la tétrazotation 3 g p, p'-diamino-stilbène, en utilisant les quantités stoéchiometriques d'azotite de sodium et d'acide chlorhydrique. Une quantité de 3,5 g aldéhyde salicylique a été introduite dans un verre Berzelius, contenant 100 ml solution d'hydroxyde de sodium 6%; un peu d'éthanol favorise la dissolution (dans une solution alcaline concentrée, l'aldéhyde salicylique précipite).

Le colorant obtenu est soluble en pyridine et dans l'eau; il teint la laine dans une nuance très belle de jaune-marron. Pour la laine teintée on a déterminé la solubilité dans l'urée-disulfite et les indices physico-mécaniques (résistance à la rupture et allongement). On a effectué les mêmes déterminations également pour la laine crue (nonteintée). Les résultats obtenus sont les suivants:

Solubilité dans l'urée-disulfite:

Laine crue	29,20%
Laine teintée avec le colorant (IV)	20,70%

Chaque résultat représente la moyenne de 10 déterminations.

Indices physico-mécaniques:

	Résistance à la rupture	Allongement
Laine crue	9,98	25,5
Laine teintée avec le colorant (IV)	11,39	21,5

Chaque résultat représente la moyenne de 100 déterminations.

De plus, la laine teintée avec le colorant (IV) n'est pas décolorée par lavage avec la pyridine chaude.

Ces résultats conduisent à l'interprétation que pendant la teinture de la laine avec de tels colorants apparaissent des liaisons covalentes entre la fibre et les molécules des colorants. À la fois apparaissent de nouvelles liaisons transversales dans la macromolécule de la kératine, qui résistent à l'action réductrice du disulfite.

La formation des ces ponts transversals explique l'augmentation de la résistance à la rupture des fibres de laine, la diminution de l'allongement et également l'abaissement de la solubilité dans l'urée-disulfite. Il faut souligner cette possibilité d'améliorer les propriétés physico-mécaniques des fibres de laine par teinture à l'aide des ces colorants.

Sans doute, les groupements aldéhydiques déterminent une réactivité plus élevée aux molécules des colorants dans le processus tinctorial, de telle sorte que ces colorants soient considérés comme une nouvelle série de colorants azoïques réactifs.

4. Conclusions

On montre la possibilité d'obtenir une nouvelle série de colorants azoïques, ayant des groupements aldéhydiques dans la structure chimique de la molécule.

Les groupements aldéhydiques peuvent parvenir dans la molécule du colorant par leur présence soit dans la molécule du composant diazotable, soit dans la molécule du composant de copulation.

Dans le processus de teinture les groupements aldéhydiques se trouvant greffés sur les molécules des ces colorants sont réactifs et ils se comportent d'une façon analogue aux ceux auxochromiques. Grâce à ces groupements aldéhydiques les colorants peuvent se lier aux fibres textiles par liaisons covalentes.

Les teintures réalisées avec de telles colorants sont très résistantes au lavage et la macromolécule de la kératine change sa structure chimique par réticulation.

On peut considérer que ces colorants azoïques, ayant des groupements aldéhydiques dans la structure chimique de la molécule, représentent une nouvelle série de colorants azoïques réactifs.

Reçue le 15 avril 1991

Institut Polytechnique, Jassy,
Chaire de Chimie générale
et Technologie chimique

BIBLIOGRAPHIE

1. Ifrim S., Mihai E., Bul. Inst. polit., Iaşi, **XV** (**XIX**), *1-2*, s. II, 99 (1969).
2. Ifrim S., Roşca I., *Chimie generală*. Ed. Tehn., Bucureşti, 1989, 563.
3. Ponchel P., Mazingue G., Overbèke M.V., Bull. I.T.F., **103**, 1155 (1962).
4. Reddie R.N., Nicholls C.H., Text. Res. J., **4**, 303 (1971).
5. Watt I.C., Morris R., Text. Res. J., **10**, 952 (1970).
6. Velmico J., Wemyss A.M., J. Text. Inst., **2**, 78 (1962).
7. Ifrim S., *Chimia lânii*. Ed. Tehn., Bucureşti, 1979, 269.
8. Ifrim S., Mihai E., Comun. şt., Univ. „Al.I.Cuza", Iaşi, Inst. pedag., 411 (1969).
9. Ifrim S., Bul. Inst. polit., Iaşi, **XIX** (**XXIII**), *3-4*, s. II, 139 (1973).
10. Riesz E., Bull. Scient. I.T.F., **11**, *43*, 61 (1982).

O NOUĂ CATEGORIE DE COLORANŢI AZOICI

(Rezumat)

Se prezintă o nouă categorie de coloranţi azoici, care au grupe aldehidice în molecule. Grupele aldehidice pot să apară în moleculele coloranţilor fie prin componenta diazotabilă, fie prin componenta de cuplare.

Se subliniază rolul auxocromic al grupării aldehidice şi proprietatea acesteia de a reacţiona cu grupele aminice libere din cheratina lânii, formând noi legături transversale.

Folosind indicii de solubilitate în uree-disulfit şi cei fizico-mecanici, se interpretează că prin vopsirea lânii cu astfel de coloranţi macromoleculele de cheratină se reticulează. În procesul de vopsire aceşti coloranţi formează legături covalente cu cheratina lânii, încât pot fi consideraţi o categorie nouă de coloranţi azoici. Se prezintă, de asemenea, sinteza a patru noi coloranţi azoici care au grupe aldehidice în structura lor moleculară.

BULETINUL INSTITUTULUI POLITEHNIC DIN IAŞI
Tomul XXXIX (XLIII), Fasc. 1–4, 1993
Secţia II
CHIMIE ŞI INGINERIE CHIMICĂ

D.C. 66.095.1; 547.533; 66.097.7; 661.183.48

SOME REMARKS ON MECHANISM OF ZEOLITE CATALYZED ALKYLATION OF TOLUENE WITH METHANOL

BY

EMIL DUMITRIU, V. HULEA and MIRCEA PALAMARU

1. Introduction

The toluene alkylation with methanol using various zeolites as catalysts was the object of a great number of studies [1]...[6]. Different autors have investigated the catalytic properties of zeolites (activity and selectivity), but information about the mechanism of this alkylation process are lack in the literature.

Here we present some data on the mechanism of the toluene alkylation with methanol taking into account the nature of the electrophile carriers.

2. Experimental

a) *Catalyst.* The HY zeolite was prepared by the common method of ionic exchange of NaY (Ventron, LZ-Y 52) with an aqueous solution of 0.1 M NH_4Cl, further deaminated and calcinated in air at 773 K for 4 h. The X-ray diffraction pattern showen that the zeolite was fully crystalline.

b) *Apparatus and Procedure.* The experiments were carried out in a down flow tubular reactor (Pyrex glass) at atmospheric pressure. The reactor was heated by a metal block furnance. The top section of the reactor which functioned as a vaporizer and preheater was paked with inert glass beads.

The reagents (methanol or toluene–methanol mixture) was fed by a calibrated syringe pump at a constant feed rate, vaporized and passed through the catalyst zone. Nitrogen was used as carrier gas which was made moisture-free using a molecular sieve trap. The flow of nitrogen was controlled by a needle valve and measured by a calibrated flowmeter. The reaction products were cooled at 273 K and analyzed by gas chromatography using a dinonil-phthalate-benton 34 column for the liquid phase and 2,4-dimethylsulfolane-squalane for the gaseous phase.

3. Results and Discussion

As is known, the reaction of toluene alkylation with methanol is part of the group of electrophilic substitution reactions at the aromatic ring. The nature of the electrophile substitution reactions because, in the most cases, the electrophile reagent is formed from the initial introduced species (in our case – methyl alcohol) through reversible or ireversible foreruner reactions. Note that by these foreruner reactions (preliminary to proper aromatic substitution) more reactive species, electrophile (E^+) and electrophile carriers ($E - Y$), can be formed.

If carbocation CH_3^+ is admitted in the electrophile alkylation as electrophil reagent (E^+), both the methanol and other reagents can be taken into account as electrophile carriers ($E - Y$). The aim of this paper is to identify the possibility of dimethylether participation as electrophile carrier.

The experiments of catalytic alkylation of toluene carried out in the presence of HY zeolite have lead to a great number of reaction products which were identified by GC and are listed in Table 1.

Table 1

The Composition of Reaction Products of the Toluene Alkylation with Methanol (T=673 K, F/N_2=5/1, W/F=17.85 g.h.mol^{-1})

Condensable phase	Noncondensable phase
benzene	dimethyl ether
toluene	methane
o-xylene	propane
m-xylene	*n*-, *i*-butane
p-xylene	ethane
1,2,4-trimethyl benzene	ethene
1,3,5-trimethyl benzene	propene
1,2,3-trimethyl benzene (trace)	butene-1
water	butene-2

As is seen from Table 1, two group of reactions in the process of zeolite catalysed alkylation of toluene with methanol can be distinguished: (i) the catalytic reactions of the aromatic hydrocarbons (alkylation, transalkylation, disproportionation, izomerization, etc.), and (ii) the catalytic conversion of methanol (formation of dimethyl ether, paraffins, olefins and even aromatics). It is necessary to emphasize that different interactions there are among these reactions either in the same group or between the two groups of reactions.

Thus, the experiments of catalytic alkylation and methanol conversion carried out on the same catalyst and the same reaction conditions (temperature, contact time and methanol feed) have clearly demonstrated the dimethyl ether participation as electrophil carrier in the toluene alkylation.

As can be seen from Fig. 1, for the methanol conversion, the dimethyl ether concentration of gazeous phase slight decreases with temperature increase but this concentration is maintained in the range of 13...17 wt%. Whereas, in the catalytic alkylation of toluene there is an important decrease of the dimethyl ether concentration which reaches a minimum at 425°C, after which a slight increase of dimethyl ether is observed. Note that this temperature (425°C) corresponds to the maximum of toluene conversion.

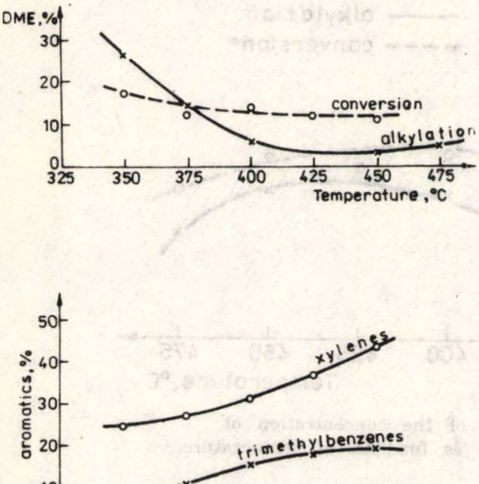

Fig. 1.– Toluene conversion and the dimethyl ether concentration in the gaseous phase vs. reaction temperature.

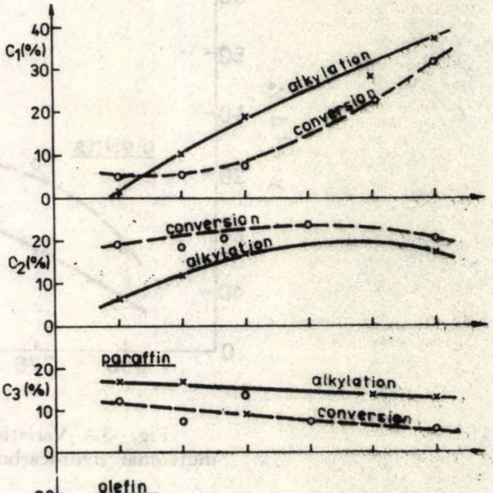

Fig. 2.– Hydrocarbon distribution in the gazeous phase vs. reaction temperature.

The participation of dimethyl ether in the toluene alkylation can be also demonstrated by the change of the hydrocarbon distribution from the gazeous phase (Fig. 2). It can be seen that the olefine proportion decreases when the

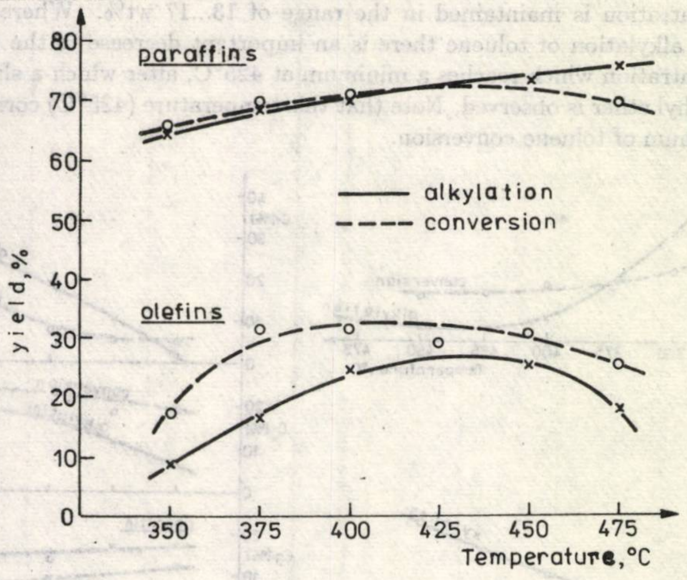

Fig. 3.- Variation of the concentration of individual hydrocarbons as function of temperature.

methanol conversion and toluene alkylation occur once. For comparison the paraffine distribution is given in Fig. 3 as well as the olefine distribution.

Though the mechanism of methanol conversion is not yet elucidated, being supposed various possibilities as: carbocation mechanism [7], carbonium-carbene mechanism [8], etc., however it is unanimously admitted that the dimethyl ether is an important link in the C–C chain propagation (both in the olefine and paraffine formation). Admitting that the mechanism of methanol conversion is not influenced by the methanol concentration (as it is normally) it would result that the methanol conversion process is disturbed by the dimethyl ether participation in the toluene alkylation and thus the different distribution of hidrocarbons in the gaseous phase can be explained.

Moreover, if it is taken into account that the zeolite catalyst posses Brönsted and Lewis acidic centers of various strength, the observed changes on the methanol conversion can be also explained by the competitive adsorbtion and desorbtion of the reagents and intermediates and by the strength of the bonds which the active centers form with the reagents and intermediates. It is of importance, in this connection, to have knowledge of the state and distribution of the active components on the catalyst surface determined by these active centers.

Received, December 16, 1990

Polytechnic Institute, Jassy,
Department of
Organic Industries

REFERENCES

1. Venuto P.B., Hamilton L.A., Landis P.S., Wise J.J., J. Catal., **5**, *81*, 484 (1966).
2. Yashima T., Ahmad N., Yamasaki K., Katsuta M., Hara N., J. Catal., **16**, 273 (1970).
3. Chen N.Y., Kaeding W.W., Dwyer F.G., J. Am. Chem. Soc., **101**, 6783 (1979).
4. Doughlan S. et al., Chem. Ind., **14**, 480 (1979).
5. Tuyen May, Dimitrov Chr., React. Kinet. Catal. Lett., **22**, 215 (1983).
6. Dumitriu E., Oprea S., Yousef K., Rev. Chim. (Bucharest), **35**, 906 (1984).
7. Anderson J.R., Foger K., Mole T., Rajadhyakaha R.A., Sanders J.V., J. Catal., **58**, 114 (1979).

CÂTEVA OBSERVAŢII ASUPRA MECANISMULUI ALCHILĂRII TOLUENULUI CU METANOL CATALIZATĂ DE ZEOLIŢI

(Rezumat)

S-au studiat alchilarea toluenului şi conversia metanolului pe câţiva zeoliţi HY. S-a remarcat participarea dimetileterului în alchilarea toluenului în calitate de purtător de electrofil. Când alchilarea toluenului şi conversia metanolului decurg simultan, distribuţia hidrocarburilor olefinice şi parafinice se modifică.

BULETINUL INSTITUTULUI POLITEHNIC DIN IAŞI
Tomul XXXIX (XLIII), Fasc. 1–4, 1993
Secţia II
CHIMIE ŞI INGINERIE CHIMICĂ

D.C. 66.097.4; 54-92

PHASE TRANSFER CATALYSIS IN POLYCONDENSATION PROCESSES

X. INTERNAL ROTATION ENERGIES IN POLYETHERS BASED ON 3,3-BIS (CHLOROMETHYL)OXETANE AND 4,4'-DIHYDROXYAZOBENZENE

BY

GH. SURPĂŢEANU, N. HURDUC and VICTOR BULACOVSCHI

1. Introduction

Many papers have been devoted to liquid crystalline (LC) polyethers in which mesogenic groups are linked together through flexible spacers [1]...[4], but less has been published on rigid-chain polymers [5], [6].

In a previous paper we showed the possibility of preparation polyethers from 3,3-bis(chloromethyl)oxetane (BCMO) and 4,4'-dihydroxy azobenzene (DHAB) under the phase transfer conditions. These polymers exhibit phase transitions by weak signals on DSC thermogram, but some of them are nonreproducible or vanish on rescanning.

To explain this aspect, conformational studies were undertaken, which were correlated with the geometry of mesogenic groups and chain stiffness [7]. Calculations were performed on a PC-386 computer by running the MMX program.

2. Results and Discussion

In order to establish the conformation of minimum energy, the calculations were undertaken upon the repeating unit of the polyether prepared from BCMO and DHAB corresponding to the Fig. 1.

Since DHAB is linked in the macromolecular chain to BCMO unit, bonds 1 and 4 appear to be equivalent and are characterised by low rotational barriers (27.44 kJ/mol) (Fig. 2). Going further, one finds that bonds 2 and 3 are more rigid, both they reveal two maxima for the potential barrier of 293 kJ/mol upon rotation by 80° and 270° (Fig. 3). The rigidity of these bonds was to be expected if one accounts for the conjugated double system in this structure.

Higher values were calculated for the corresponding maxima of potential energy upon rotation about link 5. The rotational barrier exceeds 4 000 kJ/mol and appears upon rotation by 210° and 300° (Fig. 4).

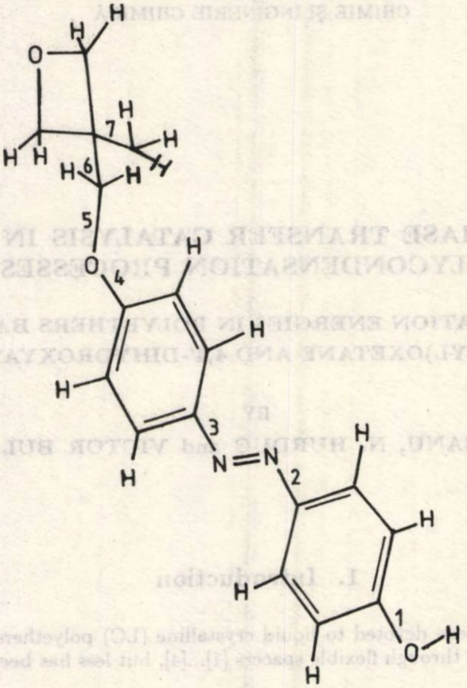

Fig. 1.– The arrangement of the DHAD and BCMO units in the repeating sequence.

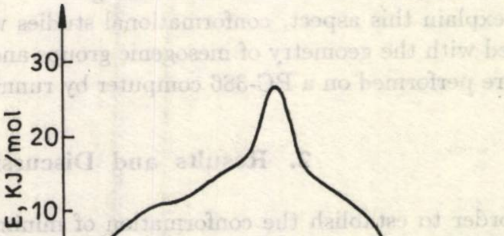

Fig. 2.– The potential energy of the polymeric chain vs. the angle of rotation upon the links *1* and *4* corresponding to Fig. 1.

The bonds 6 and 7 are equivalent and flexible. Their potential barrier does not exceed 28 kJ/mol. The energetic diagram presents three maxima of the potential energy upon rotation by 60°, 180° and 300°. In such conditions the oxetane ring might rotate, but with restrictions due to interchaine interactions at oxygen atoms (Fig. 5). Similar considerations may be done upon links 1 and 4, where sterical hindrances appear also. As a consequence, one should consider that whole structural unit behavies as a mesogenic and that LC properties are to be associated to these polyethers.

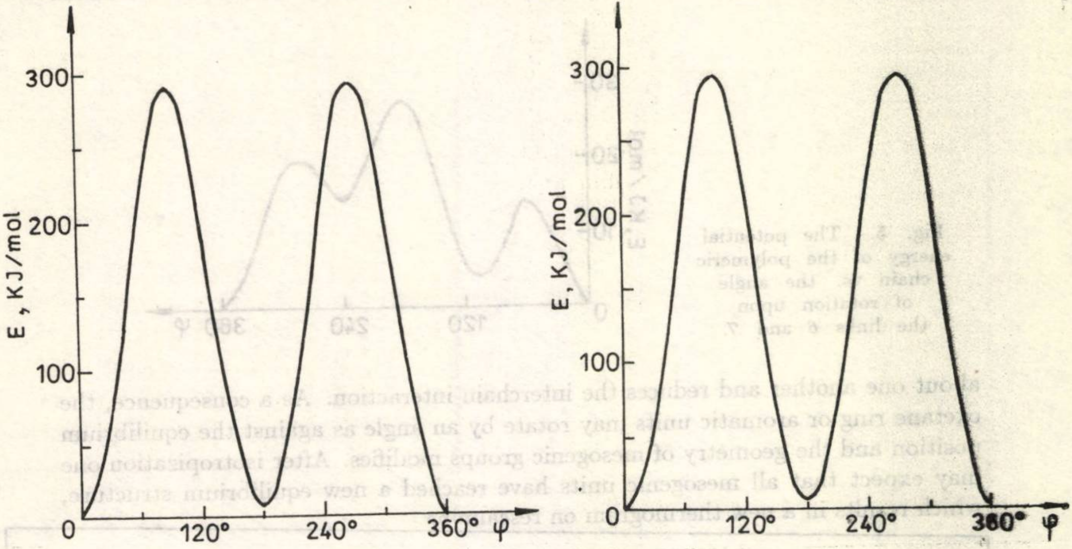

Fig. 3.- The potential energy of the polymeric chain vs. the angle of rotation upon the link *2* *(A)* and link *3* *(B)*.

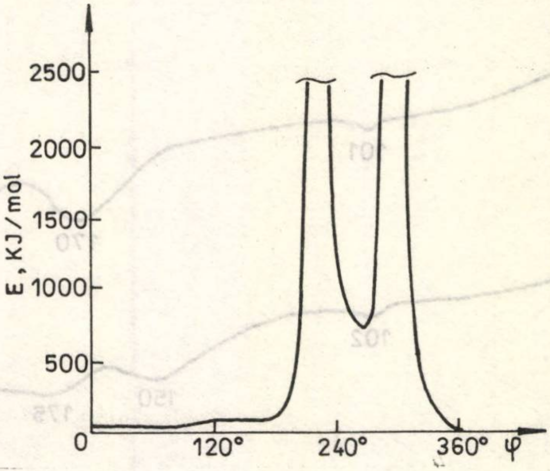

Fig. 4.- The potential energy of the polymeric chain vs. the angle of rotation upon the link *5*.

Fig. 6 presents DSC curves of a polyether synthesised from BCMO and DHAB. On the first heating (curve *A*) the glass transition temperature at 101° C is followed by three thermal modifications (150°, 175°, 199°C) and isotropization at 223°C. After cooling and reheating, on DSC thermogram (curve *B*) remains the glass transition point, but only two thermal modifications (170° and 196°C) and isotropization at 223°C appear. The shift of the phase transitions or their disappearance consist in modification of mesogenic geometry occuring on the first heating. The isotropization facilitates rotation of individual links of the chain

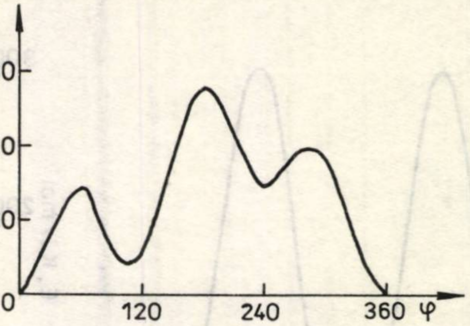

Fig. 5.– The potential energy of the polymeric chain vs. the angle of rotation upon the links *6* and *7*.

about one another and reduces the interchain interaction. As a consequence, the oxetane ring or aromatic units may rotate by an angle as against the equilibrium position and the geometry of mesogenic groups modifies. After isotropization one may expect that all mesogenic units have reached a new equilibrium structure, which results in a new thermogram on rescanning.

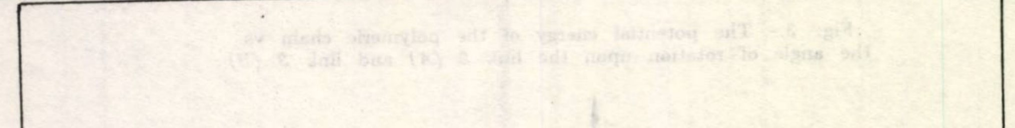

Fig. 6.– DSC thermogram for the BCMO–DHAD polyether: first heating (*A*) and second heating (*B*).

These kind of disimilarities between two succesive DSC thermograms were notified by other authors also.

3. Conclusions

The polyethers from BCMO and DHAB are rigid chain polymers and they reveal LC properties on heating. The whole structural unit might be considered as a mesogenic group due to its conformation imposed by the two monomers (BCMO and DHAB) which are tightly linked in the polymer chain. On heating there appear rotation possibilities of individual bonds of the chain about one another inducing alteration of the mesogenic geometry. This is not so sever, but can determine the shift of thermal transitions.

Received, January 12, 1993

Polytechnic Institute, Jassy,
Department of Macromolecules

REFERENCES

1. Shaffer T.D., Percec V., J. Polym. Sci., Polym. Chem. Ed., **25**, 2755 (1987).
2. Shaffer T.D., Percec V., J. Polym. Sci., Polym. Chem. Ed., **24**, 451 (1986).
3. Percec V., Nava H., Jonsson H., J. Polym. Sci., Polym. Chem. Ed., **25**, 1243 (1987).
4. Mahabadi Hadi-kh., Alexandru L., J. Polym. Sci., Part **A**, Polym. Chem., **28**, 231 (1990).
5. Hurduc N., Bulacovschi V., Bordeianu Al., Simionescu C., Polym. Bull., **28**, 639 (1992).
6. Hurduc N., Bulacovschi V., Scutaru D., Simionescu C., Ukraynian Polym. J., (in press).
7. Hurduc N., Surpăţeanu Gh., Bulacovschi V., Eur. Polym. J., **28**, 1589 (1992).
8. Alluiger N.L., Quant. Chem. Program Exchange Bull., **7**, 141 (1987).

CATALIZA CU TRANSFER INTERFAZIC ÎN PROCESELE DE POLICONDENSARE

X. Energiile de rotaţie internă la polieterii pe bază de 3,3-bis(clorometil)oxetan şi 4,4′-dihidroxiazobenzen

(Rezumat)

Polieterii pe bază de 3,3-bis(clorometil)oxetan şi 4,4′-dihidroxiazobenzen relevă însuşiri lichid-cristaline. Gruparea mezogenă în aceşti polimeri este reprezentată de unitatea structurală, a cărei geometrie influenţează tranziţiile termice ale polimerului. Această ipoteză se bazează pe calculele conformaţionale efectuate asupra unităţii structurale.

BULETINUL INSTITUTULUI POLITEHNIC DIN IAŞI
Tomul XXXIX (XLIII), Fasc. 1–4, 1993
Secţia II
CHIMIE ŞI INGINERIE CHIMICĂ

TATIANA LIXANDRU

1928–1993

On July 30, 1993, Tatiana Lixandru, a distinguished professor at the Faculty of Industrial Chemistry, "Gh.Asachi" Technical University of Jassy, genuine and remarkable scientist, having contributed to the training of several generations of chemical engineers, has passed away.

She was born in the town of Bârlad, on February 29, 1928, in a honourable and wise family who have affectionately cared for and educated their daughter. On graduating the "Iorgu Radu" High School of Bârlad in 1947, the young Tatiana will attend the courses of the Faculty of Industrial Chemistry in Jassy, getting excellent results along all her student's years. Consequently, when still a student, she becomes a preparer in the Department of Leather Industry. After graduating she moves in the Department of the Technology of Organic Substances. Surrounded by specialists and involving herself deeply in the serious and stimulative climate of work she becomes specialized in organic chemistry – in time, she is successively promoted assistant professor (1962), lecturer (1969) and, finally, full professor.

In parallels with her didactic activity, professor Tatiana Lixandru has developed a serious and impressive scientific work. As early as her first investigations, Tatiana Lixandru obtained significant results on the reactivity of some carbonylic derivatives containing phenols and aromatic amines, which have actually constituted the themes of her Ph.D. thesis, publicly defended in 1967.

In the following year (1968), professor Tatiana Lixandru initiated her researches in the chemistry of ferrocene and, in time, she succeeded in having her own team of workers in this field of investigation.

Actually, it is this domain in which Tatiana Lixandru invested must of her scientific resources, her endowment of a passionate and hardworking investigator being evidenced in the fine syntheses performed.

The constant scientific advance was recognized unanimously by her becoming, in 1977, Ph.D. supervisor. Also, her original contributions to the development of the Romanian Science were materialized in 1969, when Tatiana Lixandru was awarded the "Scientific merit" medal and the "Nicolae Teclu" prize of the Romanian Academy in 1974.

Several participations of professor Tatiana Lixandru to international conferences and meetings permitted her to make known the essential contributions of the Romanian School of Chemistry to the study of ferrocene.

Special mention has to be made here of the fact that, besides her more than 75 scientific papers, published mainly in prestigious international journals, Tatiana Lixandru is the author of several patents and research projects, as well as of some handbooks and monographs devoted to the study of ferrocene.

Along the three decades in which Tatiana Lixandru devoted her whole life to education and didactic activities, numerous generations of students had the opportunity to attend her minutely-prepared lectures, a model of both scientific vigour and teaching skill and to appreciate the precision and clarity of her ideas. The impressive conscientiousness, the passionate work, perseverance, remarkable intellectual power and unaltered ethical conduct made Tatiana Lixandru one of the most prestigious professors and the unanimous recognition and high esteem from both, her colleagues coworkers and pupils.

The passing away of Tatiana Lixandru is therefore a great loss to us all. Time will not less forget her as the loyal, unsweving and considered person she used to be will be always present in the memories of all those who knew and appreciated her.

Department of Organic Chemistry

ORSZÁGOS MŰSZAKI INFORMÁCIÓS KÖZPONT ÉS KÖNYVTÁR

1994 SEP [illegible]

ISSN 0254-7104